國立臺灣大學醫學院微生物學研究所

博士論文

Graduate Institute of Microbiology
College of Medicine
National Taiwan University

Doctoral dissertation

鈣離子如何活化切割拓樸異構酶的蛋白酶之研究

Study on calcium-induced proteolytic cleavage of DNA topoisomerases

周尚民

Shang-Min Chou

指導教授：李財坤 博士

Advisor : Tsai-Kun Li, Ph.D.

中華民國九十九年十二月

December, 2010

中文摘要

時間與空間上的嚴格控制對鈣蛋白酶來調控它的蛋白質水解活性功能是很重要的。這裡，我們證實位於細胞質中的鈣蛋白酶 2 可以切割水解位於細胞核的人類拓樸異構酶 1（hTOP1）及拓樸異構酶 2β(hTOP2β)，而拓樸異構酶 2α (hTOP2α)並不會被水解切割, 此現象可能透過 Ca^{2+}所誘導的鈣蛋白酶 2 進入細胞核而發生。此由以下的證據支持：(一)細胞處理 Ca^{2+}或 Ca^{2+}離子載體(ionophores)會造成在細胞核內的 hTOP1 及 hTOP2β蛋白質被快速切割水解。（二）兩種 Ca^{2+}螯合物都能有效地阻止 ionomycin (一種 Ca^{2+}離子載體)所引起的 hTOP1 及 hTOP2β的蛋白質切割；而且添加 Ca^{2+}可以直接活化細胞萃取物中蛋白酶切割 hTOP1 與 hTOP2β的現象；都支持細胞內的鈣離子濃度$[Ca^{2+}]_i$對於 hTOP1 與 hTOP2β蛋白質的切割是必要的。（三）進一步，我們利用重組蛋白質，實驗顯示鈣蛋白酶 2 比鈣蛋白酶 1 具有更高的效率去切割 hTOP1 蛋白質。(四)與以上概念一致，我們推論鈣蛋白酶 2 可能是主要 Ca^{2+}活化切割 hTOP1 的蛋白酶之一，因為在降低鈣蛋白酶 2 表現(si-Capn2)的細胞中 hTOP1 對於 ionomycin 誘導的蛋白質切割有高的抗性。(五)另外，我們的實驗也發現 hTOP2β與 hTOP1 均是鈣蛋白酶 2 的新受質，且 hTOP2β似乎較 hTOP1 更容易在相同濃度的 ionomycin 處理下被切割。(六)鈣蛋白酶 2 所切割 hTOP1 蛋白質的位置位於 hTOP1 的 N 端(N-terminus)第 158 及 183 個胺基酸賴胺酸(K^{158} and K^{183})上，而切割後的大片斷 hTOP1($hTOP1^{tr}$) 蛋白質則具有更強解螺旋（relaxation)的能力。（七）此外，$hTOP1^{tr}$ 蛋白質依然保有可以和 DNA 及喜樹鹼(camptothesin，CPT)形成可切割複合體（TOP1 cleavable complex，TOP1cc)，並具有與核仁蛋白質 nucleolin 的蛋白交互作用能力。（八）細胞處理 ionomycin 後，鈣蛋白酶 2 的活化似乎可以保護細胞免於 CPT 所引起的細胞毒殺害作用。總結, 我們的結果為細胞質中的鈣蛋白酶 2 如何切割細胞核內蛋白質提供了良好的說明與實驗證據支持：在被 Ca^{2+}活化後的鈣蛋白酶 2 會藉由細胞質-核穿梭運輸，讓鈣蛋白酶 2 從細胞質到細胞核從而接觸到並切割其核內受質。

關鍵字： 鈣蛋白酶，拓樸異構酶，蛋白質降解，鈣離子，細胞質核穿梭

Abstract

Crucial to calpain function is the tight regulation of its proteolytic activity, which is temporally and spatially controlled. Here, we demonstrated that the cytoplasm-located calpain 2 cleaves human nuclear topoisomerases I (hTOP1) and IIβ (hTOP2β) but not IIα (hTOP2α) possibly through the Ca^{2+}-induced nuclear translocation of active proteases. This is supported by the followings: (I) Treatments of cells with Ca^{2+} or Ca^{2+} ionophores caused a rapid proteolytic cleavage of hTOP1 and 2β in the nucleus. (II) Elevated intracelluar [Ca^{2+}] is responsible for this hTOP1 and 2β proteolysis event as suggested by the observations that two Ca^{2+} chelators could both effectively block the ionomycin-induced cleavage of hTOP1 and 2β and addition of Ca^{2+} in the *in vitro* protease activation assay caused hTOP1 and 2β proteolysis. (III) Using recombinant proteins, our *in vitro* experiments showed that calpain 2 cleaved hTOP1 more efficient than calpain 1 did.(IV) Consistent with above notion that calpain 2 as a main protease responsible for Ca^{2+}-activated proteolysis of hTOP1, hTOP1 proteins in calpain 2-knockdown (si-Capn2) cells were resistant to the ionomycin-induced proteolysis. (V) Similar to hTOP1, hTOP2β has also been identified as a novel substrate for calpain 2. In addition, Ca^{2+}-activated calpain 2 appeared to cleave hTOP2β more completed than hTOP1 in the same dose of

ionomycin treatment. (VI) The calpain 2 cleavage sites of hTOP1 were mapped at its N'-terminus K^{158} and K^{183} and the resulting $hTOP1^{tr}$ exhibited an enhanced relaxation activity. (VII) In addition, the $hTOP1^{tr}$ proteins remained the abilities to form the hTOP1-DNA-camptothecin (CPT) cleavable complex (hTOP1cc) and to interact with nucleolin proteins. (VIII) Ionomycin treatment caused a calpain 2-dependent protection of cells from cytotoxic killing by CPT. In sum, our results provided a good support for the regulation of calpain in the proteolytic cleavage of nuclear proteins via a cytoplasmic-to-nuclear trafficking of calpain 2.

Key words: Calpain, Topoisomerase, Proteolysis, Calcium, Nucleocytoplasmic shuttling

Abbreviations

a.a.	amno acid
BAPTA	1, 2-bis (o-amino-phenoxy) ethane-N, N, N', N'-tetraacetic acid
BSA	bovine serum albumin
Ca^{2+}	calcium ion
CAPN1/2	calpain 1/2
CAPN Inh I/II	calpain inhibitor I/II
CAPS Inh VI	caspase inhibitor VI
CHX	cycloheximide
CoIP	coimmunoprecipitation assay
CPT	camptothecin
DRB	5, 6-dichloro-1-β-d-ribofuranosylbenzimidazole
DTT	dithiothreitol
EDTA	ethylenediaminetetraacetic acid
EGTA	ethanedioxybis(ethylamine)-NNN'N'-tetra-acetate
ER	endoplasmic reticulum
FAK	focal adhesion kinase
GFP	green fluorescent protein
GST	glutathione-S-transferase

hTOP1	human DNA topoisomerase I
hTOP1cc	hTOP1 cleavable complex
$hTOP1^{tr}$	truncated hTOP1
IFA	immunofluorescence assay
kDa	Kilo Dalton, 1000 Dalton
LAC	lactacystin
MWs	molecular weights
PAGE	polyacrylamide gel electrophoresis
PBS	phosphate buffered saline
siRNA	small interference RNA
SDS	sodium dodecyl sulfate
TPE	Tris-phosphate-EDTA
VP-16	etoposide

Contents

Chapter 1 Preface

1.1 DNA topoisomerase family

DNA topoisomerases (type I: EC 5.99.1.2, type II: EC 5.99.1.3) are enzymes that unwind and wind DNA in order for DNA to control the synthesis of RNA and to facilitate DNA replication (*1-2*). Topoisomerases solve topological problems by transient cleavage and re-ligation half-reaction on DNA, and thus are separated into two types according to the number of strands cut in one round of reaction (*2-3*). Type I enzyme produces transient single-strand breaks on DNA, while types II topoisomerase produces double-strand breaks (*2*). As a result, type I enzyme removes supercoils from DNA one at a time, whereas type II enzyme removes supercoils two at a time. Although type II topoisomerase is more efficient in removing supercoils once at a time, this enzyme requires energy from ATP hydrolysis, but type I topoisomerase does not (*2, 4*). Type I topoisomerases can be further divided into two subclasses: type IA and type IB topoisomerases. Interestingly, type IA topoisomerases form a covalent intermediate with the 5' end of DNA, while the IB topoisomerases form a covalent intermediate with the 3' end of DNA (*2, 5*). Recently, a type IC topoisomerase has also been identified, called topoisomerase V (TOP5). While it is structurally unique from type IA and IB topoisomerases, it shares a similar catalytic mechanism with type IB topoisomerases (*2*). Type II topoisomerases which cuts both

strands of one DNA double helix with 4 base pairs (bp) apart, are also split into two subclasses: type IIA and type IIB topoisomerases, which share similar structure and catalytic mechanism (*2*).

There are four topoisomerases, including topoisomerase I (TopA), DNA gyrase, topoisomerase III (TopB) and topoisomerase IV (TopoIV), in bacteria. TopA can remove only negative supercoils. For example, during replication, the negative supercoils behind the replication fork are removed by bacterial TopA. The bacterial Top2 is also called DNA gyrase, which has two functions: (a) to remove the positive supercoils during DNA replication and (b) to introduce negative supercoils (*4*). These are two main enzymes that were responsible for the maintenance of DNA topological homeostasis. The bacterial TopoIV also belongs to the type II topoisomerase. The main catalytic activity of this enzyme is involved in decatenation and segregation between mother and daughter nucleoids.

So far, six different topoisomerases have been reported to be present in human (Fig. 1) or higher eukaryotic cells, namely topoisomerases 1 (TOP1), mitochondria topoisomerase 1 (mTOP1), topoisomerases 3α (TOP3α) and 3β (TOP3β), which are type I enzymes, and topoisomerases 2α (TOP2α) and 2β (TOP2β), two isozymes belonging to the type II family (*6*). In human, type IA topoisomerases (TOP3α and 3β) are homologous to bacterial type I topoisomerases (bacterial TopA and TopB) and,

like these bacterial enzymes, have weak activity toward negatively supercoiled DNA, but not positively supercoiled DNA substrate (*2*, *7-8*).

1.2 The important of DNA topoisomerases in antibiotics and anti-cancer therapy

DNA topoisomerases are also the known targets of many therapeutic drugs in clinical use (*9*). Both bacterial DNA gyrase and TopoIV are targets of clinically important antibiotics active against a wide spectrum of bacterial pathogens (*10*). Most of these therapeutic agents are called topoisomerase poisons due to the topoisomerase poisons convert the normal topoisomerases into DNA damaging and cell-killing nucleases by stabilizing the covalent DNA-protein intermediates. The quinolones, first represented by nalidixic acid, initiate bactericidal actions by trapping the covalent protein-DNA complexes formed by bacterial DNA gyrase or TopoIV (*10-11*). Another class of antibiotics, the aminocoumarins, such as novobiocin and coumermycin, are catalytic inhibitors of DNA gyrase and compete with ATP for binding to the gyrase B subunit (*12*).

Human type IB and type IIA topoisomerases are also important and excellent targets for anticancer drugs (*9, 13*). Camptothecin (CPT) and its more water-soluble derivatives trap the covalent DNA-enzyme intermediate formed by eukaryotic TOP1 (*13-14*). Many anticancer agents also target human TOP2. Most of them including

*m*AMSA, etoposide (VP-16) and doxorubicin are TOP2 poisons (*9, 15*). A number of TOP2 inhibitors that interfere with various steps of the enzyme's catalytic cycle have also been characterized as potential anti-cancer therapeutic agents (*16*). Thus, catalytic TOP2 inhibitors are a heterogeneous group of compounds that might interfere with either the binding between DNA and TOP2 (aclarubicin and suramin), stabilize noncovalent TOP2 dimer (merbarone, ICRF-187, and structurally related bisdioxopiperazine derivatives) or inhibit its ATP binding (novobiocin) (*16*). Since our study is mainly focused on the proteolysis of human topoisomerases by calpains, we therefore would like to introduce them in the following sections.

1.3 Topoisomerase 1 (eukaryotic)

Both positive and negative supercoils can be relaxed by eukaryotic TOP1 (type 1B). A variety of studies, both *in vitro* and *in vivo*, indicate the importance of topoisomerase I in various cellular functions. The enzyme is necessary for efficient simian virus 40 replication *in vitro* (*17*) and *Saccharomyces cerevisiae* TOP1 mutants have delayed onsets of DNA short-chain elongation during early S phase (*18*). TOP1 is known to interact with regions of actively transcribed chromatin (*19*) and has also been found to be an essential component in several *in vitro* transcriptional systems (*20*).

In 1985 experiments with yeast TOP1 deletion mutants showed that TOP1 was dispensable for cell growth (*21*). Lee M.P. et al. demonstrated that TOP1 is required for development past the blastocyst stage in *Drosophila melanogaster* (*22*). Therefore, the TOP1 gene may be more important in higher eukaryotes. Consistantly, disruption of both TOP1 alleles is embryonic lethal in mice, and the development of such embryos fails between the 4- and 16-cell stages. Both sperms and oocytes containing the inactive allele maintain viability through the fertilization point, and thus gene expression of TOP1is not required for gamete viability (*23*).

1.4 Topoisomerase 2 (eukaryotic)

Eukaryotic topoisomerase 2 (TOP2) removes supercoils and catenanes generated during DNA metabolic processes such as transcription and replication. Vertebrate cells express two genetically distinct isoforms (TOP2α and 2β) with similar primary structures and biochemical activities, but different biological roles. They share a high degree of overall sequence homology with 68% of identity and 86% of similarity (*24*). So far, the only major *in vitro* difference between the two isoforms is the preferential relaxation of positive supercoils by the TOP2α isoform (*25*), whereas other basic catalytic aspects are very similar. Human cell lines lacking the TOP2α encounter serious problems at mitosis because the deficiency in the chromosome segregation

(*26*). For the similar reasons, mouse embryos lacking the TOP2α fail to develop beyond the 4–8-cell stage (*27*). In contrast, mammalian cell lines lacking TOP2β pass normally through mitosis, and their most prominent phenotype is a decreased sensitivity towards TOP2 poisons (*28-29*). These findings indicate that all essential TOP2 functions in cell-cycle-related events, such as DNA replication and sister chromatid segregation, can be performed by TOP2α, while TOP2β is likely participated in transcription process in proliferating cells. However, Top2β$^{-/-}$ mice are not viable. They smother shortly after birth due to severe developmental defects of motor and sensory neurons and the brain (*30*). These defects also most likely reflect a requirement of TOP2β activity in regulating the expression of genes important at later stages of neuronal differentiation (*31*). This notion has convincingly been confirmed by the recent finding that the TOP2β plays an important role in the regulation of gene transcription (*32-33*).

1.5 Topoisomerase 3 (eukaryotic)

Eukaryotic TOP*3* was first identified in *Saccharomyces cerevisiae* as a gene that is required to suppress recombination between repeated sequences (*7*). Deletion of Top3 results in a slow-growth phenotype that is suppressed by the disruption of SGS1, the gene encoding the sole RecQ helicase in *S. cerevisiae* (*34*). Further analyses

revealed that the functions of Sgs1 are closely associated with that of DNA TOP3 (*35*). The close relationship between RecQ helicases and TOP3 seems to be conserved in the higher eukaryotes. Higher eukaryotic cells have two TOP3s, TOP3α and TOP3β (*8*). Knocking out the TOP3α gene (TOP3A) in mice results in embryonic lethality (*36*), while knocking out TOP3β (TOP3B) does not affect development but reduces the life span (*37*). Various TOP3 and RecQ molecules from different species have been reported to interact physically, including TOP3α and Bloom helicase (BLM) (*38*). BLM is a causative gene for Bloom's syndrome, which is an autosomal disorder characterized by predisposition to a wide-variety of cancers and premature aging phenotype. Biochemical analyses have suggested that BLM and TOP3α together affect the *in vitro* resolution of a recombination intermediate containing the double Holliday junction (HJ) via a proposed double-junction dissolution mechanism (*39*). However, the phenotypes of cells that lack TOP3 have not been characterized precisely, since TOP3α knockout is lethal.

1.6 Calpains

Since the first description of calpain (Ca^{2+}-activated neutral protease, E.C., 3.4.22.17) in 1964 by Guroff (*40*), extensive progress has been made regarding the identity, structure, activity, localization, and physiological and pathological functions

of calpains. Calpains are Ca^{2+}-dependent cysteine proteases (proteolytic enzymes with cysteine in the catalytic site) that modulate cellular functions depending on the proteolysis of substrate proteins (*41*). In human cells, 14 independent genes encode members of the calpain superfamily (Fig. 2) (*42*). There are two classes of calpains: one (comprising calpains 1, 2, 5, 7, 10, 13, and 15) is ubiquitous in the cytosol of different types of cells; the other (comprising calpains 3, 6, 8, 9, 11, and 12) express only or mainly in certain tissues (*42*). For example, calpain 8 expression is stomach-specific, and the expression of calpain 3 is largely specific to skeletal muscle, although it is also present in cardiac muscle and the liver.

In mammals, most of studies on calpain have focused on calpain 1 and 2 (also namely μ- and m-calpains, respectively), which were called "conventional" calpains. As suggested by the names, μ- and m-calpain (calpain 1 and 2) are activated by μM and mM level of Ca^{2+} concentrations *in vitro*, respectively (*42-45*). Calpains are a hetero-dimer consisted of one common calpain small regulatory subunit (30 kDa) and one distinctive large catalytic subunit of calpain 1 and 2 (80 kDa), which are 60 % identical in their amino acid sequences (*42*). Calpain 1 and calpain 2 are divided into four domains: a highly conserved, N-terminal domain I; a catalytic domain II comprising the Cys, His, Asn triad characteristic of Cys-proteases; a "connecting" domain III, and a C-terminal Ca^{2+}-binding domain IV. The small subunit comprises an

N-terminal domain V and a C-terminal Ca^{2+}-binding domain VI. Domains I and III are apparently non-homologous to any polypeptide sequenced so far; by contrast, domains IV and VI, which are approximately 80% identical and have a low (22–44%) degree of homology with calmodulin (*42*). During activation of calpain 1 or 2, the 30-kDa regulatory subunit is cleaved to yield a final 17-kDa form, while the 80-kDa catalytic subunit is converted to 76-kDa enzymatically active form (*42*, *46*). Studies have also suggested that conventional calpains recognize either specific primary structures around the scissile bond or global structural elements of the substrate proteins, or both. However, recently the determinants for calpain 1 and 2 cleavage have been analyzed with more precision: usually, amino acid preference in primary sequences extend over eleven residues around the scissile bond. The preferred residues are Leu, Thr, Val in P_2 position, Lys, Tyr, Arg in P_1, and, unexpectedly, Pro in the region flanking the P_2–P'_1 segment (*47*).

1.7 Functions of calpains

The Ca^{2+}-dependent neutral cysteine protease, calpain, is present in virtually all vertebrate cells (*42-43*, *48*). Knockout mice lacking the calpain 1 large subunit gene ($Capn1^{-/-}$) exhibit platelet dysfunction (*49*), whereas knockout mice lacking the calpain 2 large subunit gene ($Capn2^{-/-}$) or small subunit gene ($Capn4^{-/-}$) are embryonic lethal (*50*). These results suggest that calpain 2 might be critical for

embryogenesis, whereas calpain 1 is not. Additional physiological functions of calpains, including cell cycle progression (*51*), proliferation (*52*), differentiation (*53*), migration (*54*), embryonic development (*50*), meiosis (*55*), and mitosis (*56*), have been reported depending on the biological activities of substrate proteins.

Several cellular events can increase the activity of calpains: a rise in cytosolic Ca^{2+} concentration (*41, 44*), translocation of calpains to membranes (*57*), autolysis (*58*), dissociation of the calpain subunits (*59*), decreased levels of calpastatin (the endogenous inhibitor of calpain) (*60-63*), interaction with calpain activator proteins (*64*) or phospholipids (*65-66*) and phosphorylation by EGF signaling (*67-68*). Recently, the involvement of SUMOylation in the regulation of calpain 2 activity was also been suggested (*69*). The presence and interplay among these elements is critical for the fine-tuning calpain activity. In addition to the pathological roles, a number of pathologic conditions have been associated with disturbances of the calpain system (Fig. 3) (*70*). These include type 2 diabetes (*71*), cataracts (*72-73*), Duchenne's muscular dystrophy (*74*), Parkinson's disease (*75-76*), Alzheimer's disease (*77*), multiple sclerosis (*78*), liver injury (*79*), ischemia (*80-81*), stroke (*82*), brain trauma (*83*) and some types of cancer (*84*). Consistent with the calpain involvement in the cancer formation process, several oncogenes and tumor-suppressor gene products have also been demonstrated to be substrates for members of the calpain family (*46*).

Furthermore, mutations in the Capn3 gene cause LGMD2A (*85-86*), indicating that the protein that it encodes is important for muscle function.

1.8 Rationale

Ca^{2+} has been demonstrated to serve as an important secondary messenger which participates in many cellular signalings including the well-studied PKC pathway (*87*). In addition, the Ca^{2+}-mediated signaling pathways have also been shown to play important roles in various carcinogenic processes, such as tumor formation, invasion, angiogenesis and metastasis, by regulating the downstream kinases and proteases (*88*) . Here we took advantage of Ca^{2+} ionophores, ionomycin or A23187, to trigger Ca^{2+} influx resulting in elevating the cellular levels of Ca^{2+} ($[Ca^{2+}]_i$) and to study the effect of increasing $[Ca^{2+}]_i$ on DNA topoisomerases since they are critical for cell survival and proliferation.

Chapter 2 Calcium-induced cleavage of DNA topoisomerase I involving the cytoplasmic-nuclear shuttling of calpain 2

2.1 Introduction

Successful tight control of cellular proteolytic systems is crucial for maintaining cellular homeostasis (*89*). Abnormal activation of proteolytic systems has been observed in diseases and is implicated in the pathogenesis of such as muscle wasting (*90*) and neurodegenerative diseases (*70, 75-77, 83, 91*). Similarly, the impaired homeostasis of the calcium ion (Ca^{2+}) is associated with various pathological states, such as muscular atrophies (*85-86*) and ischemia (*75, 82*). The Ca^{2+} imbalance resulting from endoplasmic reticulum (ER) stress and/or dysfunction of Ca^{2+} channels often leads to the activation of proteolytic enzymes, which are mainly performed by the calpain family proteases (*70*). Interestingly, calpains are also implicated in the pathogenesis of Alzheimer's disease (*77*), sarcopenia (*92*) and tumor progression (*93-98*), which has been attributed mostly to their proteolytic cleavage of cytosolic and membrane proteins. However, the potential mechanism(s) of action and biological importance of calpain-mediated cleavage of nuclear proteins remain to be investigated.

Mammalian cells have 14 members of the calpain family. Some (e.g. calpain 1, 2, 5, 7, 10, 13 and 15) are ubiquitous enzymes, whereas others (e.g. calpain 3, 6, 8, 9, 11

and 12) are confined to specific tissues (*41-43, 48*). Among them, calpain 1 and 2 (μ- and m-calpain; CAPN1 and CAPN2) are the best characterized (*42, 45*). These two proteases require Ca^{2+}, but display differential sensitivities in Ca^{2+} concentrations ($[Ca^{2+}]$), for *in vitro* activation using purified enzymes (*42*). In the presence of Ca^{2+}, autolysis of calpain 1 occurs at the N'-termini of both subunits, resulting in a reduced $[Ca^{2+}]$ requirement for activation and providing additional regulation of its calpain activity (*42, 99*). Another central regulatory mechanism involves the natural inhibitor calpastatin (*100-103*), which has been shown to inhibit protease activity by binding to both subunits of calpain in the cytoplasm (*60-61, 104*). Moreover, localizations of calpains are also involved in their regulation (*41-42*). In this regard, calpain 2 has been shown to be present in the cytoplasm and nuclear compartments of mouse myogenic cells (*105-106*)and is implicated in the control of the cell cycle (*42*). Despite the above reports, the potential regulatory mechanisms by which calpains are activated, especially in the nucleus, remain poorly defined.

Calpain proteases hydrolyze most of their substrates in a limited proteolysis manner and subsequently lead to alterations in biochemical activities rather than loss of function and/or degradation of substrates (*42, 48*). These calpain-mediated alterations in the activities of targeting substrates are thus mainly responsible for all observed cellular phenotypes and pathological conditions associated with abnormal

calpain activation (*42, 45*). For example, through proteolysis of cytoskeletal talin and vinculin proteins as well as the signaling FAK kinase, calpains may be involved in the remodeling of the cytoskeleton anchorage complex and the regulation of cell adhesion, migration and fusion (*42, 107-108*). Notably, many calpain substrates (e.g. FAK and talin) identified *in vitro* are located either in the cytoplasm or on the membrane, which is in agreement with the primarily cytoplasmic location of these proteases (*42, 107*). However, a few recent reports have revealed that proteins in the nuclear pore complex or nucleus itself are potential calpain substrates, thereby suggesting the potential nuclear functions of calpains (*109*). The underlying mechanism(s) and regulation(s) of the calpain-mediated cleavage of nuclear proteins thus require further investigation.

DNA topoisomerases belong to a ubiquitous family of nuclear enzymes functioning in all aspects of DNA-tracking processes, such as DNA replication, RNA transcription (*110*) and recombination repair (*1-2*). Based on their catalytic mechanisms, these enzymes can be further categorized into two types: type I (TOP1) and type II topoisomerases (TOP2) (*1*). Both human TOP1 (hTOP1) and hTOP2 have been proven to be therapeutic targets for anticancer therapy (*111-112*). Clinically useful camptothecin (CPT) induces cell killing via the formation of hTOP1 cleavable complexes (hTOP1cc) (*13-14, 113*). Here, we report that the nucleocytoplasmic shuttling of cytosolic calpain 2 contributes to its Ca^{2+}-activated proteolysis of hTOP1.

Pharmacological inhibitor and RNA interference experiments suggest that calpain 2 plays an important role in this Ca^{2+}-activated hTOP1 proteolysis. Using *in vitro* fractionation and reconstitution approaches, our results revealed that Ca^{2+} activated cytosolic protease(s) to cleave hTOP1 and that the nuclear membrane served as a barrier against the access of calpain 2 to hTOP1 proteins. We also observed that Ca^{2+} influx not only activates the proteolytic activity of calpain 2 but also promotes its nuclear entry. Interestingly, the natural inhibitor calpastatin reduced Ca^{2+}-activated cleavage of hTOP1 by restricting calpain 2 in the cytoplasm, whereas catalytic inhibitors had no effect on the nuclear entry of calpain 2. Calpain 2-mediated cleavage sites were further mapped at N-terminal K^{158} and K^{183} of hTOP1. The resulting N-terminus-truncated hTOP1 ($hTOP1^{tr}$) proteins exhibit greater relaxation activity but retain its ability to be poisoned by CPT and to interact with nucleolins. Furthermore, this calpain 2-mediated hTOP1 proteolysis seemed to be associated with ionomycin-mediated protection from CPT-induced cell killing. In sum, we have found a mechanism of action for calpain 2 in which this protease cleaves nuclear hTOP1. This calpain 2-mediated hTOP1 proteolysis not only impacts its biochemical activities but also alters some cellular functions of hTOP1. Additionally, a novel regulatory mechanism of calpastatin on the nuclear proteolytic activity of calpain 2 has also been suggested.

2. 2 Materials and methods

2.2.1 Drugs, chemicals, reagents and cell cultures

5, 6-dichloro-1-β-d-ribofuranosylbenzimidazole (DRB), 1, 2-bis (*o*-amino-phenoxy) ethane-N, N, N', N'-tetraacetic acid (BAPTA) (*114*), caspase inhibitor VI, calpain inhibitor I/II (*115*), lactacystin (*116*), calpain 1 (from human erythrocytes) and calpain 2 (rat, recombinant) (*117*) were purchased from Calbiochem. Other chemicals were obtained from Sigma. The HCT116 colorectal cancer cell line was a generous gift from Dr. L.F. Liu (Univ. Med. Den. NJ, USA). The AGS gastric, MCF7 breast, HT29 and SW480 colorectal cancer cell lines were from Drs. M-C Huang and J-T Wang (National Taiwan Univ. College of Med, NTUCM, Taiwan).

2.2.2 Antibodies, immunoblotting and immunofluorescence

Antibodies against eEF1α, hTOP1 N'-terminal 100-200 a.a. ($TOP1_{\alpha\text{-}Nt}$) and nucleolin were generous gifts from Drs. S. Chang, S-C Lu (NTUCM, Taiwan), J. Hwang (Academia Sinica, Taiwan) and S.H. Yoshimura (Kyoto U, Japan). Antibodies against hTOP2α (sc-13058), calpain 1 (sc-13990) and hTOP1 C'-terminus ($TOP1_{\alpha\text{-}Ct}$) (sc-5342) were from Santa Cruz Biotech. Antibodies against GADPH (H86504M) and hTOP1 central region 400-600 a.a. ($TOP1_{\alpha\text{-}Cn}$) (ab3825) were purchased from Biodesign and Abcam, respectively. PARP1 (556362, BD Biosciences) and calpain 2

antibodies (3372-100, BioVision, for immunoblotting assay & 208727, Calbiochem, for immunofluorescence analysis) were obtained commercially. The immunoblotting assays were performed as previously described (number of replicates, n = 2 or 3) (*118-119*). All antibodies in immunoblotting analyses were used at a ratio of 1:1,000 except for anti-$TOP1_{\alpha\text{-Nt}}$ and anti-GAPDH antibodies, which were used with 5,000 X and 50,000 X dilutions, respectively.

For the immunofluorescence assay (n = 3), HCT116 cells were plated onto cover slips (coated with FBS) a day before drug treatments. Drug-treated cells were washed with PBS and then fixed with 3% paraformaldehyde and 2% sucrose in PBS. After 10-min fixation at room temperature and three PBS washes, cells were permeated via an incubation in buffer A (20-mM HEPES, 50-mM NaCl, 3-mM $MgCl_2$, 300-mM sucrose and 0.5% Triton X-100) at room temperature for 10 min. Cover slips were washed with PBS, blocked in buffer B (5% FBS and 0.05% Tween-20 in PBS) for 3 hours and incubated with primary antibodies in buffer B for another 16 hours at 4^0C. After washing three times with PBS, cells were incubated with AlexaFluor488- or Rhodamine-conjugated secondary antibodies (Molecular Probe) in Hoechst 33342 (10 μM)-containing buffer B at 37^0C for an hour. After the PBS washes, cells were then mounted in Fluoromount-G (Douthern Biotechnology Associates). Images were captured with a TCS SP2 confocal microscope (Lecia) equipped with a CCD camera

(Optronics) or an epi-fluorescence microscope (Nikon Eclipse 80i) with a CCD camera (Nikon DS-Ri1). Hoechst DNA staining was used to indicate the location of the nucleus. Typically, images of nuclear staining were scanned with 14 sections along the Z-axis with an objective lens (HCX PL APO 63.0 X 1.32 OIL PH3 UV) for image collection after determining the edges of the cells. After initial localization of the nucleus by Hoechst staining, the representative images for nuclear staining of calpain 2 were directly scanned/captured in the single section with the largest nuclear diameter.

2.2.3 *In vitro* protease activation assay

The protease activation assay was performed similar to the published procedure for the calpain activation assay (*120*). Briefly, 2 X 10^7 HCT116 cells were washed with PBS twice and cells were then lysed directly with 200 μl of a calpain activation buffer containing 50-mM NaCl, 10-mM EGTA, 0.1% Triton X-100 and 100-mM HEPES (pH 7.5). Different divalent cations (5-mM Ca^{2+}, Mg^{2+} or Mn^{2+}) with or without 5-mM EGTA were added to activate proteases (n = 1 using $TOP1_{\alpha\text{-Nt}}$ antibodies, n = 1 using $TOP1_{\alpha\text{-Ct}}$ antibodies). After a 10-min incubation at room temperature, reactions were stopped by the sample buffer. (50-mM Tris-HCl pH 6.8, 2% SDS, 0.1% bromophenol blue, 10% glycerol and 0.1-M β-mercaptoethanol).

Immunoblotting analysis was performed to analyze the integrity of hTOP1 proteins.

2.2.4 Nuclei isolation and cellular fractionation

HCT116 cells (~ 5 X 10^6) were pelleted and washed twice with PBS. The cell pellet was then re-suspended in 200 μl of hypotonic buffer (10-mM Tris-HCl pH 7.9, 140-mM KCl, 5-mM $MgCl_2$, and 1-mM DTT). After a 5-min incubation on ice, NP40 (0.25%) was added to the cell mixtures with an additional 3-min incubation and then followed with gentle taps to break down cellular membrane. The supernatant was collected as cytoplasmic extract after a 5-min centrifugation at 800 Xg with a microfuge (4^0C). The nucleus pellet was re-suspended with 1 ml of washing buffer (20-mM Tris-HCl pH 7.9, 140-mM KCl and 20% glycerol), span at 800 Xg for 5-min and collected as the fraction of intact nuclei. To prepare the nuclear extract, isolated nuclei were dissolved in 100 μl of nuclear extraction buffer (10-mM HEPES pH 7.5, 350-mM NaCl, 5-mM EDTA, 5-mM DTT) with 30-min gentle rotation. The nuclear mixture were then subjected to centrifugation at 12,000 Xg for 10 min and the supernatants were collected as nuclear extracts (n = 2).

2.2.5 Purification of TOP1 and GST-fused TOP1 fragments

Recombinant full-length of hTOP1 proteins were expressed in a baculovirus

system and purified following a published procedure. Plasmids expressing different length of GST-fused hTOP1 fragments were obtained from Dr. E.H. Rubin (Cancer Institute of NJ, USA) (*121*). After transformation of the constructs into *E. coli* BL21, bacteria were grown at 26^0C in Luria Broth containing 100 μg/ml of ampicillin and shaken until the A_{600} reached ~ 0.6. After 4 hours of incubation with 0.5-mM isopropyl-β-D-1-thiogalactopyranoside (IPTG), cells were harvested and then washed once with STE buffer (10-mM Tris pH 8.0, 150-mM NaCl and 1-mM EDTA). Bacteria were re-suspended in STE buffer containing 100-μg/ml lysozyme and incubated for 15 min on ice for cellular lysis. After addition of 5-mM DTT and 1.5% N-lauryl-sarcosine, bacterial lysates were further sonicated on ice. After spinning briefly, supernatants were incubated with prepared glutathione sepharose beads (Pharmacia) for 1 hour at 4^0C. Beads were washed four times with cold PBS. GST-fused proteins (e.g., GST-$TOP1_{141-166}$ containing the hTOP1 fragment from amino acid 141 to 166) were eluted with an elution buffer (10-mM reduced glutathione and 40-mM Tris pH 8.0).

2.2.6 Identification of calpain 2 cleavage sites in hTOP1, *in vitro* calpain cleavage assay and DNA relaxation analysis

Reaction mixtures in the calpain cleavage (CC) buffer (10-mM Tris pH 7.5,

50-mM NaCl, 1-mM DTT, 1-mM EDTA and 0.1-mg/ml BSA) containing purified hTOP1 (~ 0.5 μg) were mixed with or without 5-mM Ca^{2+} and 0.8-U calpain 2 . In these experiments, we used 0.8-U calpain to achieve a nearly complete digestion of recombinant hTOP1 and thereby optimized conditions for the *in vitro* assays. Reactions were stopped by the addition of EGTA (final concentration of 5 mM) after a 10-min incubation at room temperature. Reaction mixtures were subjected to both the immunoblotting assay and DNA relaxation analysis. The DNA relaxation assay was performed in a 30-μl mixture consisting of 0.5 μg of supercoiled DNA substrate (pBR322) with intact hTOP1, the $hTOP1^{tr}$-containing mixture or various cellular extracts (~ 20 μg) in the relaxation buffer (10-mM Tris pH 7.5, 50-mM NaCl, 1-mM EDTA, 1-mM DTT and 100 μg/ml of BSA). After a 10-min incubation at 37^0C, an adequate amount of stop solution (final 1% SDS, 0.0005% Bromophenol blue, 6% glycerol and 10 μg of protease K) was added and followed by an incubation at 37^0C for 30 min. The activity of hTOP1 in relaxing DNA was analysed with a 0.8% agarose gel with 1.2 V/cm at 4^0C for 15 hours in 0.5X Tris-phosphate-EDTA (TPE) buffer.

For the identification of calpain 2-cleaved sites on hTOP1, two GST-fused hTOP1 fragments (GST-$TOP1_{141-166}$ or GST-$TOP1_{166-210}$, ~ 1.5 μg) were subjected to the calpain cleavage assay with 0.8 U calpain 2 as described above (with the exception of a longer incubation time of 15 min). The cleavage mixtures were then

loaded into Microcon YM-10 (Millipore) and spun to eliminate proteins with molecular weights (MWs) larger than 12.4 kDa (> 95%, according to the manufacturer's report). Eluted samples containing non-GST-fused cleaved products were collected and delivered to Mission Biotech (Taiwan) for MALDI-TOF/Mass spectrometry analysis.

2.2.7 Lentivirus-mediated small RNA interference (siRNA)

Knockdown of calpain 2 expression was achieved by a lentivirus-packaged siRNA approach as described previously (http://rnai.genmed.sinica.edu.tw/). Five different pLKO.1-shRNA plasmids expressing calpain 2-targeting siRNAs (siCapn2 #39-43) were obtained from the National RNAi Core Facility (Taiwan). The calpain 2-targeting sequences for siCapn2 #39 and siCapn2 #43 are listed below: GCGCTCAGACACCTTCATCAA and CCCGAGAATACTGGAACAATA. Plasmid pLKO.1-shRNA (with puromycin resistant gene), pMD.G (VSV envelope protein) and pCMVDR8.91 (gag, pol and rev proteins) were co-transfected into 293T cells (~ 1.2 x 10^6) with a 1:0.1:1 ratio by Lipofectamine plus (Invitrogen). Culture media containing released viruses were collected every 24 hours for 3 days after transfection and the viral soups were then used for viral infection. One day after separated viral infection with five different si-Capn2-expressing lentiviruses (n = 1), HCT116 cells

were subjected to clonal selection with puromycin (2 μg/ml) for an additional three days. Surviving cells were then pooled and further cultivated into stable five clones (HCT116 si-Capn2 #39-43). Immunoblotting analysis with anti-calpain 2 antibodies was used to examine the knockdown efficiencies of pooled clones (data no shown for HCT116 si-Capn2 #40-42 cells). HCT116 si-Capn2 #39 and #43 cells were selected for further experiments.

2.2.8 The coimmunoprecipitation (CoIP) assay

Approximately 2 X 10^7 HCT116 cells were treated with 10-μM ionomycin for 15 min., harvested and then washed with PBS twice. After a brief spin at 13,000 Xg, cells were lysed with calpain activation buffer containing an additional 1X protease inhibitor cocktail (Roche). Supernatants were collected after 20-min centrifugation at 13,000 Xg. After addition of pre-immune mouse serum or anti-nucleolin antibodies to the collected supernatants, reaction mixtures were immediately rotated at 4^0C for 1 hr. Protein G-Sepharose beads were then added to the mixtures and further incubated overnight at 4^0C with gentle rotation. The beads were washed once with calpain activation buffer and four times with PBS. After the addition of sample buffer, immunoblotting analyses with two kinds of antibodies against the hTOP1 (n = 2, with either $TOP1_{\alpha\text{-}Ct}$ or $TOP1_{\alpha\text{-}Cn}$) or with nucleolin antibodies were carried out to

determine the interaction between hTOP1 and nucleolin.

2.2.9 Assays for human TOP1 cleavable complex (hTOP1cc)

For detection and characterization of hTOP1cc and hTOP1^{tr}cc, 10^6 of HCT116 cells were treated with or without 5-μM ionomycin for 15 min. and co-incubated with CPT (5 μM) for another 30 min at 37^0C. For the band depletion assay, the drug-treated cells were lysed with alkaline lysis and then subjected to immunoblotting analysis to examine CPT-induced formation of hTOP1cc and/or hTOP1^{tr}cc (*118*). In the medium reversal experiments, an additional incubation in CPT-free media 30 min prior to lysis was carried out to determine the reversible nature of hTOP1cc and hTOP1^{tr}cc (*122*). The alkaline lysis was performed with one appropriate volume of alkaline lysis buffer (0.2-N NaOH, 2-mM EDTA), which was then neutralized with a 1/10 volume of 10X neutralization solution (10% NP-40, 1-M Tris pH 7.4, 100-mM $MgCl_2$, 100-mM $CaCl_2$, 10-mM dithiothreitol, 1-mM EGTA and a protease inhibitor cocktail) with a 1/10 volume of 2 N HCl. For the release of hTOP1cc or hTOP1^{tr}cc from chromatin DNA, neutralized cell lysates were further incubated with *S. aureus* DNA nuclease S7 (60 U per reaction) on ice for 30 min. Reactions were terminated using sample buffer.

2.2.10 Colony formation assay

The clonogenic assay was performed as described (*119*) (n = 3) to examine the potential effect of ionomycin on CPT-induced cell killing. Sub-confluent cells were pre-treated with or without 5-μM ionomycin for 15 min and then co-treated with or without CPT for another 30 min. Drug-treated cells (4-to-8 X 10^2 per plate) were re-seeded onto 60-mm culture dishes with drug-free medium. Surviving cells were allowed to grow into colonies in a 5% CO_2 incubator at 37^0C for 12 days. Colonies were stained (with 0.03% crystal violet and 2% ethyl alcohol) and scored.

2.2.11 Quantitative and statistical analyses

Immunoblotting results were scanned and saved as electronic files. The intensities of individual bands were then graphed and determined with the ImageQuant program (Molecular Dynamics). In the medium reversal and S7-release experiment, the level of free $hTOP1^{tr}$ protein in the ionomycin-treated sample was taken as 100%. For the quantitative analysis of IFA results, both nuclear staining of calpain 2 and nucleolar enrichment of hTOP1 were scored as positive ones from several fields of confocal microscope images (up to ~50 or 100 cells/per field). In control cells, hTOP1 proteins locate in both nucleoplasm and nucleoli. After ionomycin treatments, cells with a much reduced immuno-fluorescent signal of

hTOP1 in nucleoplasm compartment and increased hTOP1 signals in nucleoli were scored as positive in nucleolar enrichment of hTOP1. Statistical analysis for differences between the numbers of survival rates, protein levels of hTOP1 and calpain 2, percentage values of hTOP1 proteolysis and nuclear calpain 2 staining was performed with Student's *t*-test. Data were considered statistically significant when *P*-values were < 0.05 and <0.01, which are shown with single (*) and double asterisks (**) respectively.

2.3 Results

2.3.1 Ca^{2+} influx promoted by calcium ionophores induces rapid and limited cleavage on human DNA topoisomerase I (hTOP1)

Different cells were treated with Ca^{2+} ionophores (*123*) (ionomycin or A23187) and immunoblotting analysis was used to examine the effect of Ca^{2+} influx on the protein integrity of hTOP1. In Fig. 4A, cellular exposure to 10-μM ionomycin caused limited proteolysis of hTOP1 in four different cancer cell lines with different efficiencies but not in SW480 cells (see quantitative results in Fig. 4B). Furthermore, in Fig. 5A we also took advantage of immunological approaches by using different hTOP1 antibodies ($TOP1_{\alpha\text{-Nt}}$ for recognition of N'-terminal 100-200 a.a., $TOP1_{\alpha\text{-Cn}}$ for recognition of the central 401-600 a.a. and $TOP1_{\alpha\text{-Ct}}$ for recognition of C'-terminus) to dissect the cleavage patterns of hTOP1. Interestingly, similar cleavage products were observed in ionomycin-treated HCT116 cells, suggesting the proteolytic sites of hTOP1 are likely located within its N'-terminal 200 amino acids according to the epitope specificity of TOP1 antibodies (Fig. 5B). In addition, this calcium ionophores-induced hTOP1 proteolysis was time- and dosage-dependent (HCT116 cells, Figs. 6A, B and C). Notably, HT29 cells exhibited the highest basal level of hTOP1 proteolysis (23.8 $\pm$ 4.8 %, Fig. 4B) among the five cell lines examined.

To confirm the contribution of intracellular [Ca^{2+}] to the above mentionable hTOP1 proteolysis effect of ionomycin, we used Ca^{2+} chelator EGTA. As shown in Fig. 7A, 2-mM EGTA abolished the ionomycin-induced proteolysis of hTOP1. Moreover, extracellular addition of Ca^{2+} in culture media also caused a dose-dependent hTOP1 proteolysis in HCT116 cells (Fig. 7B), providing further support for the direct role of Ca^{2+} in this limited proteolysis of hTOP1. Consistently, co-treatment of cells with 5-mM Ca^{2+} and 20-μM ionomycin caused a significant increase in hTOP1 proteolysis (~ 52%) compared to HCT116 cells treated with 20-μM ionomycin only (~ 25%). No hTOP1 proteolysis was observed in the presence of additional10-mM EGTA (Fig. 7C). In sum, our data suggest that Ca^{2+} influx activates the limited proteolysis of nuclear hTOP1.

2.3.2 Cytosolic protease(s) participates in Ca^{2+}-activated cleavage of hTOP1

Next, we sought to identify the protease(s) responsible for this Ca^{2+}-activated hTOP1 proteolysis. First, we demonstrated that adding Ca^{2+} into total cell lysates obtained from HCT116 cells lysed with calpain activation buffer could fully cause the cleavage events on hTOP1 *in vitro* (Fig. 8A) which was similar to results observed from *in vivo* treatment. Therefore, supporting a specific involvement of Ca^{2+} is in this limited proteolytic processing of hTOP1. Second, the fractionation and reconstitution

approaches as well as the *in vitro* cleavage assay were first used to identify and localize the responsible protease(s). In Fig. 8B, we found that the Ca^{2+}-activated hTOP1 proteolysis could only occur when cytosolic (C) and nuclear extracts (N) were mixed together, suggesting the cytoplasmic location of the protease(s). In addition, when intact nuclei (Ni') were combined with the Ca^{2+}-activated cytosolic fraction, a reduction in the level of hTOP1 proteolysis was observed (Fig. 8C, compare lane 5 to 6). From these observations support the notion that the nuclear shuttling of cytosolic proteases might play a major part in Ca^{2+}-activated hTOP1 proteolysis

2.3.3 Only calpains but not caspases, proteasome or *de-novo* synthesized proteases involve in Ca^{2+} influx mediated cleavage of hTOP1

The pharmacological approach using specific inhibitors was then used to examine the potential involvement of proteases. First, we found that the proteasome and caspases are likely not involved in this process, since hTOP1 proteolysis was not affected by co-treatment of either the proteasome inhibitor lactacystin (LAC, Fig. 9C) or caspase inhibitor VI (CASP Inh VI, Fig. 9A). Furthermore, the pretreatment of DRB (transcription inhibitor) or cycloheximide (CHX, translation inhibitor) before ionomycin treatment, there was no any obvious reduction in the proteolytic level of hTOP1 compared with that in the presence of ionomycin alone (Fig. 9C). The calpain

family included the most well-known proteases activated by Ca^{2+}. As expected, calpain inhibitor I (CAPN Inh I) effectively blocked the ionomycin-induced hTOP1 proteolysis (Fig. 9B). Similar blockage was also observed with calpain inhibitor II (data not shown). We have also examined whether ionomycin treatment induces proteolysis of other nuclear proteins. We found that only hTOP2β and lamin A/C proteins, but not hTOP2α or PARP proteins, were cleaved into visible smaller fragments upon exposure to 10-μM ionomycin. Similarly, these proteolyses of hTOP2β and lamin A/C proteins induced by ionomycin could also be greatly diminished by either EGTA or calpain inhibitor co-treatment (appendix Fig. 1).

2.3.4 Calpain 2 has better proteolytic activity than calpain 1 on hTOP1

Within the calpain family, calpain 1 and 2 are the main proteases activated by Ca^{2+} (*42*). We thus examined the ability of recombinant calpain 1 and 2 to cleave purified hTOP1 proteins. In Figs. 10A-B, we observed that both calpain 1 and 2 limitedly cleaved hTOP1 into fragments with a pattern similar to that induced by ionomycin treatment in the above cell culture experiments. Recombinant calpain 2 appeared to exhibit a much higher specific cleavage activity on hTOP1 than recombinant calpain 1 (Fig. 10C). Notably, this *in vitro* hTOP1 proteolysis by recombinant calpain 2 was also inhibited in the presence of calpain inhibitor I or

Ca^{2+}-chelating EGTA (Fig. 10D).

2.3.5 Calpain 2 contributes to the Ca^{2+}-activated hTOP1 proteolysis *in vivo*

Above *in vitro* experiments have identified hTOP1 as a potential substrate, that is preferentially cleaved by calpain 2 compared with calpain 1 (Figs. 10A-B). A genetic approach using RNA interference technology was employed to examine the involvement of calpain 2 in Ca^{2+}-induced hTOP1 proteolysis. Cells were infected with lentiviruses expressing different small interference RNAs specifically targeting calpain 2 (si-Capn2 #39 or #43) and then incubated in the presence of puromycin. Pooled clones of drug-resistant HCT116 cells were collected after three days of drug selection and further cultivated into stable lines. As shown in Figs. 11A-B, the expression of calpain 2 was knocked-down in both HCT116 si-Capn2 #39 (42.5 $\pm$ 12.0 % remained) and #43 clones (17.0 $\pm$ 2.8 % remained) with a greater efficiency in si-Capn2 #43 cells. Moreover, hTOP1 remained mostly intact upon exposure to 10-μM ionomycin in both HCT116 si-Capn2 #39 and #43 cells (Fig. 11C). Furthermore, knockdown of calpain 2 expression did not cause any significant change in the level of hTOP1 proteins (Fig. 11D). Together, our results thus suggest that calpain 2 is one of the protease responsible for Ca^{2+}-activated hTOP1 proteolysis.

2.3.6 Ca^{2+} influx triggers nucleocytoplasmic shuttling of calpain 2

The main cellular location of calpain 2 has been reported to be in the cytoplasm and most of its *in vitro* substrates are either membrane-associated or cytosolic proteins (*42, 47*). Consistently, we showed that calpain 2 proteins were mainly resident in the cytoplasm of untreated cells (Figs. 12A-B). Inspection of Fig. 12A or B reveals that a small proportion of calpain 2 re-distributed into the nuclear fraction after Ca^{2+} influx, whereas both activated and intact calpain 1 protease remained in the cytosolic fraction (Fig. 12A). In addition, nuclear staining of calpain 2 became visible after 10-μM ionomycin treatment (~ 28 % of cells with positive nuclear staining using an epi-fluorescence microscope shown in Fig. 12C).

To further eliminate interference of imaging of cytosolic calpain 2, we took advantage of using confocal microscopy. As shown in Figs .12D and 13A, the positive nuclear entry of calpain 2 was observed upon Ca^{2+} influx induced by ionomycin treatment. Quantitative analysis further revealed that ionomycin treatment induced nuclear entry of calpain 2 in a dosage-dependent manner (Figs. 13B-C). These results therefore suggest that Ca^{2+} influx not only activates the protease activity of calpain 2 but also causes its nuclear entry. Moreover, both processes are likely needed for Ca^{2+}-activated hTOP1 proteolysis.

2.3.7 Nuclear entry of calpain2 is dependent on Ca^{2+} but not its catalytic activity

To test the above hypothesis, EGTA and calpain inhibitors were used to block Ca^{2+} influx and protease activity, respectively. As shown, EGTA abolished both proteolysis of hTOP1 (Fig. 14A) and nuclear entry of calpain 2 after ionomycin treatment (Fig. 14B). The catalytic inhibitor of calpains (CAPN Inh I) blocked the Ca^{2+}-activated hTOP1 proteolysis (Fig. 14C) but had no effect on the nucleocytoplasmic shuttling of calpain 2 (Figs. 14D-E).

2.3.8 Ca^{2+} induced nuclear entry of calpain 2 is regulated by calpastatin

Moreover, it is generally believed that the natural inhibitor calpastatin regulates the activation of calpain proteases and inhibits their catalytic activity by binding to them (*60-61, 102-103*). We thus transfected GFP-fused calpastatin into HCT116 cells to examine its effects on the Ca^{2+}-activated hTOP1 proteolysis and nuclear entry of calpain 2. As scored by the GFP-positive signal, ~ 30% of HCT116 cells transiently expressed calpastatin. To our surprise, calpastatin not only reduced the Ca^{2+}-activated hTOP1 proteolysis (Fig. 15B), but also blocked the ionomycin-induced nuclear entry of calpain 2 (Figs. 15A and C). With 10-μM ionomycin treatment, force expression of calpastatin decreased the nuclear staining of calpain 2 from 25.3 ± 1.2 % to 5.1 ± 1.0 % ($P < 0.01$, Fig. 15C). In sum, our results suggest a novel role for calpastatin in

regulating the Ca^{2+}-activated nuclear entry of calpain 2.

2.3.9 Calpain 2 cleaves hTOP1 at two N'-terminal lysine residues, K^{158} and K^{183}

The above epitope mapping results (Fig. 5B) suggest that hTOP1 proteolysis by calpain 2 likely occurs within its N'-terminal 200 amino acids. To further identify the cleavage sites, various GST-fused recombinant hTOP1 fragments were purified for the *in vitro* calpain 2 cleavage assay. As shown in Fig. 16A, two bacterially expressed GST-fused TOP1 proteins, GST-$TOP1_{141-166}$ (the TOP1 fragment containing amino acid 141 to 166) and GST-$TOP1_{166-210}$ were purified to nearly homogeneity (upper panel with coomassie staining).Treatment of calpain 2 and Ca^{2+} caused proteolysis of both the GST-$TOP1_{141-166}$ and GST-$TOP1_{166-210}$ fragments, but not the GST proteins alone (Fig. 16A). Reaction mixtures containing cleaved products were loaded into Microcon YM-10 columns, and the flow-through parts were then collected for molecular weight (M.W.) determination by MALDI-TOF mass spectrometry analysis. In Fig. 16B, the truncated hTOP1 peptides in the flow-through part of the GST-$TOP1_{141-166}$/calpain 2/Ca^{2+} eluents produced a major peak at position 1633.583 M/Z (arrow #1, upper panel), and those from the GST-$TOP1_{166-201}$/calpain 2/Ca^{2+} eluents showed three major peaks at 4243.953, 3123.813 and 1137.576 M/Z (arrow #2, 3 and 4, lower panel). Based on the above data and theoretical calculation of

molecular weight (Fig. 16C), we thus concluded that calpain 2 cleaves hTOP1 at its N'-terminal K^{158} and K^{183}. The cleavage site at the E^{207} is most likely due to the additional six amino acids generated from cloning.

Consistently, we used the polyclonal antibodies against $hTOP1_{100-200}$ fragment ($TOP1_{\alpha-Nt}$) and showed that the more complete cleavage of recombinant hTOP1 by higher unit of calpain 2 (0.8 U) resulted in four proteolytic products with MWs of ~ 18, 21, 69 and 72 kDa (Fig. 16D). In addition, we also constructed the full length of hTOP1 into the expression plasmid pEGFP-C1 to produce a chimera protein with N-terminus fused with GFP (Fig. 17A). In Fig. 17B, the Ca^{2+}-activated proteolysis on hTOP1 resulted in two GFP-fused truncated products with MWs of ~44 and 47 KDa (Fig. 17B) corresponding to the above part of *in vitro* cleavage (Fig. 16D). Together, our results suggest that calpain 2 cleaves hTOP1 at the N'-terminal K^{158} and K^{183} residues.

2.3.10 Nucleolin interacts with two N-terminal truncated forms of hTOP1

Moreover, GFP-hTOP1 was force expressed in HCT116 cells and its protein was concentrated in nucleoli with a diffuse pattern in the nucleoplasm (Figs. 17C-D). As reported (*121*), the nucleolin-interacting domain is located on the N'-terminal 166 to 210 a.a. of hTOP1. Since the calpain 2 cleavage sites, K^{158} and K^{183}, are located

within the nucleolin-binding domain of hTOP1, we thus examined the interaction between calpain 2-truncated hTOP1^{tr} proteins and nucleolin using an immuno-coprecipitation approach. Two calpain 2 cleavage sites ($K^{158, 183}$), three caspase cleavage sites ($D^{123, 146, 170}$) and the nucleolin-interacting domain (amino acid 166 to 210) located on the N'-terminus of hTOP1 are illustrated in Fig. 18A. Interestingly, not only hTOP1 but also two large fragments of calpain 2-truncated hTOP1 (hTOP1^{tr}) were all co-precipitated by anti-nucleolin antibodies (Fig. 18C, lane 2 and 4).Input proteins were shown in Fig. 18B. Therefore, calpain 2-mediated hTOP1 proteolysis does not disrupt the interaction between hTOP1 and nucleolin, further suggesting $hTOP1_{183\text{-}210}$ as the nucleolin-interacting domain.

2.3.11 Calcium-influx mediated nucleolar accumulations of hTOP1 is independent of calpain 2

Nucleolin staining indicates the nucleolar location. As shown in Fig. 19A, hTOP1 proteins seem to be more concentrated in the nucleoli after ionomycin treatment (62.0 ± 4.0 % in HCT116 si-Vector cells, n = 3). This ionomycin-induced change of hTOP1 location is likely independent of calpain 2, since it also occurs efficiently in HCT116 si-Capn2 #43 cells (58.1 ± 2.2 %, Figs. 19B and C).

2.3.12 hTOP1^{tr} proteins exhibit greater relaxation activity

Above results suggest that a part of the regulatory N'-terminus of hTOP1 is truncated by calpain 2. We examined the specific relaxation activity of the intact hTOP1 (hTOP1$_{1-765}$) and hTOP1^{tr} (hTOP1$_{158-765}$ and hTOP1$_{183-765}$) proteins. In Fig. 20A, addition of 5-mM Ca^{2+} and 0.8-U calpain 2 triggered autolysis of the protease and complete proteolysis of recombinant hTOP1. Different reaction mixtures were then diluted 2-fold and the relative activities of diluents relaxing supercoiled (SC) DNA were compared. Interestingly, the DNA relaxation activity of the hTOP1-containing mixture was increased (by roughly two-fold) when Ca^{2+} and calpain 2 were both presented (Fig. 20B).

To support the above finding, we treated HCT116 si-Vector or si-Capn2 #43 cells with ionomycin (20 μM) and then collected their extracts for immunoblotting analysis and the DNA relaxation assay. Ionomycin treatment activated proteolysis of hTOP1 in HCT116 si-Vector cells (Fig. 20C), and thus the derived cell extract is regarded as the hTOP1^{tr}-containing extract. After ionomycin treatment, the relaxation activity of the si-Vector cell extract was also approximately 2-fold higher than that of the si-Capn2 #43 cell extract (Fig. 20D). It is generally believed that DNA TOP1 provides the main supercoiling activity in mammalian cells (*1, 124*). The enhancement of this relaxation activity of by calpain 2-truncated hTOP1^{tr} is thus likely responsible for the increased

relaxation activity of ionomycin-treated cell lysates. Together, these results are consistent with reports showing that the N'-terminal domain of hTOP1 plays a distinct role in its DNA relaxation activity (*125-126*). In addition, our results also suggest the novel regulation of hTOP1 activity by calpain 2.

2.3.13 Both two hTOP1^{tr} are trapped on chromosome by CPT

TOP1 has also been proven to be an excellent therapeutic target for anticancer therapy. CPT induces cell killing by the formation of a cleavable complex (TOP1cc) (*13-14*), in which TOP1 is trapped on chromatin and cannot be resolved by SDS-PAGE analysis (*118*). As expected, CPT treatment resulted in the disappearance of detectable hTOP1 in the free form (Fig. 21A, compared lane 2 to 1) since hTOP1cc is covalently trapped on chromatin DNA. In Fig. 21A, cells were pre-treated with ionomycin (5 μM, 15 min) to generate truncated hTOP1 (hTOP1^{tr}, lane 3). We further showed that CPT treatment induced trapping of hTOP1^{tr}cc (Fig. 21A, compared lane 3 to 4-8) on chromatin DNA in a similar dose-dependent manner. Moreover, characteristics of the cleavable complex were examined for those of hTOP1^{tr}cc. First, both hTOP1^{tr}cc and hTOP1cc on chromatin are released as free hTOP1^{tr} and hTOP1 after a combination of medium reversal and S7 nuclease treatment (Fig. 21B). Together, our results show that hTOP1^{tr}cc is formed upon CPT treatment and exhibits

characteristics similar to those of hTOP1cc.

2.3.14 Calpain 2 is involved in the ionomycin-induced protection from CPT cytotoxicity

Next,we also found that pretreatment with 5-μM ionomycin could protect cells from CPT-mediated cell killing (Fig. 22A). A reduced protective effect of ionomycin on the CPT-induced cell killing was observed in HCT116 si-Capn2 #39 and #43cells (Figs. 22C-D), suggesting the involvement of calpain 2 in this protective effect. Furthermore, calpain 2-deficient HCT116 si-Capn2 #39 and #43 cells were both more sensitive to CPT treatment than HCT116 si-Vector cells (Fig. 22C). Taken together, our results suggest that calpain 2 might protect cells from CPT-mediated cell killing. This protective effect is not due to change in the expression level of hTOP1 proteins or change in their ability to form hTOP1cc responding CPT treatment, since hTOP1 levels and CPT-induced hTOP1cc formation were not altered in HCT116 si-Capn 2 cells (Figs. 22B and E; see quantitative results in Figs. 11D and 19F, n = 3).

2.3.15 On hTOP1 HT29 cells has better basal proteolytic activity in which calpains may involve

As stated above, we also found that HT29 cells exhibit an elevated level of

endogenous hTOP1 proteolysis (Figs. 4A-B) suggesting a higher level of calpain 2 activation. To dissect their correlation, we therefore examined the endogenous levels of calpain 1, 2 and hTOP1 in different cell lines and found that

HT29 and MCF7 cells have lower level of calpain 2 protein compared to HCT116, AGS or SW480 cells (Fig. 23A). Furthermore, HT29 cells contain the highest level of hTOP1 protein (Figs. 23B and 24A, 1.31 $\pm$ 0.09-fold, compared to HCT116, n = 3, $P < 0.01$). Other cell lines did not exhibit any significant differences in the hTOP1 protein levels compared to HCT116 cells. Consistent with the notion that calpains and Ca^{2+} are responsible for this higher endogenous level of hTOP1 proteolysis, our results demonstrated that long-term (6-hour) treatment with either Ca^{2+} chelator BAPTA or calpain inhibitor I could effectively reduce hTOP1 proteolysis to ~ 58 % (lane 3) and 37 % (lane 4) of levels in control cells (lane 1), respectively (Fig. 24B). Our above results indicated HT29 cells has better calpain activity on proteolysis of hTOP1.

2.3.16 HT29 cells exhibits properties with more nuclear shuttling of calpain 2 and better resistant to CPT cytotoxicity

On the other hand, ionomycin treatment did not induce hTOP1 proteolysis in SW480 cells (Figs. 4A-B and 25A). Thus, the levels of activated endogenous nuclear

calpain 2 in the three colorectal cancer cell lines are as follows: HT29 (23.8 ± 4.8 %) >> HCT116 (2.3 ± 1.9 %) = SW480 (3.0 ± 1.2 %; Fig. 4B, n = 3). In agreement with this finding, we have also observed that HT29 cells have the highest level of both endogenous basal (5.0 ± 0.4 %, n = 3) and ionomycin-induced nuclear immunoreactivity for calpain 2 (49.4. ± 6.3 %, n = 3) (Figs. 25B and C). In agreement with the protective role of calpain 2 in CPT-induced cell killing, we have also found that HT29 cells with the highest endogenous activated calpain 2 are more resistant to CPT-induced cell killing (Fig. 25D).

2.4 Summary

Calpains, mostly through their proteolytic cleavage of the cytosolic and membrane proteins, have been suggested to contribute to the pathogenic progression of neuronal diseases (*75*), muscle dysfunctions (*92*) and tumors (*94-95, 98*). Nevertheless, the action mechanism(s) and the biological importance of the calpain-mediated cleavage on nuclear proteins remain to be explored. Here, we reported a cytoplasmic-nuclear shuttling of calpain 2 and its association with the observed Ca^{2+}-mediated truncation on human nuclear DNA topoisomerase I (hTOP1) (Fig. 26). Using hTOP1 as the nuclear substrate, we had provided scientific evidence on a potential underlying mechanism for the calpain 2-mediated proteolysis of nuclear proteins. As reported, Ca^{2+} influx activates both calpain 1 and 2. Surprisingly, we found that calpain 2, but not calpain 1, shuttles from cytoplasm to nucleus upon ionomycin treatment. This nuclear entry of calpain 2 is regulated by Ca^{2+}, but is independent of its protease activity. In addition, our study had also revealed a novel inhibitory mechanism for calpastatin by limiting the nuclear entry of calpain 2. Therefore, we reasoned that Ca^{2+} influx activates the proteolysis of nuclear hTOP1 through activation on both the proteolytic activity of calpain 2 and its nuclear entry. Interestingly, the calpain 2-truncated hTOP1 ($hTOP1^{tr}$) exhibits a higher supercoiling activity and remains sensitive to its targeting drug camptothecin (CPT). A protective

role of calpain 2 on the CPT-induced cell killing has also been observed.

2.5 Discussions

Calpain 1 and calpain 2 are the two calpain proteases that have been extensively studied (*42*). Common features are shared by these two proteases include the following: both enzymes require Ca^{2+} for activation (although a great difference in the Ca^{2+} concentration required for activation exists; purified calpain 1 and 2 require concentrations of 3-50 and 400-800 μM of Ca^{2+} for half-maximal activity *in vitro*) (*42*), both enzyme exhibit a cytoplasmic localization and both proteases are under inhibitory regulation by calpastatin (*102*). In addition, common substrates have also been identified via the *in vitro* cleavage approach (*47*). From our *in vitro* cleavage assay, it is interesting to note that that calpain 2 cleaves hTOP1 more efficiently than calpain 1 with an identical pattern. Experimental results from the cellular fractionation and reconstitution approaches further suggest that this Ca^{2+}-activated hTOP1 proteolysis occurs in the nucleus and that the nuclear membrane limits the access of cytosolic calpains to nuclear hTOP1 proteins. Interestingly, we have found that only calpain 2, but not calpain 1, enters the nucleus upon Ca^{2+} influx. This nucleocytoplasmic shuttling of proteases thus provides a novel regulatory mechanism for the calpain 2-mediated proteolysis of nuclear proteins. In agreement with this notion, nuclear hTOP2β and lamin A/C proteins also cleaved by calpain 2 upon 10 μM ionomycin treatment (appendix Fig. 1).

How is this calpain 2-mediated proteolysis of hTOP1 regulated? Recent studies suggest that calpain 2 might reside in or translocate into nucleus and then mediate the proteolysis of nuclear proteins. During Ca^{2+}-mediated degeneration of neuron, calpain-mediated changes in the nuclear pore permeability also cause an abnormal nuclear accumulation of large proteins (*109*). In our study, we found that both Ca^{2+} and calpastatin regulate the nucleocytoplasmic shuttling of calpain 2 and hTOP1 proteolysis. Calpain catalytic inhibitors only block Ca^{2+}-activated hTOP1 proteolysis but have no effect on the nuclear entry of calpain 2. Therefore, we reason that the ionomycin-induced nuclear entry of calpain 2 is most likely not due to calpain-mediated alterations in nuclear permeability. We have further described a novel regulatory mechanism in which calpastatin regulates calpain 2-mediated proteolysis of nuclear hTOP1, possibly by limiting the nuclear entry of proteases.

Calpains are known to mediate cellular functions through their ability to limitedly cleave substrates involved in different pathways (*42, 127-130*). However, the potential nuclear function(s) of calpains remains largely unknown. Here, we have found that ionomycin treatment, through calpain 2, stimulates proteolysis of hTOP1. In addition, calpain 2 also seems to contribute to the modest protection effect of ionomycin from the CPT-mediated cell killing. It has been reported that the N'-terminal domain plays a direct role in the DNA relaxation and binding ability of

hTOP1 (*125-126*, *131*). Consistent with this finding, our data show that N'-terminus, calpain 2-truncated hTOP1^{tr} exhibits greater DNA relaxation activity than intact hTOP1, while hTOP1tr still retains the ability forming CPT-DNA-hTOP1^{tr} cleavable complex (hTOP1^{tr}cc). How calpain 2 protects cells from CPT-induced cell killing remains complicated to explain. It is well documented that CPT-sensitivity is determined by several parameters in different cancer cells, and the formation and retention of cleavable complexes on DNA is the key sensitivity/resistance determinant (*132-133*). With regard to the formation and retention of cleavable complexes induced by CPT, our results have revealed that cellular levels of calpain 2 do not affect the levels of hTOP1 proteins. In addition, CPT induced a similar extent of hTOP1^{tr}cc and hTOP1cc formation (the concentrations trapping 50% of hTOP1 proteins in the form of cleavable complexes are ~ 3.0 and 3.2 μM for hTOP1cc and hTOP1^{tr}cc in HCT116 cells, respectively.). How calpain 2 proteins affect CPT sensitivity thus remains to be further investigated. In our limited screening using colorectal cancer cell lines, we have found that the basal level of calpain 2-truncated hTOP1^{tr} proteins is higher in HT29 cells and this cellular phenotype also correlates with an elevated level of nuclear calpain 2 staining in HT29 cells. Consistent with the notion that activated calpain 2 protects cells from CPT-mediated cell killing, we have observed that HT29 cells are more resistant to CPT-induced cell killing than two other colorectal cancer

cell lines. However, the calpain 2 abundance is decreased in the HT29 cells. This might be due to the following reasons: reduction in expression at the transcription and/or translation level, increased protein instability and higher activation level of calpain 2. Because HT29 cells also exhibit the highest endogenous cleavage level of hTOP1 by calpain 2 among three cell lines tested, we therefore suggested that the higher activation level of calpain 2 might contribute to the lower calpain 2 abundance in HT29 cells. Since CPT sensitivity is determined by many other parameters in different cancer cell lines and these three colorectal cancer cells are not isogenic, the relative contribution of calpain 2 in CPT sensitivity is therefore experimentally challenging to determine. Nevertheless, it is interesting to note that several recent reports have revealed a potential relationship between elevated calpain activity and poor prognosis in or advanced tumorigenic status of different types of cancer. For example, the calpain 2-mediated cleavage of the androgen receptor (AR) has been proposed as a mechanism for androgen independence in prostate cancer (*98*).

To the best of our knowledge, our study on the calpain 2-mediated hTOP1 proteolysis provides the first demonstration that calpain 2 can effectively cleave nuclear proteins through Ca^{2+}-activated nucleocytoplasmic shuttling of proteases. Notably, the Ca^{2+} concentrations (e.g., 5 mM) that we used in our *in vitro* study are much higher that the intracellular Ca^{2+} concentrations (nM to μM) and it is thus hard

to translate our in vitro findings into *in vivo* consequences. Nevertheless, considering the potential roles of calpain-mediated cellular destruction in various diseases with elevated intracellular Ca^{2+} levels (*75, 83, 91, 109, 134*), our discovery may have an important biological and/or clinical implication. It is thus reasonable to speculate that calpain 2-mediated proteolysis of nuclear proteins might also contribute to the pathological progress of diseases found to have altered Ca^{2+} homeostasis. In this regard, the fact that DNA topoisomerases exhibit essential cellular functions supports such a possibility.

Chapter 3 Calcium influx-induced proteolytic cleavage of topoisomerase 2β

3.1 Introduction

Change and regulation of DNA topology are necessary for a number of cellular processes, including chromosome segregation, DNA replication, transcription, recombination, and chromatin organization (*1-2*). Topoisomerases are isomerase enzymes that act on DNA to resolve these topological changes and are separated into two types by the number of strand-cut in one round of action (*2, 5, 135*). Type I enzymes act by forming a transient single-strand break (ssb) through which the other DNA strand passes to achieve relaxation; while type II, usually ATP and Mg^{2+}-dependent, is able to do so with the two strands that make up duplex DNA, creating a DNA-linked protein gate through which another intact duplex passes (*2-3*). In human, there are six topoisomerases including topoisomerase1 (hTOP1) (*136*), mitochondria topoisomerase I (mTOP1) (*137*), topoisomerases 3α (hTOP3α) (*36*) and 3β (hTOP3β) (*138*), which are type I, and topoisomerases 2α (hTOP2α) (*136*) and 2β (hTOP2β) (*24*), two isozymes belonging to type II. Both type I and type II enzymes are proficient in relaxing supercoiled DNA, while only TOP2 can decatenate intertwined DNA molecules *in vitro* (*1, 3*). Therefore, TOP2 is important for cellular survival, being required for segregation of daughter chromosomes at the end of DNA replication (*6, 25, 27*). Moreover, mice embryo lacking TOP2α gene fail to develop

revealing the TOP2α is essential for cell proliferation (*27*). In contrast, mammalian cell lines lacking TOP2β pass normally through mitosis (*26*), and their most prominent phenotype is a decreased sensitivity towards TOP2 poisons (*28-29*). Actually, Top2β$^{-/-}$ mice are not viable. They smother shortly after birth due to developmental defects of motor and sensory neurons and the brain suggesting TOP2β is required only for aspects of nerve growth and brain development (*30*). This implication has been recently confirmed by the findings that TOP2β plays an important role in the regulation of gene transcription, in as much as it introduces double-strand breaks at promoter regions of several genes, which are required for the proper signal-dependent activation of these genes (*31-33*).

Ca^{2+} homeostasis controls and manages many kinases and proteases relative to diverse cellular responses upon different stimulus (*45, 87, 139*). Moreover, the cytosolic free Ca^{2+} concentration ($[Ca^{2+}]$) is tightly regulated and maintained at approximately 100 nM against a large extracellular/intracellular gradient with the assistance of a series of channels, exchangers, and ion pumps (*140*). Here we hence used a Ca^{2+} ionophore, ionomycin, to trigger Ca^{2+} influx for a purpose to mimic the cellular microenvironment of elevated intracellular $[Ca^{2+}]$. Interestingly, hTOP2β was rapidly cleaved upon cellular exposure to ionomycin treatment. This proteolytic cleavage of hTOP2β requires the activation of calpains in the presence of Ca^{2+}-influx

suggesting hTOP2β is a novel substrate to calpains. In addition, the overexpression of natural calpain inhibitor calpastatin or calpain 2-targeting siRNA could dramatically abolish the Ca^{2+} influx –induced cleavage events of hTOP2β. Corresponding to the above statement, cells with knockdown of calpain 2 had more protein level of hTOP2β than si-vector control cells implying that calpains might regulate the stability of hTOP2β protein and therefore have a potential function to improve cell resistance to VP-16 (TOP2 poison) treatment. In this study we report hTOP2β is a novel nuclear substrate of calpains with the possible involvement of calpain 2.

3.2 Materials and Methods

3.2.1 Drugs, chemicals, reagents and cell cultures

1, 2-bis (*o*-amino-phenoxy) ethane-N, N, N', N'-tetraacetic acid (BAPTA) (*114*), caspase inhibitor VI, calpain inhibitor I (*115*), lactacystin (*116*), calpain 2 (rat, recombinant) (*117*) were purchased from Calbiochem. Other chemicals were obtained from Sigma. The HCT116 colorectal cancer cell line was a generous gift from Dr. L.F. Liu (Univ. Med. Den. NJ, USA). The SK-N-MC and SK-N-SH neuroblastic, AGS gastric, MCF7 breast, HT29 and SW480 colorectal cancer cell lines were from Drs. W-B Wang, F-L Kung, M-C Huang and J-T Wang (National Taiwan Univ. College of Med, NTUCM, Taiwan). The cells were grown in Dulbecco's modified Eagle's medium (DMEM) supplemented with 10% foetal bovine serum (FBS) at 37℃ and 5% CO_2 atmosphere.

3.2.2 Transfection and preparation of cell extracts

Cells were seeded on 35-mm dishes at a density of 2.5 X 10^5 cells in DMEM containing 10% FBS and then incubated at 37℃ for 24 hr. Transfection was performed by means of PolyJet™ *in vitro* transfection reagent (SignaGen®) or Lipofectamine plus (Invitrogen), followed by incubation at 37℃ for 24 hr. Cells were washed with 1XPBS twice before lysed with cold RIPA buffer (25-mM Tris-HCl pH 7.5, 150-mM NaCl, 1% NP-40, 1% sodium deoxycholate, 0.1% SDS) containing

protease inhibitors cocktail (Roche). Gather the lysate to one side using a cell scraper, collect the lysate and transfer to a microcentrifuge tube. Centrifuge samples at ~14,000 Xg for 15 minutes to pellet the cell debris. Transfer supernatant to a new tube for further analysis.

3.2.3 Immunoblotting analysis (Western blotting)

Samples were resolved by SDS–PAGE on 8% gels, and then transferred to NC membranes (Pall) at 330-mA for 2.5 hr at 4℃. The membranes were blocked with 5% non-fat milk in 1X TBS (Tris buffered saline, 50-mM Tris-HCl pH 7.4 and 150-mM NaCl) for 1 hr at room temperature. The membranes were then washed two times with 1X TBS and incubated with the primary antibody for 12 hr at 4℃. The membranes were then washed three times with 1X TBS containing 0.2% Tween 20 and then incubated with HRP (horseradish peroxidase) conjugated anti-rabbit or mouse IgG antibody for 1 hr at room temperature. The membranes were finally washed three times with 1X TBS containing 0.2% Tween 20, and then subjected to enhanced chemiluminescence detection (PerkinElmer Life Science). Antibodies for GAPDH were used as the internal loading standard.

3.2.4 Cellular fractionation assay

The isolation of nuclear and cytosolic extracts were performed as previously described (*141*). Briefly, HCT116 cells (~ 5 X 10^6) were pelleted and washed twice with 1X PBS. The cell pellet was then re-suspended in 200 μl of hypotonic buffer (10 -mM Tris-HCl pH 7.9, 140-mM KCl, 5-mM $MgCl_2$, and 1-mM DTT) and incubated on ice for 5 min. NP40 (0.25%) was added to the cell mixtures with an additional 3-min incubation and then followed with gentle taps to break down cellular membrane. The supernatant was collected as cytoplasmic extract after a 5-min centrifugation at 800 Xg with a microfuge (4^0C). The nucleus pellet was re-suspended with 1 ml of washing buffer (20-mM Tris-HCl pH 7.9, 140-mM KCl and 20% glycerol), span at 800 Xg for 5-min and collected as the fraction of intact nuclei. To prepare the nuclear extract, isolated nuclei were dissolved in 100 μl of nuclear extraction buffer (10-mM HEPES pH 7.5, 350-mM NaCl, 5-mM EDTA, 5-mM DTT) with 30-min gentle rotation. The nuclear mixture were then subjected to centrifugation at 12,000 Xg for 10 min and the supernatants were collected as nuclear extracts.

3.2.5 Immunofluorescence assay (IFA)

The immunofluorescence assay was performed as described (*141*) to determine the location of interested proteins. First, HCT116 cells were plated on cover slips (coated with FBS) a day before drug treatments. Drug-treated cells were washed with 1X PBS

and then fixed with 3% paraformaldehyde and 2% sucrose in PBS. After 10-min fixation at room temperature and three PBS washes, cells were permeated via an incubation in buffer A (20-mM HEPES, 50-mM NaCl, 3-mM $MgCl_2$, 300-mM sucrose and 0.5% Triton X-100) at room temperature for 10 min. Cover slips were washed with PBS, blocked in buffer B (5% FBS and 0.05% Tween-20 in PBS) for 3 hours and incubated with primary antibodies in buffer B for another 16 hours at 4^0C. After washing three times with PBS, cells were incubated with AlexaFluor488- or Rhodamine-conjugated secondary antibodies (Molecular Probe) in Hoechst 33342 (10 μM)-containing buffer B at 37^0C for an hour. After the PBS washes, cells were then mounted in Fluoromount-G (Douthern Biotechnology Associates). Images were captured with a TCS SP2 confocal microscope (Lecia) equipped with a CCD camera (Optronics) or an epi-fluorescence microscope (Nikon Eclipse 80i) with a CCD camera (Nikon DS-Ri1). Hoechst DNA staining was used to indicate the location of the nucleus.

3.2.6 Lentivirus-mediated small RNA interference (siRNA)

The lentivirus-packaged siRNA approach was employed to knock down expression of calpain 2 as described previously (details please also see chapter 2) (*141*) .

3.2.7 Colony formation assay

The clonogenic assay was performed as described (*119*) to examine the potential effect of downregulation of calpain 2 on the VP-16-induced cell killing. Sub-confluent cells were treated with or without 10 μM VP-16 for 30 min. After treatment, cells (4 to 8 X 10^2 per plate) were re-seeded onto 60-mm culture dishes with drug-free medium. Surviving cells were allowed to grow into colonies in a 5% CO_2 incubator at 37℃ for 12 days. Colonies were then stained with 0.03% crystal violet and 2% ethyl alcohol and scored.

3.3 Results

3.3.1 The ionomycin-promoted Ca^{2+} influx causes rapid and limited proteolytic cleavage of hTOP2β

Ionomycin (Ca^{2+} ionophore) has been used in research to raise the intracellular level of Ca^{2+} and as a research tool to understand Ca^{2+} transport across biological membranes or downstream effects of Ca^{2+} signaling (*123, 142-143*). Different human cancer cells were treated with ionomycin for a short incubation time (15 min.) to trigger Ca^{2+} influx. Surprisingly, we found the protein integrity of hTOP2β was differential lost in various cancer cells, but the truncated form of hTOP2β with MWs of ~160 KDa was also observed in all of treated cells (Fig. 27A). In addition, this Ca^{2+} ionophore-induced proteolysis of hTOP2β was dosage-dependent in both MCF7 breast and HCT116 colorectal cancer cells (Fig. 27B) suggesting the increasing intracellular [Ca^{2+}] contributes to the above proteolysis of hTOP2β.

3.3.2 The Ca^{2+} dependent proteolytic processing of hTOP2β

To further confirm the involvement of Ca^{2+}, we used two Ca^{2+} chelators, EGTA and the cell permeable BAPTA-AM. As shown in Figs. 27C and D, both EGTA and BAPTA-AM repressed the ionomycin-induced proteolysis of hTOP2β. Moreover, elevating extracellular [Ca^{2+}] by directly adding $CaCl_2$ in culture media also caused a

higher level of Ca^{2+}-influx-induced proteolysis of hTOP2β protein. Constantly, diminishing extracellular [Ca^{2+}] by replacing media with PBS buffer resulted in no hTOP2β proteolysis, providing further support for the direct role of Ca^{2+} in this limited and rapid proteolysis of hTOP2β.

3.3.3 The proteolytic cleavage of hTOP2β occurs in the nucleus whereas cytosolic proteases might be mainly responsible for the proteolysis on hTOP2β

In the next step, we sought to identify the protease(s) responsible for this Ca^{2+} -activated hTOP2β proteolysis. First, HCT116 cells exposed to ionomycin were collected and the cellular fractionation assay was performed to examine the integrity and location of hTOP2β protein. We showed that the proteolyzed hTOP2β proteins appeared within nucleus as shown in Fig. 28A. Second, the reconstitution with cellular fractionations was used to identify and localize the responsible protease(s). In Fig. 28B, we have found that there was the most efficient cleavage of Ca^{2+}-activated hTOP2β proteolysis when cytosolic (C) and nuclear extracts (N) were mixed together; suggesting the dominant protease(s) locates in the cytoplasm. However, the nuclear extracts alone in the presence of Ca^{2+} could still caused the minor cleavage of hTOP2β implying there might be protease(s) responsible for this proteolytic processing of hTOP2β in the nucleus. However, we could not totally rule out the

potential contamination of nuclear fractions with cytosolic protease(s) during the fractionation procedures. In addition, when nuclear extracts were combined with the Ca^{2+}-activated recombinant calpain 2, similar cleavage patterns of hTOP1 and hTOP2β were observed in Fig. 28C, suggesting that Ca^{2+}-dependent protease calpain 2 is involved in this processing of hTOP2β.

3.3.4 Ca^{2+} influx-activated calpains including calpain 2 participate in the cleavage of hTOP2β

It is believed that the calpain proteolytic system has more than one mechanism of activation depending on the cellular condition and autolysis (*58, 99, 144-145*). Several aspects on the activity regulation of calpains in relation to autolysis have been investigated, including the effect of autolysis on Ca2+ sensitivity (*146*), substrate specificity (*147*), subunits interaction and proteolytic activity (*59*). It is important to note that autolysis of calpains was observed in pathological conditions associated with aberrant rise in the concentration of intracellular Ca^{2+} ($[Ca^{2+}]_i$) (*70*). Therefore, we took advantage of immunoblotting assay with antibodies against the "conventional" calpains, calpain 1 and 2, to examine whether autolysis of calpain 1 or 2 had occurred or not during cellular exposure to ionomycin. As shown in Fig. 29A, the autolysis of calpain 1 was obviously observed compared with the control treatment. Moreover,

both intact calpain 1 and 2 were dosage-dependently decreased indicating that the Ca^{2+} influx-activated autolysis occurs on calpain 1 and 2. To further support this observation, cells with ectopic expression of the calpain 2 large subunit fused with HA-tag on its N-terminus were incubated in the absence or presence of ionomycin. We found that the autolysis of N-terminus of calpain 2 indeed occurred (Fig. 29C) when cellular exposure to ionomycin, therefore suggesting the ionomycin-induced Ca^{2+} influx causes activation of both calpain 1 and 2. As expected, the pre-treatment of calpain inhibitor I (CAPN Inh I) (Figs. 29B and C) or EGTA (Fig. 29C) before ionomycin treatment, reduced in the proteolytic level of hTOP2β and calpain 2 compared to that observed in the presence of ionomycin alone. In addition, the caspases and proteasome are likely not involved in this cleavage of hTOP2β, since the ionomycin-induced hTOP2β proteolysis was not affected by co-treatment of either the caspases inhibitor VI (CASP Inh VI) or proteasome inhibitor lactacystin (LAC) (Fig. 29B). Above results suggest that the most well-known Ca^{2+}-activated protease, calpains (possible, calpain 1 and 2), may play a critical role in the proteolytic processing of hTOP2β.

We have also examined whether ionomycin treatment induces proteolysis of other cellular proteins. We found that hTOP1, lamin A/C and p53 proteins were cleaved into visible smaller fragments upon exposure to ionomycin corresponding to

the previous reports they are substrates of calpains (Figs. 29C and D) (*128, 148*). Next, a genetic approach using RNA interference technology was employed to examine the involvement of calpain 2 in the Ca^{2+}-induced hTOP2β proteolysis. HCT116 cells were infected with lentiviruses expressing different small interference RNAs specifically targeting calpain 2 (si-Capn2 #43) and then incubated in the presence of puromycin to establish stable lines. As shown in Fig. 29D, the hTOP1, hTOP2β and p53 proteins were more resistant to the ionomycin-induced cleavage of in the si-Capn2 #43 cells compared with those in the si-Vector cells with the same treatment. Together, our results thus suggest that calpain 2 is one of the protease responsible for the Ca^{2+}-activated hTOP2β proteolysis.

3.3.5 Calpastatin, a natural calpain inhibitor, reduces Ca^{2+}-activated cleavage of hTOP2β

Moreover, calpastatin has been demonstrated an endogenous, protein inhibitor of calpains to inhibit their activation and catalytic activity by binding to them (*62-63, 102-103*). We thus transfected a plasmid expressing GFP-fused calpastatin into HCT116 cells and then examined its effects on the Ca2+-activated hTOP2β proteolysis. In agreeing with the inhibitory action on calpains in the previous reports, the calpain-mediated cleavage of hTOP2β was abolished by expression of calpastatin

further supporting that the hTOP2β protein is a novel substrate of calpains (Figs. 29E and F).

3.3.6 Ca^{2+} influx-induced nuclear translocation of hTOP2β and down regulation of protein level of hTOP2β by calpain 2 contributes to the cell survival to VP-16 treatment (TOP2 poison)

Interestingly, we also observed that the location of hTOP2β has changed in the presence of Ca^{2+} influx (Fig. 30A), which shows a nucleolus-accumulating pattern. Since calpain 2 has been demonstrated to be one of the protease responsible for the Ca^{2+}-influx activated cleavage of hTOP2β, we thus purposed a possibility that calpain 2 might also regulate protein stability of hTOP2β. Therefore, we examined the protein level of hTOP2β in two calpain 2-knockdown cell lines (HCT116 and HT29 cells). As shown in Figs. 29D and 30B, the intact protein level of hTOP2β was much more in si-Capn2 #43 cells compared to that in si-Vector cells in the absence of ionomycin suggesting the protein stability of hTOP2β may be regulated by calpain 2 *in vivo*. Corresponding to the above mention, the si-Vector cells were more resistant to VP-16 (TOP2 poison) mediated cell killing than si-Capn2 #43 cells (Fig. 30C) since mammalian cell lines lacking TOP2β with most prominent phenotype is a decreased sensitivity towards TOP2 poisons (*28-29*).

3.4 Discussions

Calpain is regarded as a bio-modulator, because the properties of the substrate proteins are often modulated upon hydrolysis by calpain (*149-151*). For example, treatment of protein kinase C with calpain produces an intact kinase domain that is active by itself indepentent of effectors such as diacylglycerol and Ca^{2+} (*150, 152*). Calpain 1 and calpain 2 are the two calpain proteases that have been extensively studied (*42*). They catalyze the proteolysis of proteins involved in various important biological functions, such as cytoskeletal remodeling, cell-cycle regulation, signal transduction, cell differentiation, apoptosis and necrosis, embryonic development, and vesicular trafficking (*42, 48, 153*). For this reason, calpain activity needs to be tightly regulated both temporarily and spatially in order to be effective and limited in various cellular stages (*42*). Here we first demonstrated that the hTOP2β is a nuclear substrate for Ca^{2+} influx -activated protease(s), calpains, since calpain 1and 2 have been showed to be cytoplasmic and nuclear shuttling proteins (*105, 141, 154-155*). From our downregulation of calpain 2 experiments, it is interesting to note that the reducing protein level of calpain 2 not only caused decreasing cleavage efficiency of hTOP2β but also reduced the autolysis level of calpain 1. Moreover, calpastatin, a natural calpain inhibitor, could abolish the Ca^{2+} influx-activated hTOP2β proteolysis.

In addition, the increasing protein level of hTOP2β in si-Capn2 #43 cells

compared with that in si-Vector cells suggests limited digestion of hTOP2β by calpain 2 may result in a more unstable truncated hTOP2β protein. The topoisomerase -targeting drugs have been used as anti-cancer drugs to stop the proliferation of malignant cells (*9, 16, 29*). Since the protein level of hTOP2β could be down-regulated by calpain 2 in culture cells, calpain 2 might therefore contribute to cell survival to VP-16 mediated cytotoxicity and our data support this hypothesis, further suggesting the calpain 2 is a potential target to be considered in cancer chemotherapy.

Cells maintain a ~2 X 10^4-fold gradient of Ca^{2+} between extracellular free Ca^{2+} (~1.2 mM) and resting cytoplasmic free Ca^{2+} (~100 nM). Depending upon the stimulus, the intracellular [Ca^{2+}] can exceed more than 1 μM (*156-157*). The spatio-temporal nature of changes in the free Ca^{2+} might be involved in cancer initiation, tumor formation, tumor progression, metastasis, invasion and angiogenesis (*156-158*). In our experiments to mimic the microenvironment of elevating intracellular [Ca^{2+}] by the ionomycin-induced Ca^{2+} influx, the location and protein integrity of hTOP2β are both modulated implicating a possibility of Ca^{2+} mediated transcription of hTOP2β by Ca^{2+} itself or Ca^{2+}-activated calpains, since theTOP2β has been proved to have an important role in the regulation of gene transcription.

4. Figures

DNA topoisomerase	Type	Structure	M.W. (KDa)	DNA cleavage	Gene localization (Human chromosome)	Function
I	IB	Monomer	100	ssb	20	Replication, transcription, recombination
I (mitochondria)	IB	Monomer	72	ssb	8	Replication, transcription (mitochondria)
IIIα	IA	2 isoforms (alternative solicing)	110	ssb	17	Recombination, rDNA metabolism
IIIβ	IA	3 isoforms (alternsative Splicing)	96	ssb	22	Recombination
IIα	II	Homodimer	170	dsb	17	Condensation and segregation of chromosome, replication
IIβ	II	Homodimer	180	dsb	3	Transcription

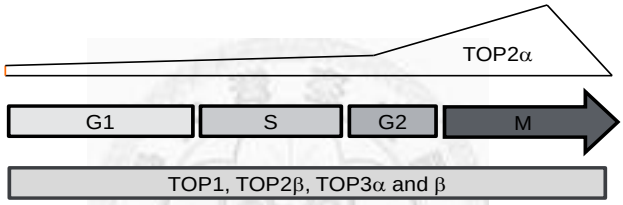

(Adapted from Mutation Research, 2003, Vol. 543, P.59)

Fig. 1 Human DNA topoisomerases and their expression throughout the cell cycle.

At least 6 topoisomerases have been discovered in human. Type I enzymes (topoisomerase 1,mitochondrial topoisomerase 1, 3α and 3β) act by forming a transient single-strand break (ssb) in DNA to achieve relaxation of the supercoiled molecule before resealing, while type II topoisomerases (topoisomerase 2α and 2β) form double-strand breaks (dsb) to facilitate unknotting or decatenation of entangled DNA molecules. Levels of topoisomerase 2α mRNA increase in late S and G2/M, whereas other topoisomerases are expressed constitutively in a less cycle-dependent manner.

Human calpain genes							
	Gene	Other names	Tissue distribution	Gene localization	Amino acid residues	Protease activity	Association with 30K
Calpain large catalytic subunit							
Calpain 1	*CAPN1*	μ-calpain large subunit	Ubiquitous	11q12-13.1	714	+	+
Calpain 2	*CAPN2*	m-calpain large subunit	Ubiquitous	1q32-41	700	+	+
Calpain 3	*CAPN3*	P94, nCL-1	Skeletal muscle	15q15	821	+	_
Calpain 5	*CAPN5*	hTRA-3, nCL-3	Ubiquitous	11q14	640	+	_
Calpain 6	*CAPN6*	CANPX	Placenta, embryonic muscles	Xq23	641	_	_
Calpain 7	*CAPN7*	PalBH	Ubiquitous	3p24	813	+	_
Calpain 8	*CAPN8*	nCL-2	Stomach	1q32-41	703	+	_
Calpain 9	*CAPN9*	nCL-4	Digestive tract	1q42.1-43	690	+	+
Calpain 10	*CAPN10*	__	Ubiquitous	2q37.3	672	ND	ND
Calpain 11	*CAPN11*	__	Testis	6p12	702	ND	ND
Calpain 12	*CAPN12*	__	Hair follicle	19q13	720	ND	ND
Calpain 13	*CAPN13*	__	Ubiquitous	2p21-22	423	ND	ND
Calpain 14	*CAPN14*	__	ND	2p21-22	?	ND	ND
Calpain 15	*SOLH*	SOLH	Ubiquitous	16p13.3	1086	ND	ND
Calpain small regulatory subunit, 30K							
CAPNS1	*CAPNS1*		Ubiquitous	19q13	268	_	+
CAPNS2	*CAPNS2*		Ubiquitous	16q13	248	_	+

(Adapted from Diabetes, 2004, Vol. 53, SUPPLEMENT 1)

Fig. 2 Human calpain family members.

At present, 14 human genes have been identified as members of the calpain large catalytic subunit family, together with two genes for small regulatory subunit (30K). As shown in this figure, their gene products are also summarized and characterized.

Examples of pathogenic conditions that have been associated with calpains	
Diseases	Observations
Limb-girdle muscular dystrophy type 2A	This disease is associated with mutations in the gene encoding calpain 3 (*CAPN3*) and probable loss of calpain 3 proteolytic activity.
Gastric cancer	This type of cancer is associated with down-regulation of *CAPN9*.
Type 2 diabetes mellitus	Mutations in intron 3 of *CAPN10* are associated with an increased incidence of type 2 diabetes in some populations.
Duchenne's and Becker's muscular dystrophies	These dystrophies are associated with the absence or deficiency of dystrophin, a membrane-associated protein, resulting in an increased Ca^{2+} level in muscle, loss of Ca^{2+} homeostasis, and inappropriate calpain activities.
Alzheimer's disease	There is an increased amount of calpain 2 in the cytosolic but not the membranous fraction of the brain and in the neurofibrillary tangles of the brain.
Cataract formation	Ca^{2+} influx activates calpain 2, the predominant calpain in the lens, cleaving α- and β–crystallins but not γ-crystallins; the crystallin fragments aggregate to form cataracts.
Myocardial infarction	Ca^{2+} homeostasis is lost in ischemic areas, triggering inappropriate calpain activities; desmin and α-spectrin are degraded in ischemic heart; protein and mRNA levels of calpain 1 and 2 increase after myocardial infarction.
Multiple sclerosis	Levels of the 150-kD calpain-specific degradation product of α-spectrin increase 50% in human multiple sclerosis plaques; degradation of the 68-kD neurofilament protein is inhibited by a synthetic calpain inhibitor.
Obsessive–compulsive disorder	Erythrocytes from patients with obsessive–compulsive disorder have significantly higher calpain activities than normal controls, a finding that could not be attributed to differences in memory function.
Neuronal ischemia (stroke)	Calpastatin is degraded by calpain to a membrane-bound 50-kD polypeptide in ischemic brain tissue; calpains participate in both apoptosis and necrosis in tissue damage in ischemic areas.

(Adapted from the New England Journal of Medicine, 2005, Vol.352, P.2413)

Fig. 3 Calpains associated diseases

A number of pathologic conditions have been associatedwith disturbances of the calpain system. They include type 2 diabetes, cataracts, Duchenne's muscular dystrophy, Parkinson's disease, Alzheimer's disease, rheumatoid arthritis, ischemia, stroke and brain trauma, various platelet syndromes, hypertension, liver dysfunction, and some types of cancer.

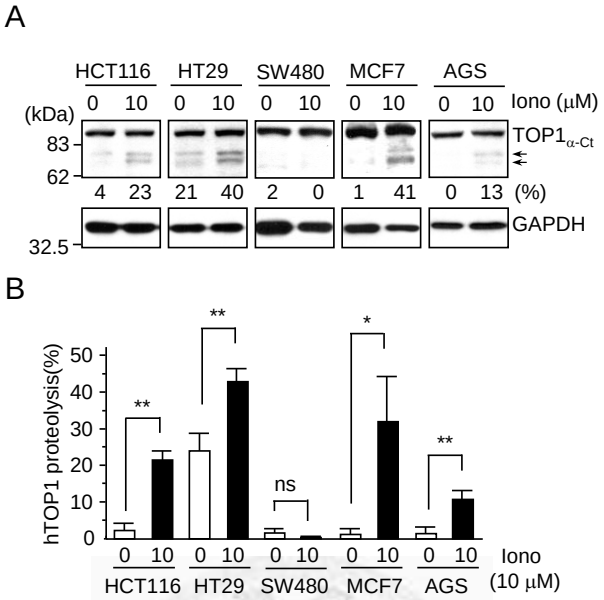

Fig. 4 Ionomycin-induced cleavage of hTOP1.

(A) Cellular exposure to ionomycin resulted in the cleavage of hTOP1 proteins in various cell lines. Colorectal cancer cell lines (HCT116, SW480 and HT29), breast cancer cell line (MCF7) and gastric cancer cell line (AGS) were treated with ionomycin (Iono, 10 μM) for 15 min. The harvested cell lysates were displayed on 8% SDS-PAGE, and immunoblotting was performed to detect hTOP1 with antibodies against the C-terminus of TOP1 ($TOP1_{\alpha\text{-}Ct}$). GAPDH serves as a protein loading control. (B) Ionomycin-induced proteolysis of hTOP1 was quantified from three independent experiments. Arrows indicate the truncated hTOP1 fragments. **, $P < 0.01$; *, $P < 0.05$; ns, statistically non-significant

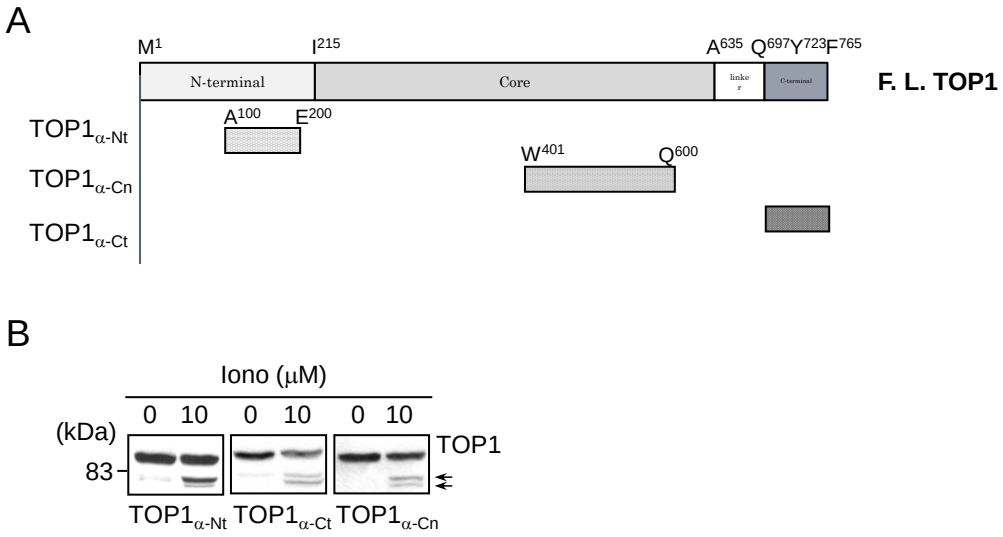

Fig. 5 Detection of truncated hTOP1 with antibodies against different epitopes.

(A) Domains of full length of hTOP1 and its correspondent sequences recognized by antibodies against hTOP1. (B) The proteolysis of hTOP1 induced by ionomycin is likely caused by the protease-mediated cleavage at the N'-terminus. Cell lysates harvested from 10 μM ionomycin treated HCT116 cells were resolved by 8% SDS-PAGE and immunoblotted with antibodies against the central domain, N-terminus and C-terminus of hTOP1 (named $TOP1_{\alpha\text{-Cn}}$, $TOP1_{\alpha\text{-Nt}}$ and $TOP1_{\alpha\text{-Ct}}$, respectively) used for the epitope-mapping of potential proteolytic sites on hTOP1. Arrows indicate the truncated hTOP1 fragments.

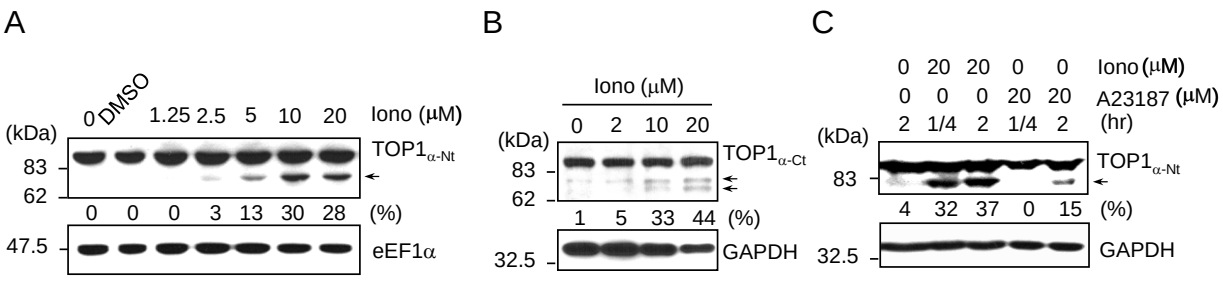

Fig. 6 Ca^{2+} ionophores induced cleavage of hTOP1 in dosage and time course dependent manners.

HCT116 cells were treated with ionomycin (doses as indicated) for 15 min. and then subjected to perform immunoblotting analysis with $TOP1_{\alpha\text{-Nt}}$ (A) and $TOP1_{\alpha\text{-Ct}}$ (B) antibodies. (C) Cell lysates collected from HCT116 cells treated with ionomycin (20 μM) and A23187 (20 μM) for 15 min. or 2 hr were analyzed by immunoblotting with $TOP1_{\alpha\text{-Nt}}$ antibodies. eEF1α and GAPDH are as the loading control. Arrows indicate the truncated hTOP1 fragments.

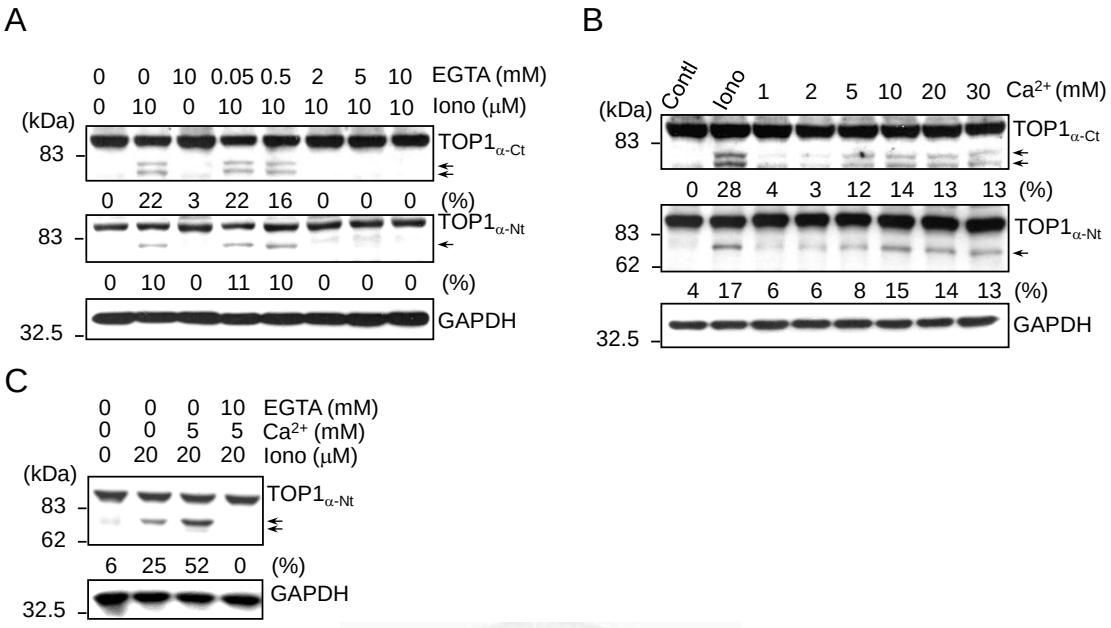

Fig. 7 Ca^{2+} influx mediated proteolytic processing of hTOP1.

(A) HCT116 cells were pre-treated with EGTA for 30 min and then underwent co-treatment with ionomycin for 15 min. (B) Different concentrations of Ca^{2+} (as indicated in figure) were add directly into the media and HCT116 cells were further incubated for 15 min. (C) HCT116 cells were treated with different combinations of 5-mM Ca^{2+}, 10-mM EGTA (pre-treatment for 30 min.) and 20-μM ionomycin for 15 min. Above cells were lysed, and immunoblotting analyses were carried out. Arrows indicate the truncated hTOP1 fragments.

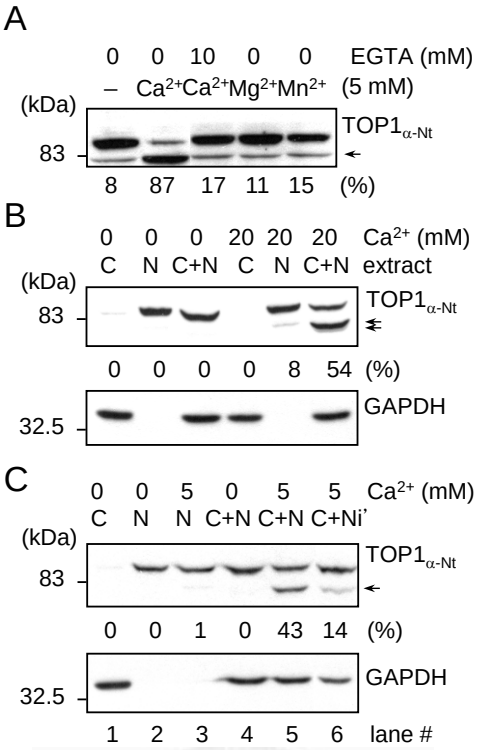

Fig. 8 Cytosolic extracts have the most proteolytic activity on hTOP1.

(A) HCT116 cells were lysed with calpain activation buffer and then performed *In vitro* protease activation assay using total extracts in the absence or presence of different divalent cations (5 mM) as described in Materials and Methods. (B) Cellular fractionations isolated from HCT116 cells were used to reconstitute *in vitro* proteolysis of hTOP1 as described in Materials and Methods. (C) The Ca^{2+}-activated hTOP1 proteolytic reaction was reconstituted by various combinations of cytosolic extract (C), nuclear extract (N) and isolated nuclei (Ni') as described in Materials and Methods. Ca^{2+} (5 mM) was added to activate the protease(s). After incubation at room temperature for 10 min, the mixtures were subjected to immunoblotting analysis with $hTOP1_{\alpha\text{-Nt}}$ antibodies. Arrows indicate the truncated hTOP1 fragments.

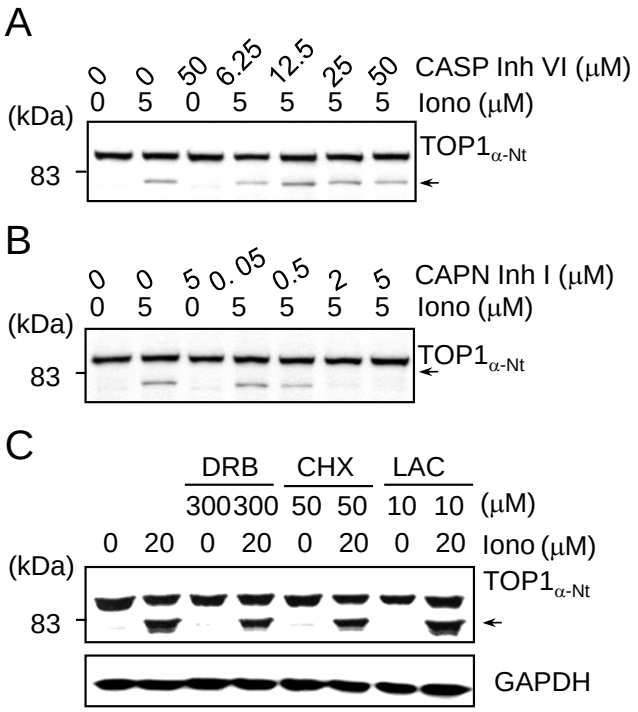

Fig. 9 Only calpains but not caspases, proteasome or *de-novo* synthesized proteases involve in Ca^{2+} influx mediated cleavage of hTOP1.

HCT116 cells were individually pretreated with caspase inhibitor VI (CASP Inh VI) (A), calpain inhibitor I (CAPN Inh I) (B), 5,6-dichloro-1-β-d-ribofuranosyl benzimidazole (DRB), cycloheximide (CHX) or lactacystin (LAC) (C) for 30 min. before ionomycin treatment for one another 15-min. incubation. Immunoblotting assay was performed to detect the proteolytic processing of hTOP1. Arrows indicate the truncated hTOP1 fragments.

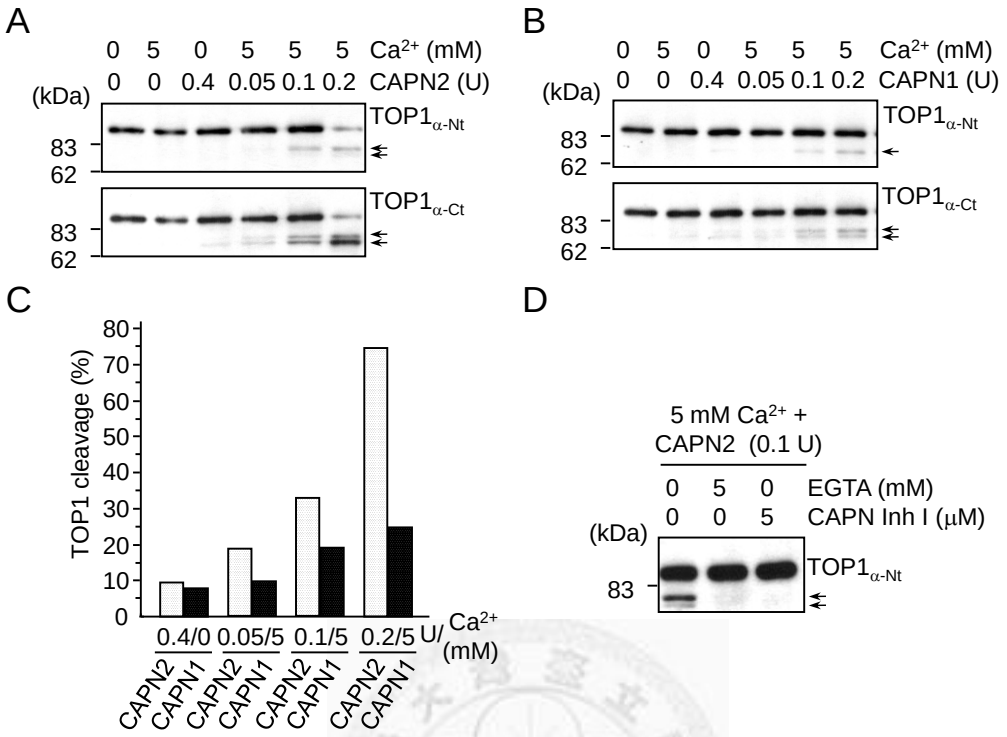

Fig. 10 Calpain 2 has better proteolytic activity than calpain 1 on hTOP1.

(A-B) Purified calpains (human CAPN1 or rat CAPN2, at indicated units) with or without Ca^{2+} (5 mM) were mixed with recombinant hTOP1 (0.05 μg) and incubated for 10 min at room temperature; then, reactions were stopped using sample buffer. The quantitative data has been plotted in (C). (D) Both Ca^{2+}-chelating EGTA and calpain inhibitor I efficiently blocked *in vitro* proteolysis of hTOP1 mediated by the Ca^{2+}-activated recombinant calpain 2. Arrows indicate the truncated hTOP1 fragments.

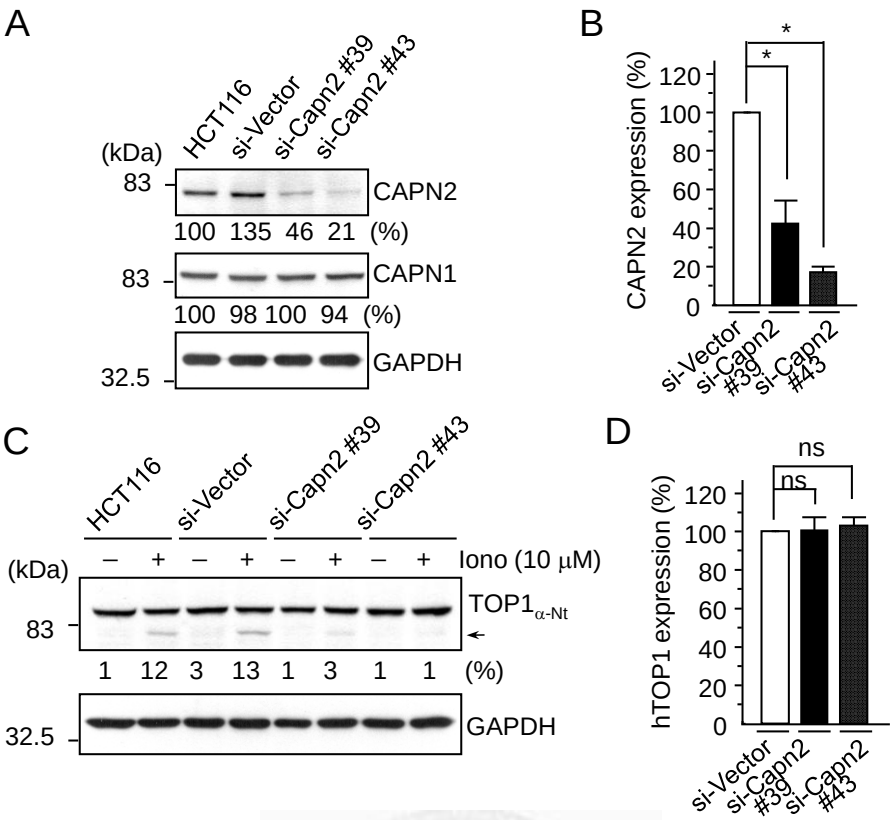

Fig. 11 Knockdown of calpain 2 represses cleavage of hTOP1.

(A) HCT116 cells were infected with lentivirus that carried sequences of si-calpain 2. After proper selection, pooled clones of calpain 2-deficient cell lines were established. The knockdown efficiency and specificity values for these two clones (HCT116 si-Capn2 #39 and #43) are shown in (A-B) (B, n=3). (C) Ionomycin-induced hTOP1 proteolysis was then performed with two knockdown clones and HCT116 si-Vector cells as described. (D) The expression levels of hTOP1 are not altered in two si-Capn2 cell lines (n = 3). Arrows indicate the truncated hTOP1 fragments. *, $P < 0.05$; ns, statistically non-significant

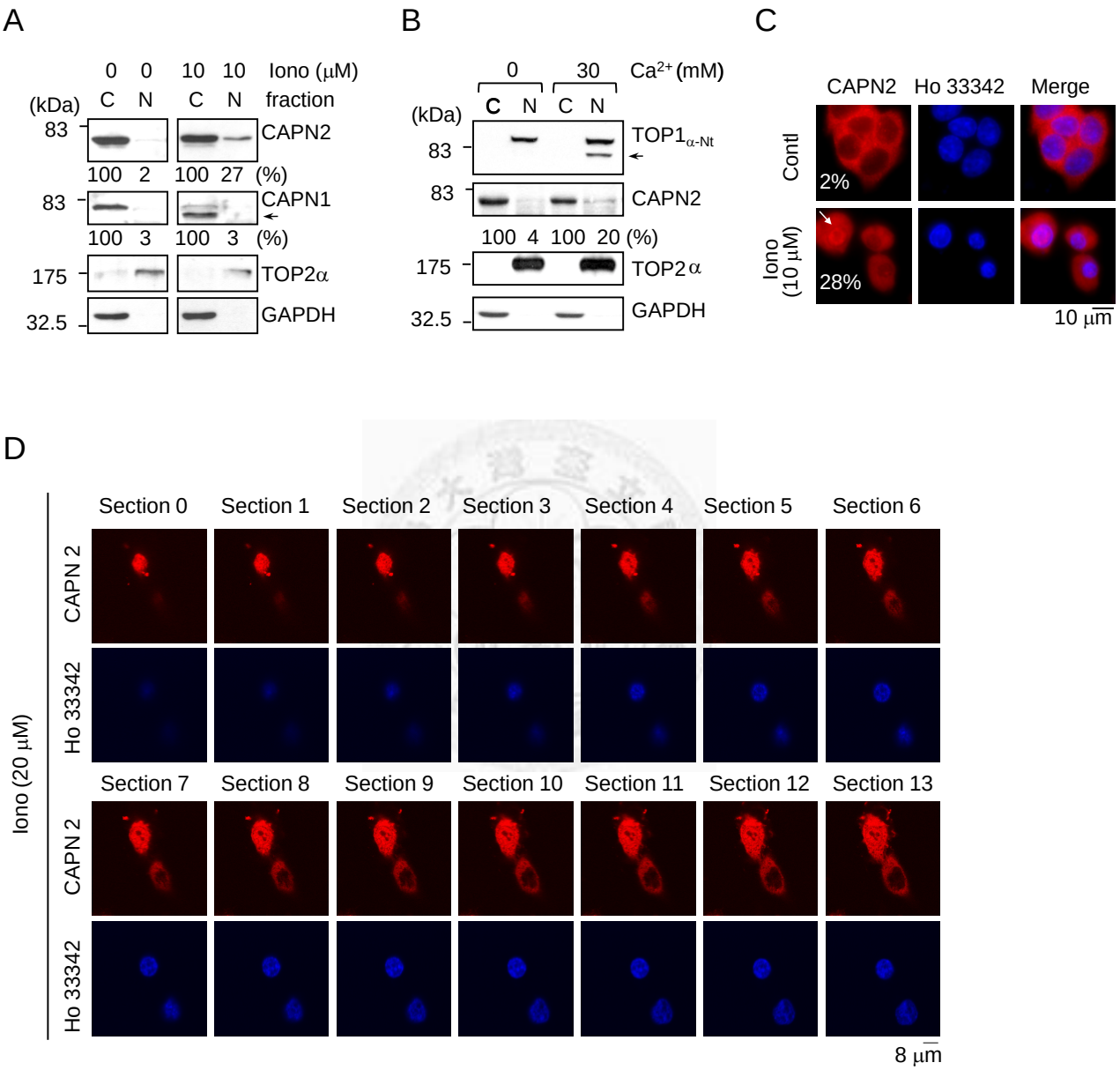
A
0 0 10 10 Iono (μM)
(kDa) C N C N fraction
83
CAPN2
100 2 100 27 (%)
83
CAPN1
100 3 100 3 (%)
175
TOP2α
32.5
GAPDH
B
0 30 Ca2+ (mM)
(kDa) C N C N
83
TOP1α-Nt
83
CAPN2
100 4 100 20 (%)
175
TOP2α
32.5
GAPDH
C
CAPN2 Ho 33342 Merge
Contl
2%
Iono (10 μM)
28%
10 μm
D
Iono (20 μM)
Section 0 Section 1 Section 2 Section 3 Section 4 Section 5 Section 6
CAPN 2
Ho 33342
Section 7 Section 8 Section 9 Section 10 Section 11 Section 12 Section 13
CAPN 2
Ho 33342
8 μm

Fig. 12 Ca^{2+} influx triggers the nuclear translocation of calpain 2.

(A-B) Fractionation experiments were performed with HCT116 cells treated with or without ionomycin (10 μM, 15 min.) and with or without Ca^{2+} (30 mM, 30 min.). Cytosolic and nuclear extracts were then analyzed by immunoblotting analysis using anti-calpain 1, 2 and $TOP1_{\alpha\text{-Nt}}$ antibodies. GAPDH and hTOP2α were used as cytosolic and nuclear markers, respectively. For immuno-fluorescent analysis (IFA), HCT116 cells were first seeded onto cover-slips for 24 hours before ionomycin treatment (10 μM for 15 min.). Cells were fixed with paraformaldehyde, permeabilized with Triton X-100 and stained for calpain 2 and DNA as described in Materials and Methods. Cellular DNA was stained with Hoechst 33342. (C) Approximate 50~100 cells were counted under fluorescence microscopy and scored as the percentages of cells with positive nuclear staining (%) were indicated. (D) HCT116 Cells were treated with ionomycin (20 μM, 15 min.) and subjected to perform IFA by confocal microscopy described in Materials and Methods. 14 sections were collected. Nuclear location was indicated by Hoechst 33342 staining. Arrows indicate the fragments of truncated calpain 1 and hTOP1. White arrows indicate the cells with nuclear staining of calpain 2.

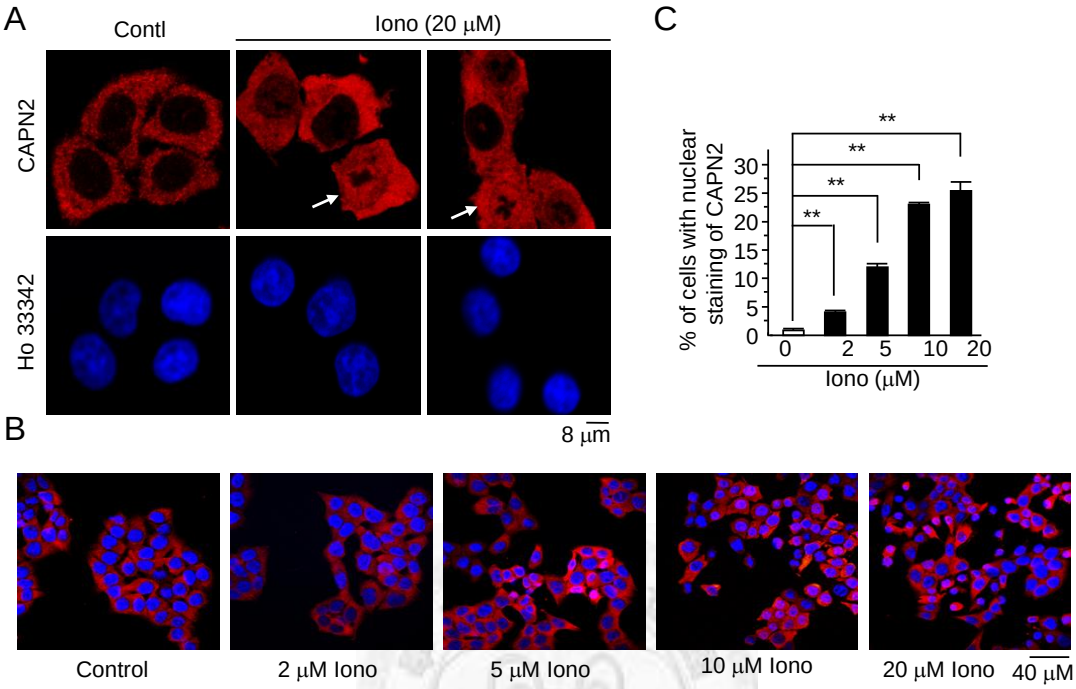

Fig. 13 Ca^{2+} ionophore mediated nuclear translocation of calpain 2 in a dosage dependent manner.

(A) HCT116 cells were treated with or without ionomycin (20 μM, 15 min.) and IFA were carried out to detect the nuclear entry of calpain 2 by a confocal microscope. (B) HCT116 cells exposures to different doses of ionomycin (15min.) were analyzed with IFA and observed under confocal microscopy. (C) Quantitative results for the dosage dependence of ionomycin-induced nuclear entry of calpain 2 (n = 3). White arrows indicate the cells with nuclear staining of calpain 2. **, $P < 0.01$

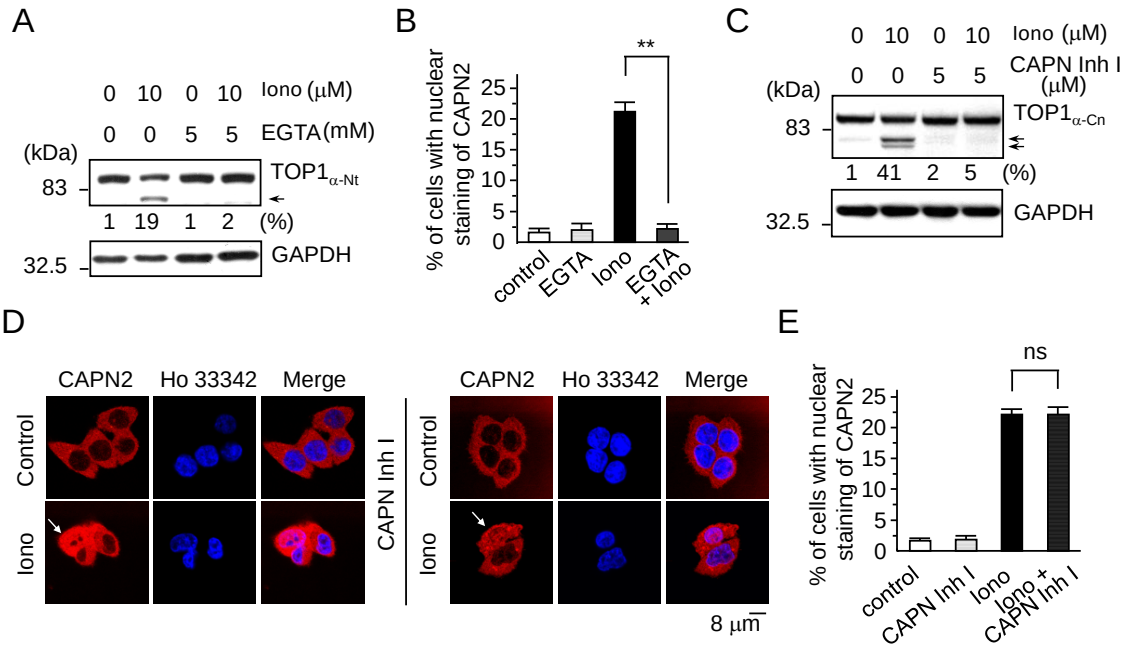

Fig. 14 Only EGTA not calpain inhibitor I could abolish nuclear shuttling of calpain 2.

(A) HCT116 cells were pretreated with EGTA (5 mM, 30 min.) and added ionomycin (10 μM) for another 15-min. incubation. Cells were collected to be analyzed with immunoblotting using $TOP1_{\alpha\text{-Nt}}$ antibodies or performed IFA as described in Materials and Methods. (B) Quantitative results for inhibition of EGTA on ionomycin-induced nuclear entry of calpain 2 (n = 3). (C) HCT116 cells upon calpain inhibitor I (CAPN Inh I, 5 μM) treatment for 30 min. were co-treated with ionomycin (10 μM, 15 min.). After treatment, immunoblotting analysis and IFA were performed to detect the Ca^{2+}-mediated truncated hTOP1 and monitor the translocation of calpain 2 (D), respectively. The nuclear entry of calpain 2 was examined as described in Materials and Methods and quantitative results were shown (E). Arrows indicate the fragments

of truncated hTOP1. White arrows indicate for the cells with nuclear staining of calpain 2. **, $P < 0.01$; ns, statistically non-significant

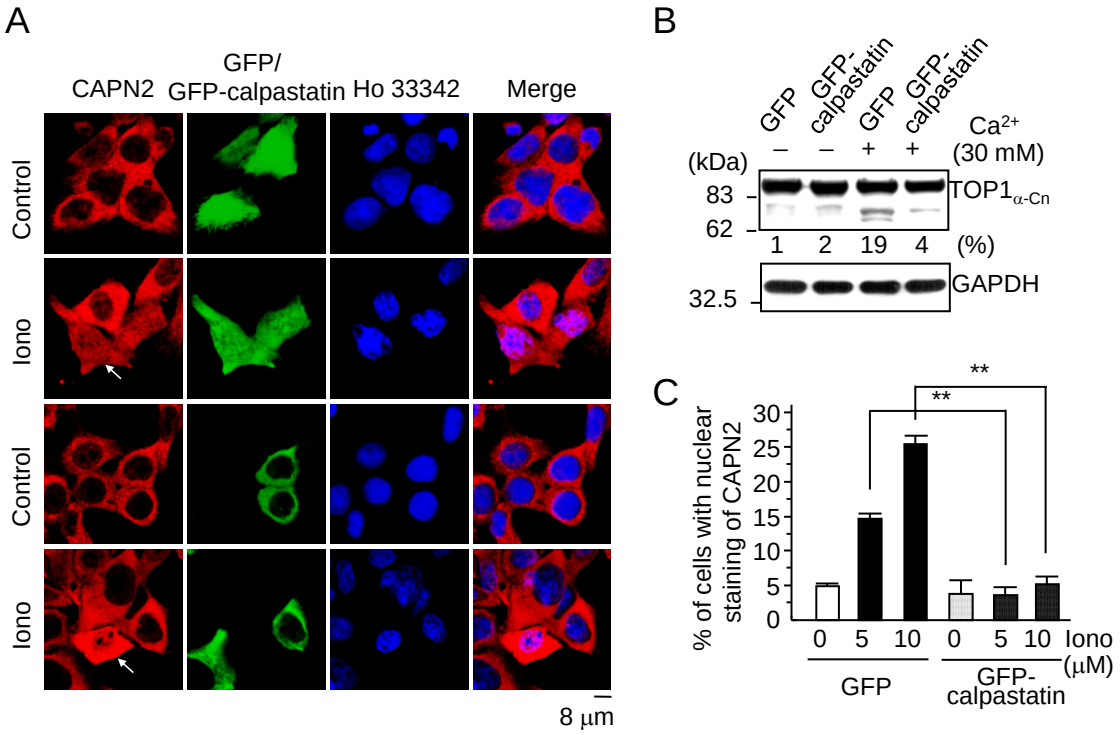

Fig. 15 Forced expression of calpastatin reduces cleavage of hTOP1 and nuclear accumulations of calpain 2.

(A) HCT116 cells were transfected with either a control vector or the GFP-calpastatin fusion-expressing construct. After 48 hours, IFA was used to examine the cells with nuclear staining of calpain 2. (B) After 48 hr post transfection as above, the cells were harvested and displayed on 8% SDS-PAGE for immunoblotting with $TOP1_{\alpha\text{-Cn}}$ antibodies. (C) Quantitative analysis of the effect of calpastatin expression on ionomycin-induced nuclear entry of calpain 2 (n = 3). Columns represent percentages of nuclei containing calpain 2 in GFP-positive cells. Arrows indicate the fragments of truncated hTOP1. White arrows indicate the cells with nuclear staining of calpain 2. **, $P < 0.01$; ns, statistically non-significant

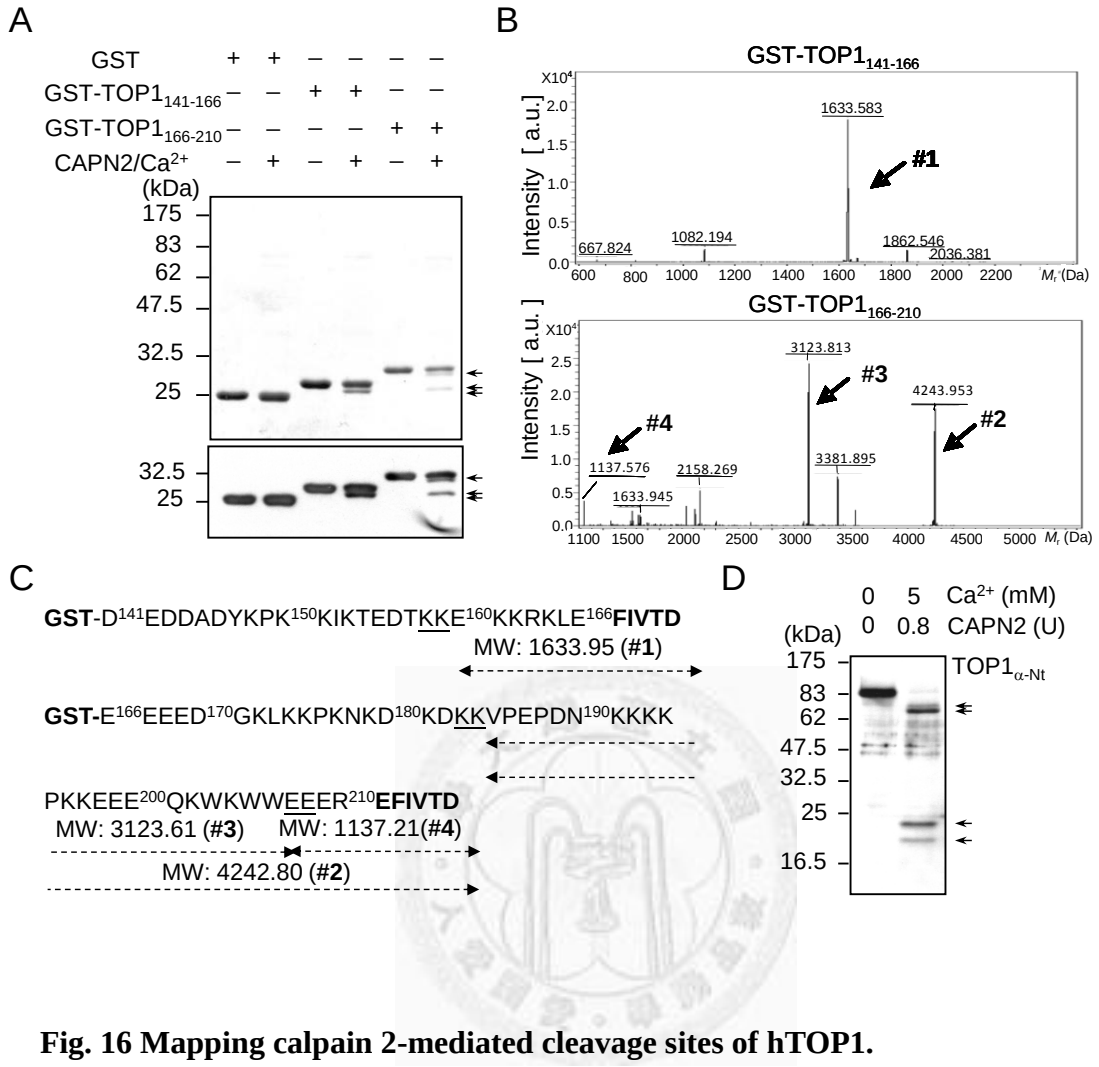

Fig. 16 Mapping calpain 2-mediated cleavage sites of hTOP1.

(A) Two GST-fused hTOP1 fragments, GST-TOP1$_{141\text{-}166}$ and GST-TOP1$_{166\text{-}210}$ proteins (with amino acid 141-to-166 and 166-to-210 of hTOP1, respectively), were expressed and purified from bacteria. The calpain 2 proteolytic reactions were performed with these two GST-fused tagged hTOP1 fragments and the reaction mixtures were then subjected to SDS-PAGE separation (A, upper panel; stained with coomassie blue), immunoblotting analysis with anti-GST antibodies (A, lower panel) and MALDI-TOF/MS analysis (B). The calpain 2-truncated products, the intact and

truncated GST-containing hTOP1 fragments in the reaction mixtures were loaded into Microcon YM-10 columns. The flow-through parts were collected for molecular weight determination by MALDI-TOF mass spectrometry analysis. The molecular masses determined for the calpain 2-cleaved hTOP1 short fragments in the flow-through are shown underlined on the top of the peaks (B, units = Da). (C) Schematic mapping containing hTOP1 amino acid sequences of GST-TOP1$_{141-166}$ and GST-TOP1$_{166-210}$ peptides and the theoretical molecular masses for the calpain 2-cleaved fragments (arrows #1-4 shown in B). The non-hTOP1-derived amino acids FIVTD and EFIVTD (in bold) are encoded from the backbone of the pGEX-1λ-T vector after cloning, and the two calpain 2 cleavage sites in hTOP1 are underlined. (D) After the *in vitro* calpain 2 cleavage of hTOP1, the reaction mixtures were subjected to immunoblotting analysis. Arrows indicate the cleaved hTOP1 fragments. MW, molecular weight; a.u., arbitrary units.

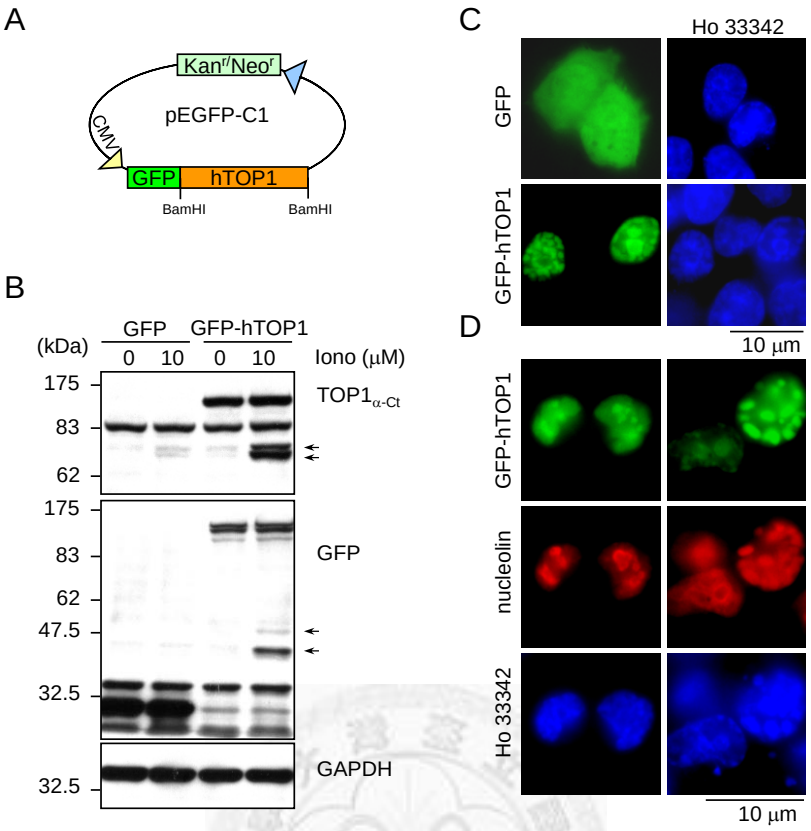

Fig. 17 Construction of GFP-hTOP1 and its expression in HCT116 cells.

(A) Construction of GFP-fused hTOP1 expressing plasmid through ligation PCR products of hTOP1into BamHI cutting site. (B) HCT116 cells were transfected with GFP fusion of hTOP1 expressing plasmid and control vector. At 36 hr post transfection, cells were treated with ionomycin (10μM, 15 min.) before lysing cell and immunoblotting was used to dissect the fragments of truncated hTOP1 with anti-GFP and $TOP1_{\alpha\text{-}Ct}$ antibodies. (C-D) The transfected HCT116 cells were collected and IFA was performed using anti-nucleolin antibodies under fluorescent microscopy. Cellular DNA was stained by Hoechst 33342. Arrows indicate the truncated hTOP1 fragments.

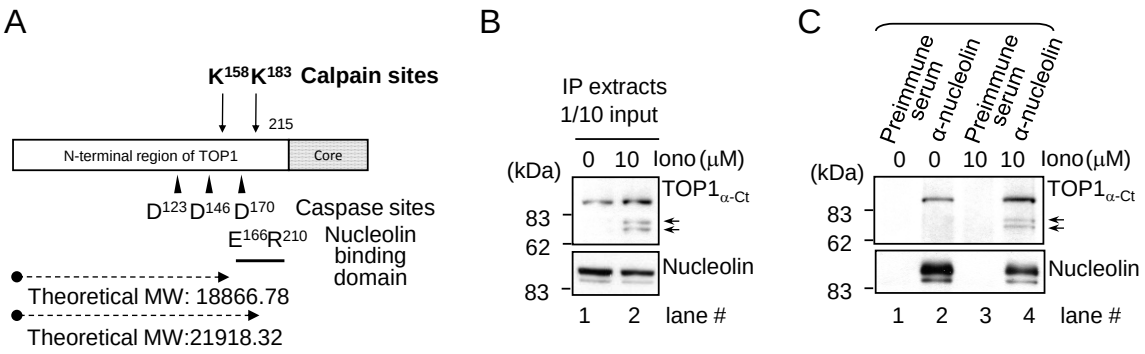

Fig.18 Nucleolin interacts with two N-terminal truncated forms of hTOP1.

(A) The two calpain 2 cleavage sites (K^{158} and K^{183}) mapped in this study and three caspase cleavage sites (D^{123}, D^{146} and D^{170}) are indicated by the arrows and arrowheads, respectively. The nucleolin-binding domain (E^{166} to R^{210}) of hTOP1 is also presented. (B) Full-length hTOP1 and calpain 2-truncated $hTOP1^{tr}$ both interacted with nucleolin. Ionomycin-treated or control HCT116 cell lysates were subjected to the immune-precipitation (IP) assay using antibodies against nucleolin as described in Materials and methods. MW, molecular weight; arrows indicate the truncated hTOP1 fragments.

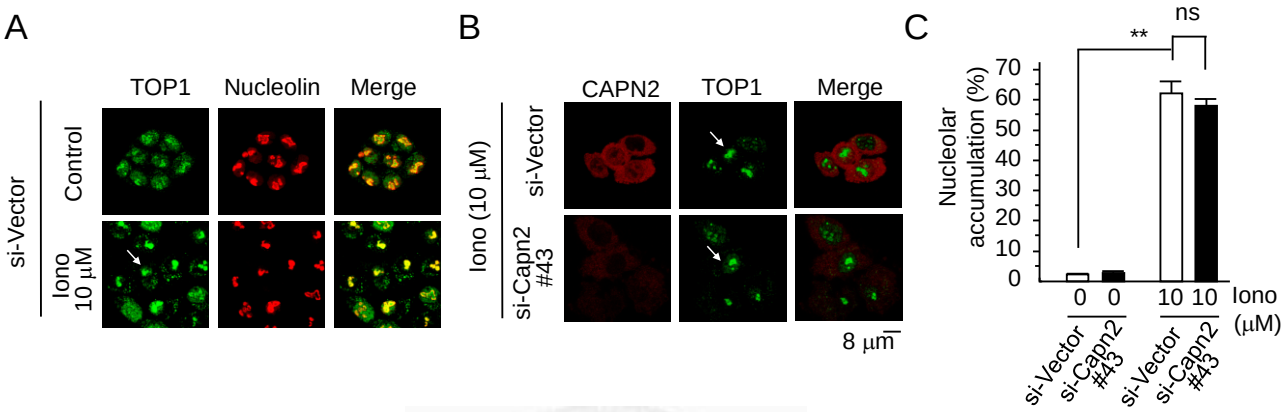

Fig.19 Ca^{2+} influx mediated nucleolar accumulations of hTOP1 is independent of calpain 2.

(A) HCT116 (si-Vector) cells treated with or without ionomycin (10 μM, 15 min.) were subjected to IFA using anti-nucleolin and $TOP1_{\alpha\text{-}Cn}$ antibodies. (B) HCT116 (si-Vector and si-Capn2 #43) cells upon ionomycin treatment (10 μM, 15 min.) were collected and IFA was carried out with anti-calpain 2 and $TOP1_{\alpha\text{-}Cn}$ antibodies under confocal microscopy. (C) The representative nucleolar accumulation of hTOP1 was calculated and scored (n=3) by a confocal microscope. White arrows indicate the cells with nucleolar accumulation of hTOP1. **, $P < 0.01$; ns, statistically non-significant

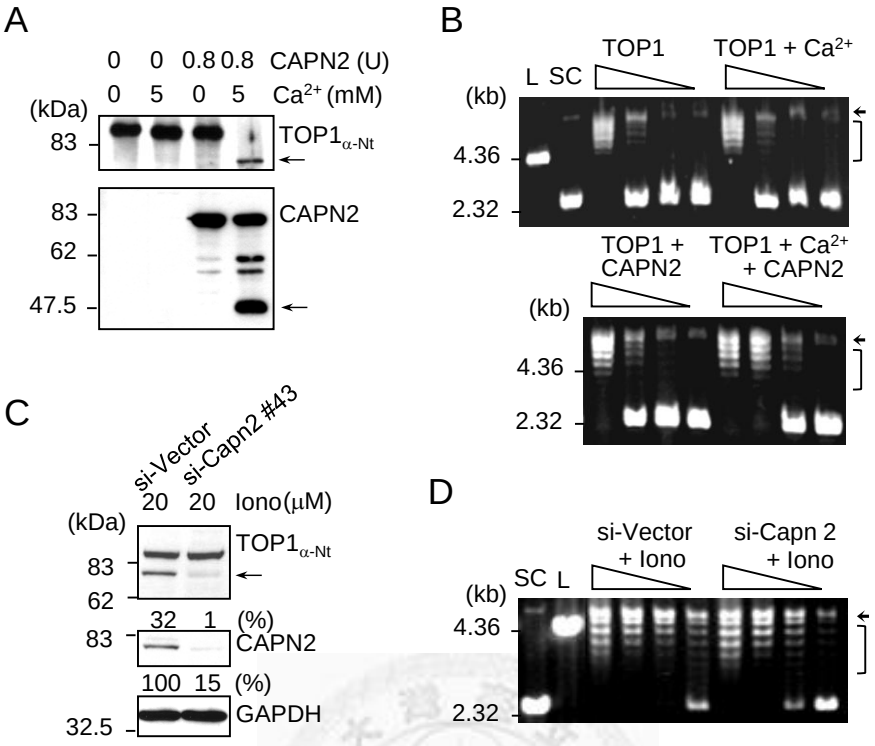

Fig. 20 N-terminal truncated hTOP1 has better supercoiling activity than full length of hTOP1.

(A) Equal amounts of purified hTOP1 proteins were mixed with Ca^{2+} and/or calpain 2 and the reaction mixtures were incubated for 10 min at room temperature. One half of mixtures were resolved in 8% SDS-PAGE and subjected to immunoblotting analysis with anti-calpain 2 and $TOP1_{\alpha\text{-Nt}}$ antibodies. The other mixtures were taken for relaxation assay. (B) The relative relaxation activities of reaction mixtures were determined with a 2-fold serial dilution as described in Materials and Methods. (C-D) HCT116 si-Capn2 #43 and si-Vector cells were treated with 20-μM ionomycin for 15 min, lysed and collected for the immunoblotting analysis (C) and relaxation assay (D).

Arrows, truncated hTOP1 or calpain 2 fragments (A and C); arrow heads, nick-from DNA (B and D); L, linearized DNA; SC, supercoiled DNA; Bracket, DNA topoisomers

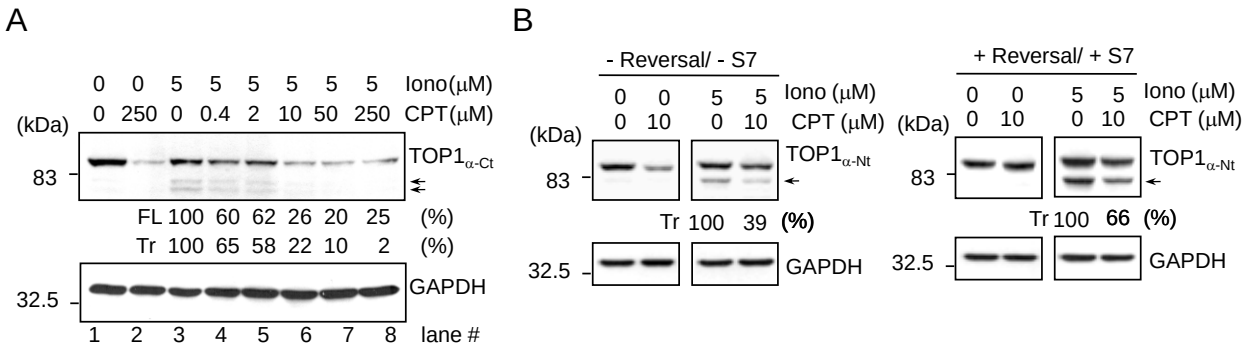

Fig. 21 Truncated forms of hTOP1 are trapped on chromosome by CPT.

(A) HCT116 cells were pretreated with ionomycin (5 μM) for 15 min. before added CPT (concentrations as indicated on the top of panel) for an another 30-min. co-incubation. Immunoblotting analysis was performed to determine the efficiency of formation of truncated hTOP1 cleavable complex (hTOP1^{tr}cc). The formation of CPT-induced hTOP1cc and hTOP1^{tr}cc in the trapping assay is indicated by the disappearance of hTOP1. The levels of full-length (FL) and truncated (Tr) hTOP1 proteins in the ionomycin-treated sample were both taken as 100%. (B) HCT116 Cells were pretreated with ionomycin (5 μM, 15 min). This treatment was followed by co-treatment with CPT (10 μM) for an additional 30 min., and then medium reversal with S7 nuclease treatment was performed as described in Materials and Methods. The percentage (%) indicates the proportion of the free-form hTOP1^{tr} proteins and the amount of hTOP1^{tr} in the ionomycin-treated control was taken as 100%. Arrows

indicate the truncated hTOP1 fragments. FL, full-length hTOP1; Tr, calpain 2-truncated hTOP1 fragments.

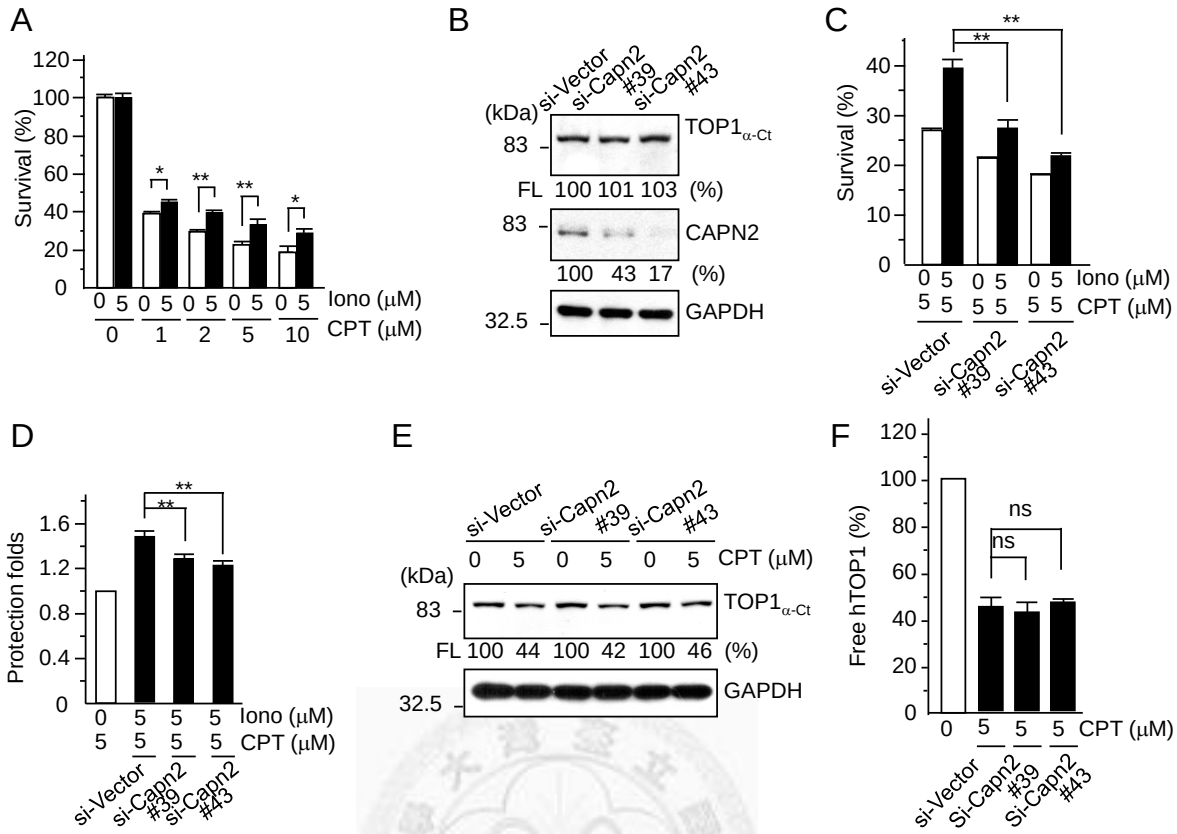

Fig. 22 Calpain 2 is involved in the ionomycin-induced protection from CPT cytotoxicity.

(A) HCT116 cells pretreated with or without ionomycin (5 μM, 15 min.) were co-incubated with CPT (concentrations as indicated in the panel) for 30 min. The colony formation assay was performed as described in Materials and Methods and quantified results were represented as CPT-induced cell killing (n = 3). (B) Expression profiles of hTOP1 and calpain 2 proteins in HCT116 (si-Vector, si-Capn2 #39 or #43) cells. (C) HCT116 (si-Vector, si-Capn2 #39 or #43) cells were exposed to ionomycin (5 μM) and CPT (5 μM) and cell survival was determined in three independent

experiments (n = 3). The relative protective effects of ionomycin against CPT-induced cell killing in different cell lines were further quantified using the ratio of survival rates in the presence and absence of ionomycin and represent as “protection folds” in (D). (E-F) HCT116 si-Vector and si-Capn 2 cells were treated with 5-μM CPT for 30 min and lyzed for immunoblotting analysis. The quantification of free hTOP1 related to si-Vector and si-Capn 2 cells were also shown in Fig.19F (n=3). FL, full-length hTOP1; **, $P < 0.01$; *, $P < 0.05$; ns, statistically non-significant

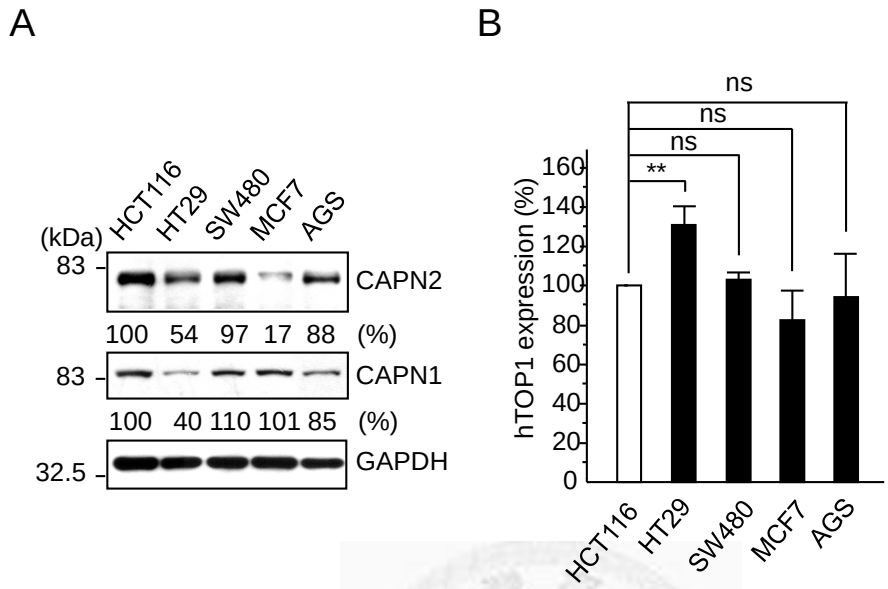

Fig. 23 Expression profiles of cellular calpain 1, 2 and hTOP1 proteins in different kinds of cancer cells.

(A) Cells lysates harvested from three colorectal cancer cell lines (HCT116, SW480 and HT29), one breast cancer cell line (MCF7) and one gastric cancer cell line (AGS) were subjected to immunoblotting analysis with antibodies against calpain 1, 2 and hTOP1. GAPDH was served as the protein loading control. (B) Quantification of hTOP1 protein from immunoblotting assay was also shown in Fig.20C (n=3). **, $P < 0.01$; *, $P < 0.05$; ns, statistically non-significant

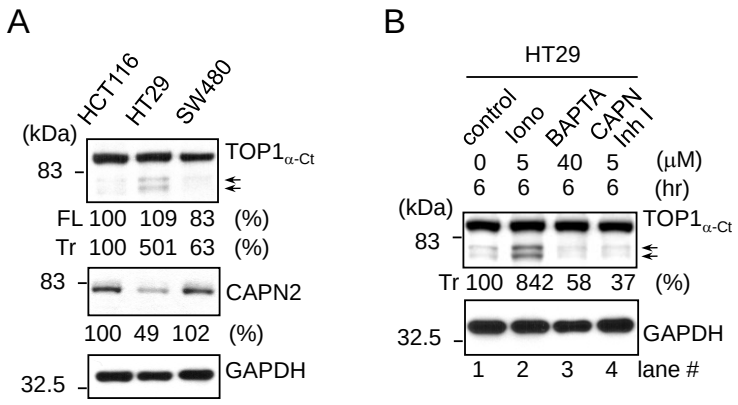

Fig. 24 On hTOP1 HT29 cells has better basal proteolytic activity in which calpains may involve.

(A) Three different colorectal cancer cell lines (HCT116, SW480, HT29) cultivated with 5% CO_2 and 37℃ were lysed and immunoblotting assay was carried out to detect the endogenous truncated forms of hTOP1. (B) HT29 cells incubated with 5-μM ionomycin, 40-μM BAPTA or 5-μM calpain inhibitor I (CAPN Inh I) for 6 hours and hTOP1 proteins were assayed as described in Materials and Methods. The endogenous level of truncated (Tr) hTOP1 in HT29 cells (lane 1) was taken as 100%. Arrows indicate the truncated hTOP1 fragments. FL, full-length hTOP1; Tr, calpain 2-truncated hTOP1 fragments

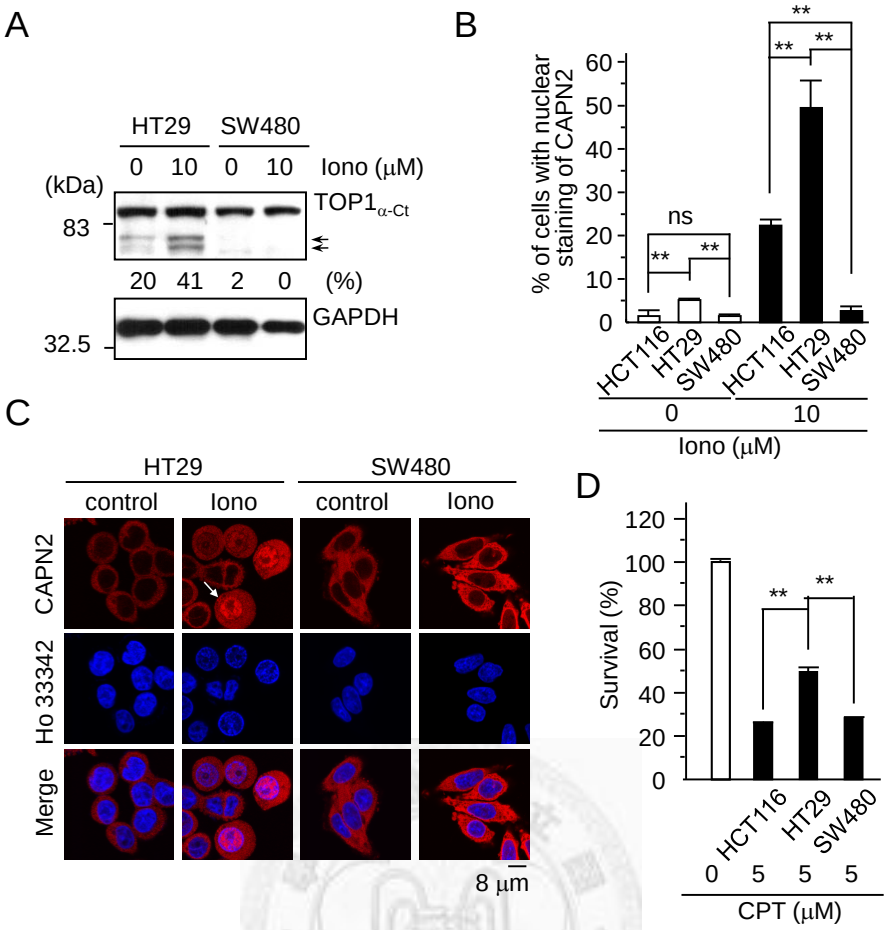

Fig. 25 HT29 cells exhibits properties with more nuclear shuttling of calpain 2 and better resistant to CPT cytotoxicity.

(A) HT29 and SW480 cells were treated with or without ionomycin (10 μM, 15 min.) and immunoblotting was performed with $TOP1_{\alpha\text{-}Ct}$ antibodies. (B-C) HCT116, HT29 and SW480 cells were seeded on coverslips for 24 hrs before treated with or without ionomycin (10 μM, 15 min.). The nuclear entry of calpain 2 was collected and scored by confocal microscopy (n=3) as described in Materials and Methods. Cellular DNA was stained by Hoechst 33342. (D) HCT116, HT29 and SW480 treated with CPT (5 μM, 30 min.) were isolated and subjected to colony formation assay as described in

Materials and Methods (n = 3). Arrows indicate the truncated hTOP1 fragments; white arrows indicate the cells with nucleolar accumulation of hTOP1. **, $P < 0.01$; ns, statistically non-significant

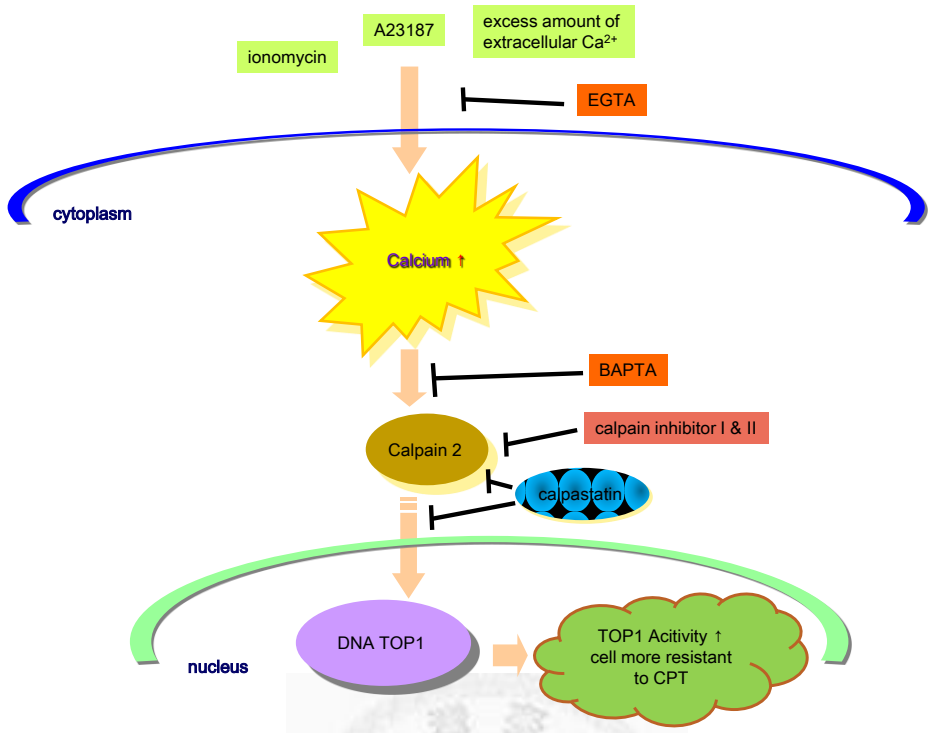

Fig. 26 Diagram of Ca^{2+}-mediated proteolytic processing of hTOP1.

Physiological or pathophysiological stresses (e.g. ischemia, hypoxia, ER stress and acidosis) could lead ER to release Ca^{2+} from ER lumen or open Ca^{2+} channel to trigger Ca^{2+} influx therefore resulting in increasing intracellular Ca^{2+} concentration ($[Ca^{2+}]$). Here we used pharmacological approaches (Ca^{2+} ionophores such as ionomycin or A23187) or directly added extracellular Ca^{2+} chloride to media to induce Ca^{2+}-influx. After $[Ca^{2+}]$ is elevated, the Ca^{2+}-dependent protease, calpain 2, would be activated and translocated from cytoplasm into nucleus. Ca^{2+} chelator (EGTA or BAPTA) and calpastatin could block the nuclear entry and proteolytic activity of calpain 2. Nevertheless, calpain inhibitor I or II only represses calpain

2-mediated cleavage of hTOP1 but not influence nuclear translocation of calpain 2. Interestingly, the truncated hTOP1 has better relaxation activity than full length of hTOP1 and the activated calpain 2 may contribute the resistant potential to CPT killing in cancer cells.

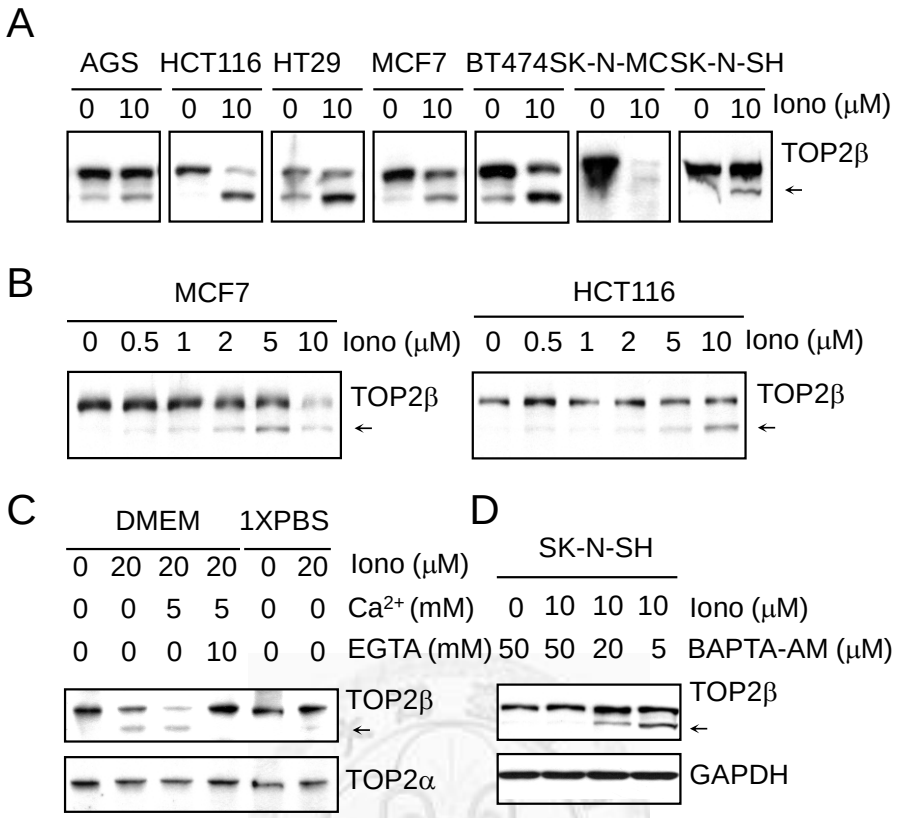

Fig. 27 Ca^{2+} influx induces proteolytic processing of hTOP2β.

(A) Gastric cancer cell line (AGS), colorectal cancer cell lines (HCT116, HT29), breast cancer cell lines (MCF7, BT474) and neuroblastoma cell lines (SK-N-MC, SK-N-SH) were treated with ionomycin (Iono, 10 μM) for 15 min. The harvested cell lysates were displayed on 8% SDS-PAGE, and immunoblotting was performed with antibodies against hTOP2β. GAPDH serves as a protein loading control. (B) Ionomycin causes cleavage of hTOP2β in a dosage dependent manner. MCF7 and HCT116 cells were treated different doses of ionomycin for 15 min. and immunoblotting was carried out to detect the cleavage of hTOP2β. (C-D) Ca^{2+} is

required for the proteolytic cleavage of hTOP2β protein. HCT116 or SK-N-SH cells were pretreated with Ca^{2+}, EGTA or BAPTA-AM for 30 min. before ionomycin treatment (15min.) and their concentration as indicated in the top of these panels. Immunoblotting analysis was used to dissect the truncated patterns of hTOP2β. Arrows indicate the truncated hTOP2β fragments.

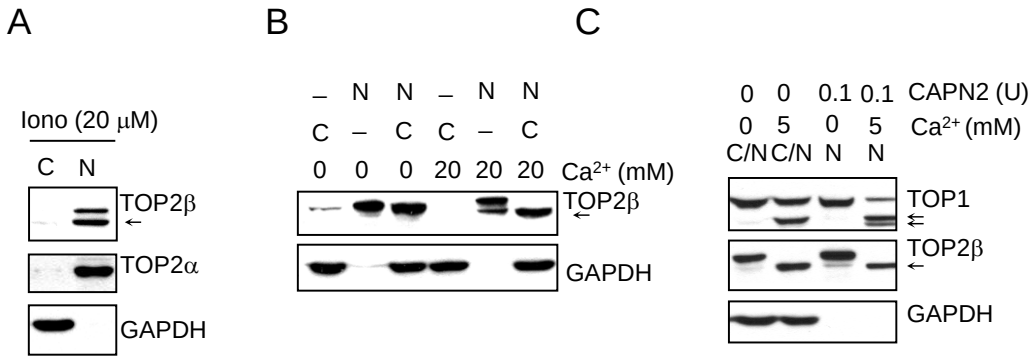

Fig. 28 Cytosolic proteases contribute to the most efficiency of cleavage.

(A) HCT116 cells were treated with ionomycin (20 μM, 15 min.) and fractionation assay was carried out as described in Materials and Methods. hTOP2α and GAPDH were blotted as controls of nuclear (N) and cytosolic (C) extracts, respectively. (B-C) *In vitro* cleavage assay as described in Materials and Methods was performed and reconstituted by combining the fractions (C or N) of fractionation or directly adding calpain 2 (0.1U) in the absent or present Ca^{2+} treatment. Immunoblotting assay was used to analyze the cleavage events of hTOP2β and hTOP1. Arrows indicate the truncated hTOP2β and hTOP1 fragments

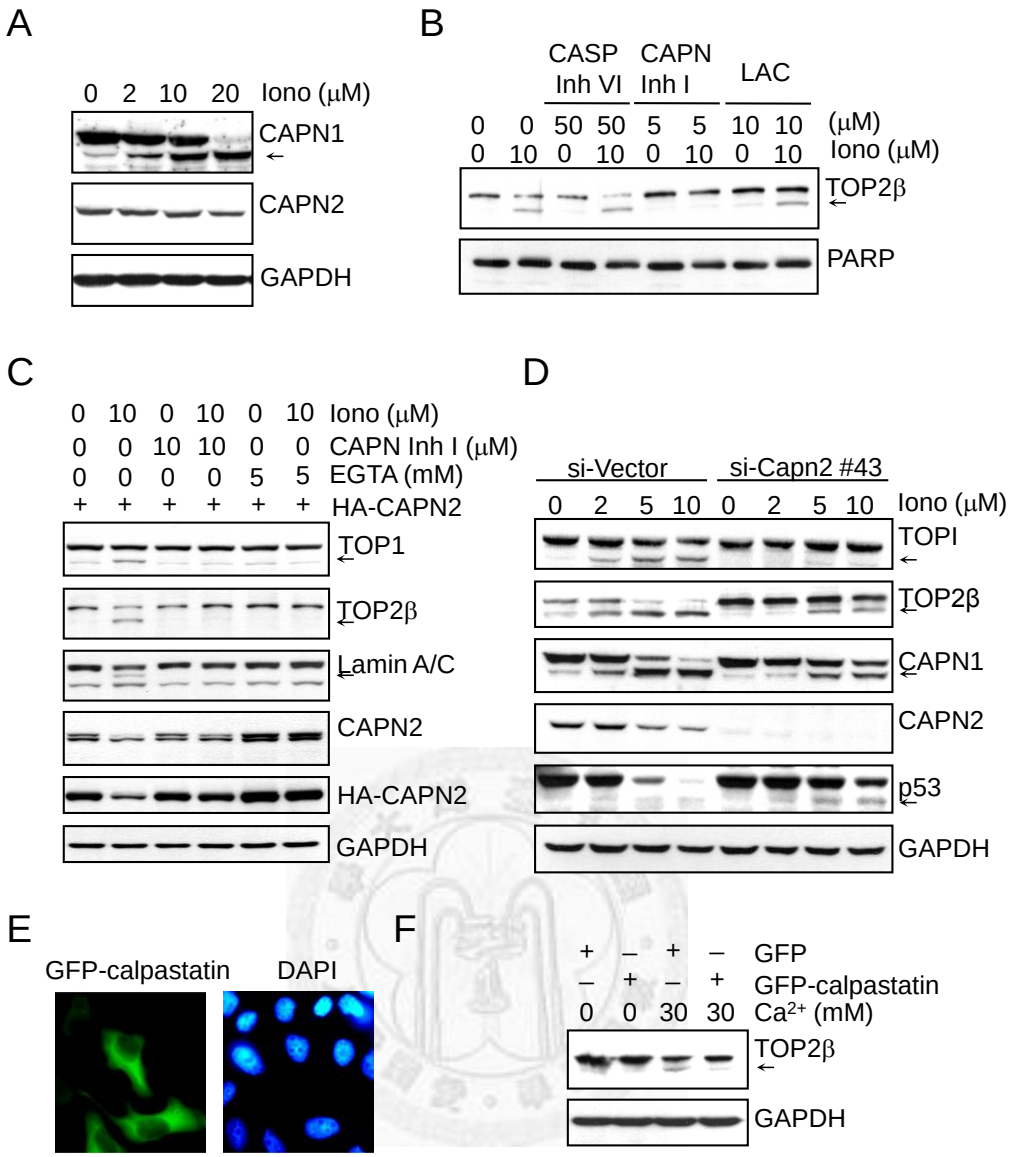

Fig. 29 Activated calpains including calpain 2 by Ca^{2+} influx are involved in the processing events of hTOP2β.

(A) Ionomycin induces activation of calpain 1 or 2. HCT116 cells were treated with ionomycin (2, 10, 20 μM, 15 min.) and the harvested cell lysates were subjected to immunoblotting with antibodies against calpain 1 or 2. (B) Only calpain inhibitor I (CAPN Inh I) not caspase inhibitor VI (CASP Inh VI) or lactacystin (Lact.) could abolish Ca^{2+} induced proteolytic cleavage of hTOP2β. HCT116 cells were pretreated

with these inhibitors for 30 min. and incubated along with ionomycin for another 15-min. treatment. (C) Calpain inhibitor I and EGTA both block the autolysis of calpain 2. Overexpression of HA-calpain 2 in HCT116 cells were exposed to calpain inhibitor I (10 μM, 30 min.) or EGTA (5 mM, 30min.) before ionomycin (10 μM, 15 min.) treatment. Immunoblotting assay was performed to determine the proteolytic processing of hTOP1, hTOP2β, lamin A/C, calpain 2 and HA-calpain 2. (D) Downregulation of calpain 2 partially reduces the cleavage events of hTOP2β and p53. HCT116 cells were infected with lentivirus system based to express siRNA against calpain 2 and selected with puromycin to generate a stable clone (si-Capn2 #43) as described in Materials and Methods. Si-Vector and si-Capn 2 #43 cells were treated with ionomycin for 15 min. with concentration as indicated on the top of the panel and the collected cell lysates were separated on 8% SDS-PAGE then subjected to immunoblotting analysis. (E-F) Force expression of calpastatin inhibits Ca^{2+} activated processing of hTOP2β. HCT116 cells seeded on coverslips for 24 hr were transfected with GFP or GFP-fused calpastatin expression plasmids. At 48 hr post-transfection, 30 mM Ca^{2+} was directly added into medium for initiating the cleavage of hTOP2β. IFA (as described in Materials and Methods) and immunoblotting assay were carried out to examine the expression of calpastatin and the Ca^{2+} mediated truncation of hTOP2β, respectively. Arrows indicate the truncated protein fragments.

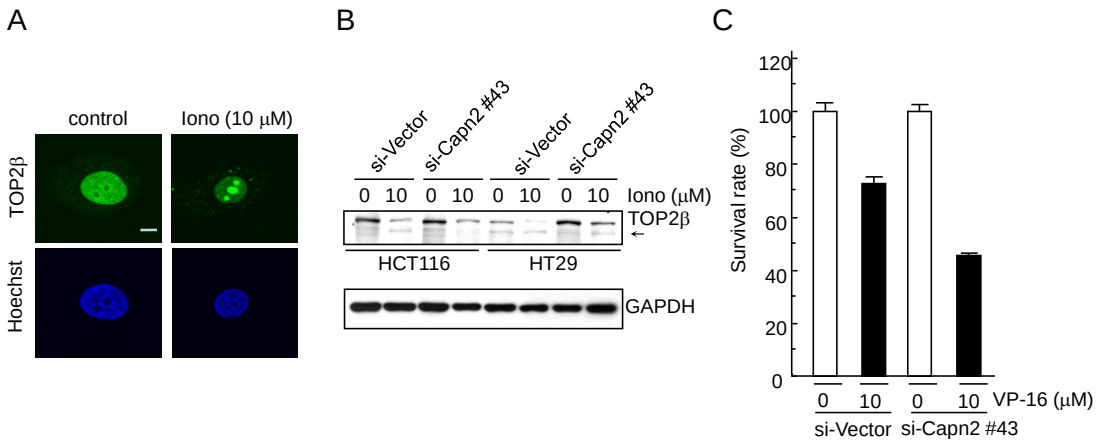

Fig. 30 Ca^{2+} influx-mediated nucleolar accumulations of hTOP2β and down regulation of protein level of hTOP2β by calpain 2.

(A) Ionomycin causes nucleolar accumulations of hTOP2β. HCT116 cells were seeded on coverslips for 24 hr and treated with ionomycin (10 μM) for 15min. IFA (as described in Materials and Methods) was used to detect the Ca^{2+} influx induced translocations of hTOP2β. (B-C) Calpain 2 participates in the regulation of protein stability of hTOP2β and contributes to cell survival upon VP-16 treatment. HCT116 and HT29 cells were chosen to establish si-Capn2 stable clones as described in Materials and Methods. Si-Vector or si-Capn2 #43 cells were treated with ionomycin (10 μM, 15 min.) and lyzed for immunoblotting analysis. The stable clones (generated from HCT116 cell line) were exposed to VP-16 (10 μM, 30 min.) and trypsinized for colony formation assay as described in Materials and Methods. Arrow indicates the truncated hTOP2β fragment. Bar, 8 μm

References

1. Wang, J. C. (2002) Cellular roles of DNA topoisomerases: a molecular perspective, *Nat Rev Mol Cell Biol 3*, 430-440.
2. Wang, J. C. (1996) DNA topoisomerases, *Annu Rev Biochem 65*, 635-692.
3. Champoux, J. J. (2001) DNA topoisomerases: structure, function, and mechanism, *Annu Rev Biochem 70*, 369-413.
4. Pietrusinski, M., and Staczek, P. (2006) [Bacterial type II topoisomerases as targets for antibacterial drugs], *Postepy Biochem 52*, 271-282.
5. Baker, N. M., Rajan, R., and Mondragon, A. (2009) Structural studies of type I topoisomerases, *Nucleic Acids Res 37*, 693-701.
6. Cortes, F., Pastor, N., Mateos, S., and Dominguez, I. (2003) Roles of DNA topoisomerases in chromosome segregation and mitosis, *Mutat Res 543*, 59-66.
7. Wallis, J. W., Chrebet, G., Brodsky, G., Rolfe, M., and Rothstein, R. (1989) A hyper-recombination mutation in S. cerevisiae identifies a novel eukaryotic topoisomerase, *Cell 58*, 409-419.
8. Seki, T., Seki, M., Onodera, R., Katada, T., and Enomoto, T. (1998) Cloning of cDNA encoding a novel mouse DNA topoisomerase III (Topo IIIbeta) possessing negatively supercoiled DNA relaxing activity, whose message is highly expressed in the testis, *J Biol Chem 273*, 28553-28556.
9. Nitiss, J. L. (2002) DNA topoisomerases in cancer chemotherapy: using enzymes to generate selective DNA damage, *Curr Opin Investig Drugs 3*, 1512-1516.
10. Mitscher, L. A. (2005) Bacterial topoisomerase inhibitors: quinolone and pyridone antibacterial agents, *Chem Rev 105*, 559-592.
11. Drlica, K., and Malik, M. (2003) Fluoroquinolones: action and resistance, *Curr Top Med Chem 3*, 249-282.
12. Maxwell, A., and Lawson, D. M. (2003) The ATP-binding site of type II topoisomerases as a target for antibacterial drugs, *Curr Top Med Chem 3*, 283-303.
13. Hsiang, Y. H., Hertzberg, R., Hecht, S., and Liu, L. F. (1985) Camptothecin induces protein-linked DNA breaks via mammalian DNA topoisomerase I, *J Biol Chem 260*, 14873-14878.
14. Liu, L. F., Desai, S. D., Li, T. K., Mao, Y., Sun, M., and Sim, S. P. (2000) Mechanism of action of camptothecin, *Ann N Y Acad Sci 922*, 1-10.
15. Wilstermann, A. M., and Osheroff, N. (2003) Stabilization of eukaryotic topoisomerase II-DNA cleavage complexes, *Curr Top Med Chem 3*, 321-338.

16. Larsen, A. K., Escargueil, A. E., and Skladanowski, A. (2003) Catalytic topoisomerase II inhibitors in cancer therapy, *Pharmacol Ther 99*, 167-181.
17. Wobbe, C. R., Dean, F. B., Murakami, Y., Borowiec, J. A., Bullock, P., and Hurwitz, J. (1987) In vitro replication of DNA containing either the SV40 or the polyoma origin, *Philos Trans R Soc Lond B Biol Sci 317*, 439-453.
18. Kim, R. A., and Wang, J. C. (1989) Function of DNA topoisomerases as replication swivels in Saccharomyces cerevisiae, *J Mol Biol 208*, 257-267.
19. Stewart, A. F., and Schutz, G. (1987) Camptothecin-induced in vivo topoisomerase I cleavages in the transcriptionally active tyrosine aminotransferase gene, *Cell 50*, 1109-1117.
20. Kretzschmar, M., Meisterernst, M., and Roeder, R. G. (1993) Identification of human DNA topoisomerase I as a cofactor for activator-dependent transcription by RNA polymerase II, *Proc Natl Acad Sci U S A 90*, 11508-11512.
21. Thrash, C., Bankier, A. T., Barrell, B. G., and Sternglanz, R. (1985) Cloning, characterization, and sequence of the yeast DNA topoisomerase I gene, *Proc Natl Acad Sci U S A 82*, 4374-4378.
22. Lee, M. P., Brown, S. D., Chen, A., and Hsieh, T. S. (1993) DNA topoisomerase I is essential in Drosophila melanogaster, *Proc Natl Acad Sci U S A 90*, 6656-6660.
23. Morham, S. G., Kluckman, K. D., Voulomanos, N., and Smithies, O. (1996) Targeted disruption of the mouse topoisomerase I gene by camptothecin selection, *Mol Cell Biol 16*, 6804-6809.
24. Austin, C. A., Sng, J. H., Patel, S., and Fisher, L. M. (1993) Novel HeLa topoisomerase II is the II beta isoform: complete coding sequence and homology with other type II topoisomerases, *Biochim Biophys Acta 1172*, 283-291.
25. McClendon, A. K., Rodriguez, A. C., and Osheroff, N. (2005) Human topoisomerase IIalpha rapidly relaxes positively supercoiled DNA: implications for enzyme action ahead of replication forks, *J Biol Chem 280*, 39337-39345.
26. Grue, P., Grasser, A., Sehested, M., Jensen, P. B., Uhse, A., Straub, T., Ness, W., and Boege, F. (1998) Essential mitotic functions of DNA topoisomerase IIalpha are not adopted by topoisomerase IIbeta in human H69 cells, *J Biol Chem 273*, 33660-33666.
27. Akimitsu, N., Adachi, N., Hirai, H., Hossain, M. S., Hamamoto, H., Kobayashi, M., Aratani, Y., Koyama, H., and Sekimizu, K. (2003) Enforced cytokinesis without complete nuclear division in embryonic cells depleting the

activity of DNA topoisomerase IIalpha, *Genes Cells 8*, 393-402.

28. Dereuddre, S., Delaporte, C., and Jacquemin-Sablon, A. (1997) Role of topoisomerase II beta in the resistance of 9-OH-ellipticine-resistant Chinese hamster fibroblasts to topoisomerase II inhibitors, *Cancer Res 57*, 4301-4308.
29. Errington, F., Willmore, E., Tilby, M. J., Li, L., Li, G., Li, W., Baguley, B. C., and Austin, C. A. (1999) Murine transgenic cells lacking DNA topoisomerase IIbeta are resistant to acridines and mitoxantrone: analysis of cytotoxicity and cleavable complex formation, *Mol Pharmacol 56*, 1309-1316.
30. Yang, X., Li, W., Prescott, E. D., Burden, S. J., and Wang, J. C. (2000) DNA topoisomerase IIbeta and neural development, *Science 287*, 131-134.
31. Lyu, Y. L., Lin, C. P., Azarova, A. M., Cai, L., Wang, J. C., and Liu, L. F. (2006) Role of topoisomerase IIbeta in the expression of developmentally regulated genes, *Mol Cell Biol 26*, 7929-7941.
32. Ju, B. G., and Rosenfeld, M. G. (2006) A breaking strategy for topoisomerase IIbeta/PARP-1-dependent regulated transcription, *Cell Cycle 5*, 2557-2560.
33. Ju, B. G., Lunyak, V. V., Perissi, V., Garcia-Bassets, I., Rose, D. W., Glass, C. K., and Rosenfeld, M. G. (2006) A topoisomerase IIbeta-mediated dsDNA break required for regulated transcription, *Science 312*, 1798-1802.
34. Gangloff, S., McDonald, J. P., Bendixen, C., Arthur, L., and Rothstein, R. (1994) The yeast type I topoisomerase Top3 interacts with Sgs1, a DNA helicase homolog: a potential eukaryotic reverse gyrase, *Mol Cell Biol 14*, 8391-8398.
35. Ira, G., Malkova, A., Liberi, G., Foiani, M., and Haber, J. E. (2003) Srs2 and Sgs1-Top3 suppress crossovers during double-strand break repair in yeast, *Cell 115*, 401-411.
36. Li, W., and Wang, J. C. (1998) Mammalian DNA topoisomerase IIIalpha is essential in early embryogenesis, *Proc Natl Acad Sci U S A 95*, 1010-1013.
37. Kwan, K. Y., and Wang, J. C. (2001) Mice lacking DNA topoisomerase IIIbeta develop to maturity but show a reduced mean lifespan, *Proc Natl Acad Sci U S A 98*, 5717-5721.
38. Wu, L., Davies, S. L., North, P. S., Goulaouic, H., Riou, J. F., Turley, H., Gatter, K. C., and Hickson, I. D. (2000) The Bloom's syndrome gene product interacts with topoisomerase III, *J Biol Chem 275*, 9636-9644.
39. Wu, L., and Hickson, I. D. (2003) The Bloom's syndrome helicase suppresses crossing over during homologous recombination, *Nature 426*, 870-874.
40. Guroff, G. (1964) A Neutral, Calcium-Activated Proteinase from the Soluble Fraction of Rat Brain, *J Biol Chem 239*, 149-155.
41. Mellgren, R. L. (1987) Calcium-dependent proteases: an enzyme system

active at cellular membranes?, *FASEB J 1*, 110-115.

42. Goll, D. E., Thompson, V. F., Li, H., Wei, W., and Cong, J. (2003) The calpain system, *Physiol Rev 83*, 731-801.
43. Perrin, B. J., and Huttenlocher, A. (2002) Calpain, *Int J Biochem Cell Biol 34*, 722-725.
44. Ono, Y., Sorimachi, H., and Suzuki, K. (1998) Structure and physiology of calpain, an enigmatic protease, *Biochem Biophys Res Commun 245*, 289-294.
45. Croall, D. E., and DeMartino, G. N. (1991) Calcium-activated neutral protease (calpain) system: structure, function, and regulation, *Physiol Rev 71*, 813-847.
46. Liu, X., Van Vleet, T., and Schnellmann, R. G. (2004) The role of calpain in oncotic cell death, *Annu Rev Pharmacol Toxicol 44*, 349-370.
47. Tompa, P., Buzder-Lantos, P., Tantos, A., Farkas, A., Szilagyi, A., Banoczi, Z., Hudecz, F., and Friedrich, P. (2004) On the sequential determinants of calpain cleavage, *J Biol Chem 279*, 20775-20785.
48. Croall, D. E., and Ersfeld, K. (2007) The calpains: modular designs and functional diversity, *Genome Biol 8*, 218.
49. Azam, M., Andrabi, S. S., Sahr, K. E., Kamath, L., Kuliopulos, A., and Chishti, A. H. (2001) Disruption of the mouse mu-calpain gene reveals an essential role in platelet function, *Mol Cell Biol 21*, 2213-2220.
50. Arthur, J. S., Elce, J. S., Hegadorn, C., Williams, K., and Greer, P. A. (2000) Disruption of the murine calpain small subunit gene, Capn4: calpain is essential for embryonic development but not for cell growth and division, *Mol Cell Biol 20*, 4474-4481.
51. Zhang, W., Lu, Q., Xie, Z. J., and Mellgren, R. L. (1997) Inhibition of the growth of WI-38 fibroblasts by benzyloxycarbonyl-Leu-Leu-Tyr diazomethyl ketone: evidence that cleavage of p53 by a calpain-like protease is necessary for G1 to S-phase transition, *Oncogene 14*, 255-263.
52. Zhang, W., Lane, R. D., and Mellgren, R. L. (1996) The major calpain isozymes are long-lived proteins. Design of an antisense strategy for calpain depletion in cultured cells, *J Biol Chem 271*, 18825-18830.
53. Patel, Y. M., and Lane, M. D. (2000) Mitotic clonal expansion during preadipocyte differentiation: calpain-mediated turnover of p27, *J Biol Chem 275*, 17653-17660.
54. Glading, A., Uberall, F., Keyse, S. M., Lauffenburger, D. A., and Wells, A. (2001) Membrane proximal ERK signaling is required for M-calpain activation downstream of epidermal growth factor receptor signaling, *J Biol Chem 276*, 23341-23348.
55. Santella, L., Kyozuka, K., Hoving, S., Munchbach, M., Quadroni, M., Dainese,

P., Zamparelli, C., James, P., and Carafoli, E. (2000) Breakdown of cytoskeletal proteins during meiosis of starfish oocytes and proteolysis induced by calpain, *Exp Cell Res 259*, 117-126.

56. Schollmeyer, J. E. (1988) Calpain II involvement in mitosis, *Science 240*, 911-913.
57. Dennison, S. R., Dante, S., Hauss, T., Brandenburg, K., Harris, F., and Phoenix, D. A. (2005) Investigations into the membrane interactions of m-calpain domain V, *Biophys J 88*, 3008-3017.
58. Melloni, E., Michetti, M., Salamino, F., Minafra, R., and Pontremoli, S. (1996) Modulation of the calpain autoproteolysis by calpastatin and phospholipids, *Biochem Biophys Res Commun 229*, 193-197.
59. Suzuki, K., and Sorimachi, H. (1998) A novel aspect of calpain activation, *FEBS Lett 433*, 1-4.
60. Moldoveanu, T., Gehring, K., and Green, D. R. (2008) Concerted multi-pronged attack by calpastatin to occlude the catalytic cleft of heterodimeric calpains, *Nature 456*, 404-408.
61. Hanna, R. A., Campbell, R. L., and Davies, P. L. (2008) Calcium-bound structure of calpain and its mechanism of inhibition by calpastatin, *Nature 456*, 409-412.
62. Nishimura, T., and Goll, D. E. (1991) Binding of calpain fragments to calpastatin, *J Biol Chem 266*, 11842-11850.
63. Yang, H. Q., Ma, H., Takano, E., Hatanaka, M., and Maki, M. (1994) Analysis of calcium-dependent interaction between amino-terminal conserved region of calpastatin functional domain and calmodulin-like domain of mu-calpain large subunit, *J Biol Chem 269*, 18977-18984.
64. Melloni, E., Averna, M., Salamino, F., Sparatore, B., Minafra, R., and Pontremoli, S. (2000) Acyl-CoA-binding protein is a potent m-calpain activator, *J Biol Chem 275*, 82-86.
65. Chakrabarti, A. K., Dasgupta, S., Gadsden, R. H., Sr., Hogan, E. L., and Banik, N. L. (1996) Regulation of brain m calpain Ca2+ sensitivity by mixtures of membrane lipids: activation at intracellular Ca2+ level, *J Neurosci Res 44*, 374-380.
66. Arthur, J. S., and Crawford, C. (1996) Investigation of the interaction of m-calpain with phospholipids: calpain-phospholipid interactions, *Biochim Biophys Acta 1293*, 201-206.
67. Shiraha, H., Glading, A., Chou, J., Jia, Z., and Wells, A. (2002) Activation of m-calpain (calpain II) by epidermal growth factor is limited by protein kinase A phosphorylation of m-calpain, *Mol Cell Biol 22*, 2716-2727.

68. Glading, A., Bodnar, R. J., Reynolds, I. J., Shiraha, H., Satish, L., Potter, D. A., Blair, H. C., and Wells, A. (2004) Epidermal growth factor activates m-calpain (calpain II), at least in part, by extracellular signal-regulated kinase-mediated phosphorylation, *Mol Cell Biol 24*, 2499-2512.
69. Wang, H. C., Huang, Y. S., Ho, C. C., Jeng, J. C., and Shih, H. M. (2009) SUMO modification modulates the activity of calpain-2, *Biochem Biophys Res Commun 384*, 444-449.
70. Vanderklish, P. W., and Bahr, B. A. (2000) The pathogenic activation of calpain: a marker and mediator of cellular toxicity and disease states, *Int J Exp Pathol 81*, 323-339.
71. Horikawa, Y., Oda, N., Cox, N. J., Li, X., Orho-Melander, M., Hara, M., Hinokio, Y., Lindner, T. H., Mashima, H., Schwarz, P. E., del Bosque-Plata, L., Oda, Y., Yoshiuchi, I., Colilla, S., Polonsky, K. S., Wei, S., Concannon, P., Iwasaki, N., Schulze, J., Baier, L. J., Bogardus, C., Groop, L., Boerwinkle, E., Hanis, C. L., and Bell, G. I. (2000) Genetic variation in the gene encoding calpain-10 is associated with type 2 diabetes mellitus, *Nat Genet 26*, 163-175.
72. Shearer, T. R., Ma, H., Shih, M., Fukiage, C., and Azuma, M. (2000) Calpains in the lens and cataractogenesis, *Methods Mol Biol 144*, 277-285.
73. Biswas, S., Harris, F., Dennison, S., Singh, J. P., and Phoenix, D. (2005) Calpains: enzymes of vision?, *Med Sci Monit 11*, RA301-310.
74. Tidball, J. G., and Spencer, M. J. (2000) Calpains and muscular dystrophies, *Int J Biochem Cell Biol 32*, 1-5.
75. Vosler, P. S., Brennan, C. S., and Chen, J. (2008) Calpain-mediated signaling mechanisms in neuronal injury and neurodegeneration, *Mol Neurobiol 38*, 78-100.
76. Samantaray, S., Ray, S. K., and Banik, N. L. (2008) Calpain as a potential therapeutic target in Parkinson's disease, *CNS Neurol Disord Drug Targets 7*, 305-312.
77. Tsuji, T., Shimohama, S., Kimura, J., and Shimizu, K. (1998) m-Calpain (calcium-activated neutral proteinase) in Alzheimer's disease brains, *Neurosci Lett 248*, 109-112.
78. Shields, D. C., Schaecher, K. E., Saido, T. C., and Banik, N. L. (1999) A putative mechanism of demyelination in multiple sclerosis by a proteolytic enzyme, calpain, *Proc Natl Acad Sci U S A 96*, 11486-11491.
79. Mehendale, H. M., and Limaye, P. B. (2005) Calpain: a death protein that mediates progression of liver injury, *Trends Pharmacol Sci 26*, 232-236.
80. Yoshida, K., Inui, M., Harada, K., Saido, T. C., Sorimachi, Y., Ishihara, T., Kawashima, S., and Sobue, K. (1995) Reperfusion of rat heart after brief

ischemia induces proteolysis of calspectin (nonerythroid spectrin or fodrin) by calpain, *Circ Res 77*, 603-610.

81. Rami, A., Agarwal, R., Botez, G., and Winckler, J. (2000) mu-Calpain activation, DNA fragmentation, and synergistic effects of caspase and calpain inhibitors in protecting hippocampal neurons from ischemic damage, *Brain Res 866*, 299-312.
82. Blomgren, K., Zhu, C., Wang, X., Karlsson, J. O., Leverin, A. L., Bahr, B. A., Mallard, C., and Hagberg, H. (2001) Synergistic activation of caspase-3 by m-calpain after neonatal hypoxia-ischemia: a mechanism of "pathological apoptosis"?, *J Biol Chem 276*, 10191-10198.
83. Huang, Y., and Wang, K. K. (2001) The calpain family and human disease, *Trends Mol Med 7*, 355-362.
84. Yoshikawa, Y., Mukai, H., Hino, F., Asada, K., and Kato, I. (2000) Isolation of two novel genes, down-regulated in gastric cancer, *Jpn J Cancer Res 91*, 459-463.
85. Ono, Y., Shimada, H., Sorimachi, H., Richard, I., Saido, T. C., Beckmann, J. S., Ishiura, S., and Suzuki, K. (1998) Functional defects of a muscle-specific calpain, p94, caused by mutations associated with limb-girdle muscular dystrophy type 2A, *J Biol Chem 273*, 17073-17078.
86. Richard, I., Broux, O., Allamand, V., Fougerousse, F., Chiannilkulchai, N., Bourg, N., Brenguier, L., Devaud, C., Pasturaud, P., Roudaut, C., and et al. (1995) Mutations in the proteolytic enzyme calpain 3 cause limb-girdle muscular dystrophy type 2A, *Cell 81*, 27-40.
87. Clapham, D. E. (2007) Calcium signaling, *Cell 131*, 1047-1058.
88. Parkash, J., and Asotra, K. (2010) Calcium wave signaling in cancer cells, *Life Sci 87*, 587-595.
89. Moldoveanu, T., Hosfield, C. M., Lim, D., Elce, J. S., Jia, Z., and Davies, P. L. (2002) A Ca(2+) switch aligns the active site of calpain, *Cell 108*, 649-660.
90. Bartoli, M., and Richard, I. (2005) Calpains in muscle wasting, *Int J Biochem Cell Biol 37*, 2115-2133.
91. Zatz, M., and Starling, A. (2005) Calpains and disease, *N Engl J Med 352*, 2413-2423.
92. Dargelos, E., Poussard, S., Brule, C., Daury, L., and Cottin, P. (2008) Calcium-dependent proteolytic system and muscle dysfunctions: a possible role of calpains in sarcopenia, *Biochimie 90*, 359-368.
93. Braun, C., Engel, M., Seifert, M., Theisinger, B., Seitz, G., Zang, K. D., and Welter, C. (1999) Expression of calpain I messenger RNA in human renal cell carcinoma: correlation with lymph node metastasis and histological type, *Int J*

Cancer 84, 6-9.

94. Kaneko, T., Yamashima, T., Tohma, Y., Nomura, M., Imajoh-Ohmi, S., Saido, T. C., Nakao, M., Saya, H., Yamamoto, H., and Yamashita, J. (2001) Calpain-dependent proteolysis of merlin occurs by oxidative stress in meningiomas: a novel hypothesis of tumorigenesis, *Cancer 92*, 2662-2672.
95. Lakshmikuttyamma, A., Selvakumar, P., Kanthan, R., Kanthan, S. C., and Sharma, R. K. (2004) Overexpression of m-calpain in human colorectal adenocarcinomas, *Cancer Epidemiol Biomarkers Prev 13*, 1604-1609.
96. Rios-Doria, J., Kuefer, R., Ethier, S. P., and Day, M. L. (2004) Cleavage of beta-catenin by calpain in prostate and mammary tumor cells, *Cancer Res 64*, 7237-7240.
97. Franco, S. J., and Huttenlocher, A. (2005) Regulating cell migration: calpains make the cut, *J Cell Sci 118*, 3829-3838.
98. Libertini, S. J., Tepper, C. G., Rodriguez, V., Asmuth, D. M., Kung, H. J., and Mudryj, M. (2007) Evidence for calpain-mediated androgen receptor cleavage as a mechanism for androgen independence, *Cancer Res 67*, 9001-9005.
99. Cong, J., Goll, D. E., Peterson, A. M., and Kapprell, H. P. (1989) The role of autolysis in activity of the Ca2+-dependent proteinases (mu-calpain and m-calpain), *J Biol Chem 264*, 10096-10103.
100. Kawasaki, H., Emori, Y., Imajoh-Ohmi, S., Minami, Y., and Suzuki, K. (1989) Identification and characterization of inhibitory sequences in four repeating domains of the endogenous inhibitor for calcium-dependent protease, *J Biochem 106*, 274-281.
101. Ma, H., Yang, H. Q., Takano, E., Hatanaka, M., and Maki, M. (1994) Amino-terminal conserved region in proteinase inhibitor domain of calpastatin potentiates its calpain inhibitory activity by interacting with calmodulin-like domain of the proteinase, *J Biol Chem 269*, 24430-24436.
102. Wendt, A., Thompson, V. F., and Goll, D. E. (2004) Interaction of calpastatin with calpain: a review, *Biol Chem 385*, 465-472.
103. Hanna, R. A., Garcia-Diaz, B. E., and Davies, P. L. (2007) Calpastatin simultaneously binds four calpains with different kinetic constants, *FEBS Lett 581*, 2894-2898.
104. Takano, E., Ma, H., Yang, H. Q., Maki, M., and Hatanaka, M. (1995) Preference of calcium-dependent interactions between calmodulin-like domains of calpain and calpastatin subdomains, *FEBS Lett 362*, 93-97.
105. Raynaud, F., Marcilhac, A., Chebli, K., Benyamin, Y., and Rossel, M. (2008) Calpain 2 expression pattern and sub-cellular localization during mouse embryogenesis, *Int J Dev Biol 52*, 383-388.

106. Raynaud, F., Carnac, G., Marcilhac, A., and Benyamin, Y. (2004) m-Calpain implication in cell cycle during muscle precursor cell activation, *Exp Cell Res 298*, 48-57.
107. Franco, S. J., Rodgers, M. A., Perrin, B. J., Han, J., Bennin, D. A., Critchley, D. R., and Huttenlocher, A. (2004) Calpain-mediated proteolysis of talin regulates adhesion dynamics, *Nat Cell Biol 6*, 977-983.
108. Carragher, N. O., Westhoff, M. A., Fincham, V. J., Schaller, M. D., and Frame, M. C. (2003) A novel role for FAK as a protease-targeting adaptor protein: regulation by p42 ERK and Src, *Curr Biol 13*, 1442-1450.
109. Bano, D., Dinsdale, D., Cabrera-Socorro, A., Maida, S., Lambacher, N., McColl, B., Ferrando-May, E., Hengartner, M. O., and Nicotera, P. (2010) Alteration of the nuclear pore complex in Ca(2+)-mediated cell death, *Cell Death Differ 17*, 119-133.
110. Liu, L. F., and Wang, J. C. (1987) Supercoiling of the DNA template during transcription, *Proc Natl Acad Sci U S A 84*, 7024-7027.
111. Li, T. K., and Liu, L. F. (2001) Tumor cell death induced by topoisomerase-targeting drugs, *Annu Rev Pharmacol Toxicol 41*, 53-77.
112. Chen, A. Y., and Liu, L. F. (1994) DNA topoisomerases: essential enzymes and lethal targets, *Annu Rev Pharmacol Toxicol 34*, 191-218.
113. Bendixen, C., Thomsen, B., Alsner, J., and Westergaard, O. (1990) Camptothecin-stabilized topoisomerase I-DNA adducts cause premature termination of transcription, *Biochemistry 29*, 5613-5619.
114. Jiang, S., Chow, S. C., Nicotera, P., and Orrenius, S. (1994) Intracellular Ca2+ signals activate apoptosis in thymocytes: studies using the Ca(2+)-ATPase inhibitor thapsigargin, *Exp Cell Res 212*, 84-92.
115. Zhang, L., Song, L., and Parker, E. M. (1999) Calpain inhibitor I increases beta-amyloid peptide production by inhibiting the degradation of the substrate of gamma-secretase. Evidence that substrate availability limits beta-amyloid peptide production, *J Biol Chem 274*, 8966-8972.
116. Fenteany, G., Standaert, R. F., Lane, W. S., Choi, S., Corey, E. J., and Schreiber, S. L. (1995) Inhibition of proteasome activities and subunit-specific amino-terminal threonine modification by lactacystin, *Science 268*, 726-731.
117. Graham-Siegenthaler, K., Gauthier, S., Davies, P. L., and Elce, J. S. (1994) Active recombinant rat calpain II. Bacterially produced large and small subunits associate both in vivo and in vitro, *J Biol Chem 269*, 30457-30460.
118. Huang, T. H., Chen, H. C., Chou, S. M., Yang, Y. C., Fan, J. R., and Li, T. K. (2010) Cellular processing determinants for the activation of damage signals in response to topoisomerase I-linked DNA breakage, *Cell Res 20*, 1060-1075.

119. Fan, J. R., Peng, A. L., Chen, H. C., Lo, S. C., Huang, T. H., and Li, T. K. (2008) Cellular processing pathways contribute to the activation of etoposide-induced DNA damage responses, *DNA Repair (Amst) 7*, 452-463.
120. Bano, D., Young, K. W., Guerin, C. J., Lefeuvre, R., Rothwell, N. J., Naldini, L., Rizzuto, R., Carafoli, E., and Nicotera, P. (2005) Cleavage of the plasma membrane Na+/Ca2+ exchanger in excitotoxicity, *Cell 120*, 275-285.
121. Bharti, A. K., Olson, M. O., Kufe, D. W., and Rubin, E. H. (1996) Identification of a nucleolin binding site in human topoisomerase I, *J Biol Chem 271*, 1993-1997.
122. Desai, S. D., Zhang, H., Rodriguez-Bauman, A., Yang, J. M., Wu, X., Gounder, M. K., Rubin, E. H., and Liu, L. F. (2003) Transcription-dependent degradation of topoisomerase I-DNA covalent complexes, *Mol Cell Biol 23*, 2341-2350.
123. Mason, M. J., and Grinstein, S. (1993) Ionomycin activates electrogenic Ca2+ influx in rat thymic lymphocytes, *Biochem J 296 (Pt 1)*, 33-39.
124. Leppard, J. B., and Champoux, J. J. (2005) Human DNA topoisomerase I: relaxation, roles, and damage control, *Chromosoma 114*, 75-85.
125. Lisby, M., Olesen, J. R., Skouboe, C., Krogh, B. O., Straub, T., Boege, F., Velmurugan, S., Martensen, P. M., Andersen, A. H., Jayaram, M., Westergaard, O., and Knudsen, B. R. (2001) Residues within the N-terminal domain of human topoisomerase I play a direct role in relaxation, *J Biol Chem 276*, 20220-20227.
126. Frohlich, R. F., Andersen, F. F., Westergaard, O., Andersen, A. H., and Knudsen, B. R. (2004) Regions within the N-terminal domain of human topoisomerase I exert important functions during strand rotation and DNA binding, *J Mol Biol 336*, 93-103.
127. Bhatt, A., Kaverina, I., Otey, C., and Huttenlocher, A. (2002) Regulation of focal complex composition and disassembly by the calcium-dependent protease calpain, *J Cell Sci 115*, 3415-3425.
128. Kubbutat, M. H., and Vousden, K. H. (1997) Proteolytic cleavage of human p53 by calpain: a potential regulator of protein stability, *Mol Cell Biol 17*, 460-468.
129. Lee, M. S., Kwon, Y. T., Li, M., Peng, J., Friedlander, R. M., and Tsai, L. H. (2000) Neurotoxicity induces cleavage of p35 to p25 by calpain, *Nature 405*, 360-364.
130. Rios-Doria, J., Day, K. C., Kuefer, R., Rashid, M. G., Chinnaiyan, A. M., Rubin, M. A., and Day, M. L. (2003) The role of calpain in the proteolytic cleavage of E-cadherin in prostate and mammary epithelial cells, *J Biol Chem*

278, 1372-1379.

131. Palle, K., Pattarello, L., van der Merwe, M., Losasso, C., Benedetti, P., and Bjornsti, M. A. (2008) Disulfide cross-links reveal conserved features of DNA topoisomerase I architecture and a role for the N terminus in clamp closure, *J Biol Chem 283*, 27767-27775.
132. Zhang, H. F., Tomida, A., Koshimizu, R., Ogiso, Y., Lei, S., and Tsuruo, T. (2004) Cullin 3 promotes proteasomal degradation of the topoisomerase I-DNA covalent complex, *Cancer Res 64*, 1114-1121.
133. Desai, S. D., Li, T. K., Rodriguez-Bauman, A., Rubin, E. H., and Liu, L. F. (2001) Ubiquitin/26S proteasome-mediated degradation of topoisomerase I as a resistance mechanism to camptothecin in tumor cells, *Cancer Res 61*, 5926-5932.
134. Bertipaglia, I., and Carafoli, E. (2007) Calpains and human disease, *Subcell Biochem 45*, 29-53.
135. Pommier, Y. (2009) DNA topoisomerase I inhibitors: chemistry, biology, and interfacial inhibition, *Chem Rev 109*, 2894-2902.
136. D'Arpa, P., Machlin, P. S., Ratrie, H., 3rd, Rothfield, N. F., Cleveland, D. W., and Earnshaw, W. C. (1988) cDNA cloning of human DNA topoisomerase I: catalytic activity of a 67.7-kDa carboxyl-terminal fragment, *Proc Natl Acad Sci U S A 85*, 2543-2547.
137. Zhang, H., Barcelo, J. M., Lee, B., Kohlhagen, G., Zimonjic, D. B., Popescu, N. C., and Pommier, Y. (2001) Human mitochondrial topoisomerase I, *Proc Natl Acad Sci U S A 98*, 10608-10613.
138. Ng, S. W., Liu, Y., Hasselblatt, K. T., Mok, S. C., and Berkowitz, R. S. (1999) A new human topoisomerase III that interacts with SGS1 protein, *Nucleic Acids Res 27*, 993-1000.
139. Mikoshiba, K. (2007) IP3 receptor/Ca2+ channel: from discovery to new signaling concepts, *J Neurochem 102*, 1426-1446.
140. Berridge, M. J. (1993) Inositol trisphosphate and calcium signalling, *Nature 361*, 315-325.
141. Chou, S. M., Huang, T. H., Chen, H. C., and Li, T. K. (2010) Calcium-induced cleavage of DNA topoisomerase I involves the cytoplasmic-nuclear shuttling of calpain 2, *Cell Mol Life Sci*.
142. Abramov, A. Y., and Duchen, M. R. (2003) Actions of ionomycin, 4-BrA23187 and a novel electrogenic Ca2+ ionophore on mitochondria in intact cells, *Cell Calcium 33*, 101-112.
143. Cavarra, M. S., Assef, Y. A., and Kotsias, B. A. (2003) Effects of ionomycin and thapsigargin on ion currents in oocytes of Bufo arenarum, *J Exp Zool A*

Comp Exp Biol 297, 130-137.

144. Molinari, M., Anagli, J., and Carafoli, E. (1994) Ca(2+)-activated neutral protease is active in the erythrocyte membrane in its nonautolyzed 80-kDa form, *J Biol Chem 269*, 27992-27995.
145. Suzuki, K., Tsuji, S., Kubota, S., Kimura, Y., and Imahori, K. (1981) Limited autolysis of Ca2+-activated neutral protease (CANP) changes its sensitivity to Ca2+ ions, *J Biochem 90*, 275-278.
146. Goll, D. E., Thompson, V. F., Taylor, R. G., and Zalewska, T. (1992) Is calpain activity regulated by membranes and autolysis or by calcium and calpastatin?, *Bioessays 14*, 549-556.
147. Schoenwaelder, S. M., Kulkarni, S., Salem, H. H., Imajoh-Ohmi, S., Yamao-Harigaya, W., Saido, T. C., and Jackson, S. P. (1997) Distinct substrate specificities and functional roles for the 78- and 76-kDa forms of mu-calpain in human platelets, *J Biol Chem 272*, 24876-24884.
148. Traub, P., Scherbarth, A., Willingale-Theune, J., Paulin-Levasseur, M., and Shoeman, R. (1988) Differential sensitivity of vimentin and nuclear lamins from Ehrlich ascites tumor cells toward Ca2+ -activated neutral thiol proteinase, *Eur J Cell Biol 46*, 478-490.
149. Saido, T. C., Sorimachi, H., and Suzuki, K. (1994) Calpain: new perspectives in molecular diversity and physiological-pathological involvement, *FASEB J 8*, 814-822.
150. Sorimachi, H., Ishiura, S., and Suzuki, K. (1997) Structure and physiological function of calpains, *Biochem J 328 (Pt 3)*, 721-732.
151. Sorimachi, H., and Suzuki, K. (2001) The structure of calpain, *J Biochem 129*, 653-664.
152. Kishimoto, A., Mikawa, K., Hashimoto, K., Yasuda, I., Tanaka, S., Tominaga, M., Kuroda, T., and Nishizuka, Y. (1989) Limited proteolysis of protein kinase C subspecies by calcium-dependent neutral protease (calpain), *J Biol Chem 264*, 4088-4092.
153. Demarchi, F., and Schneider, C. (2007) The calpain system as a modulator of stress/damage response, *Cell Cycle 6*, 136-138.
154. Gafni, J., Hermel, E., Young, J. E., Wellington, C. L., Hayden, M. R., and Ellerby, L. M. (2004) Inhibition of calpain cleavage of huntingtin reduces toxicity: accumulation of calpain/caspase fragments in the nucleus, *J Biol Chem 279*, 20211-20220.
155. Gil-Parrado, S., Popp, O., Knoch, T. A., Zahler, S., Bestvater, F., Felgentrager, M., Holloschi, A., Fernandez-Montalvan, A., Auerswald, E. A., Fritz, H., Fuentes-Prior, P., Machleidt, W., and Spiess, E. (2003) Subcellular localization

and in vivo subunit interactions of ubiquitous mu-calpain, *J Biol Chem 278*, 16336-16346.

156. Rizzuto, R., and Pozzan, T. (2006) Microdomains of intracellular Ca2+: molecular determinants and functional consequences, *Physiol Rev 86*, 369-408.

157. Rizzuto, R., Pinton, P., Ferrari, D., Chami, M., Szabadkai, G., Magalhaes, P. J., Di Virgilio, F., and Pozzan, T. (2003) Calcium and apoptosis: facts and hypotheses, *Oncogene 22*, 8619-8627.

158. Saidak, Z., Mentaverri, R., and Brown, E. M. (2009) The role of the calcium-sensing receptor in the development and progression of cancer, *Endocr Rev 30*, 178-195.

6. Appendixes

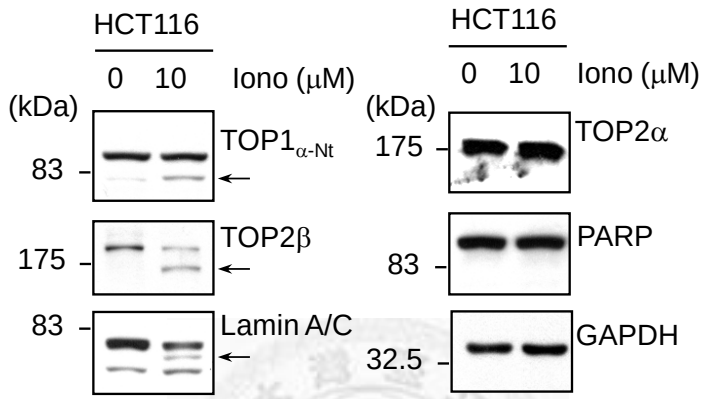

Appendix Fig. 1 Proteolytic responses of different proteins in HCT116 cells exposed to ionomycin.

HCT116 cells were treated with ionomycin (10 μM, 15 min.) and the harvested cell lysates were resolved on 8% SDS-PAGE then subjected to immunoblotting analysis with antibodies for hTOP1, hTOP2β, lamin A/C, hTOP2α, PARP, and GAPDH. Arrows indicate the truncated protein fragments

.

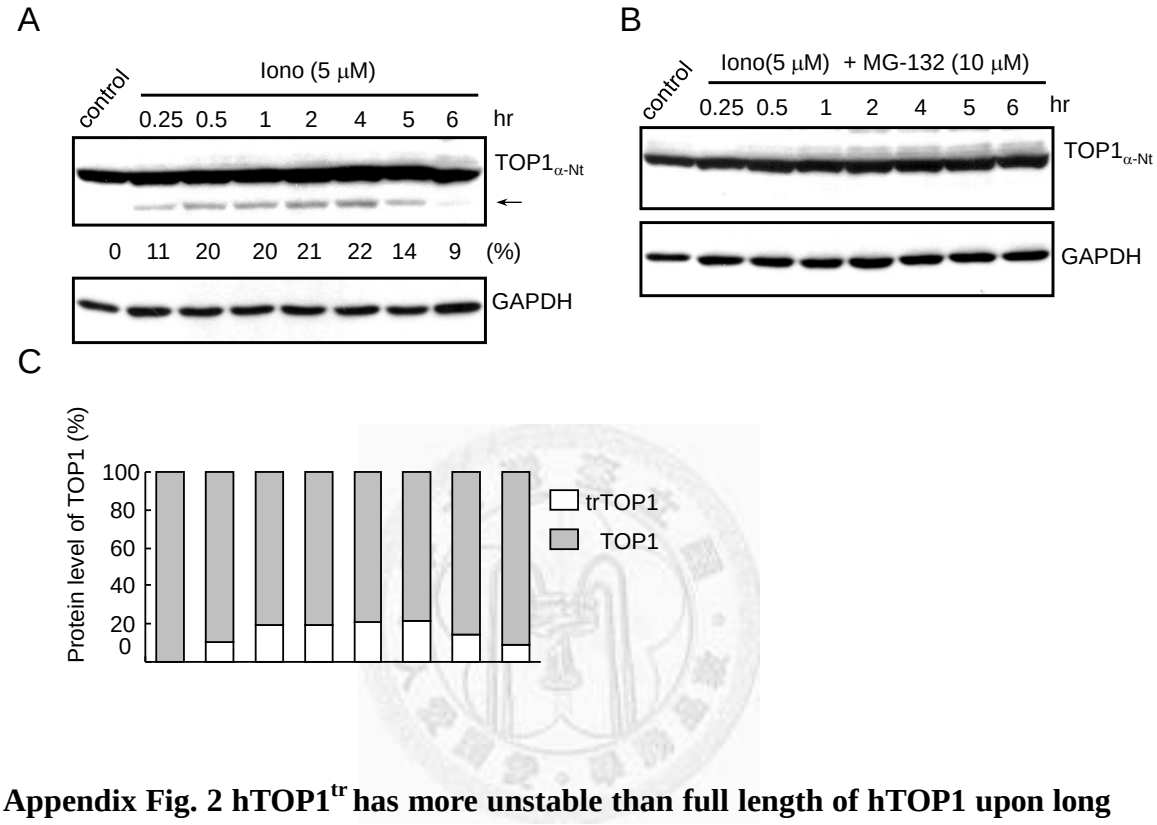

Appendix Fig. 2 hTOP1^{tr} has more unstable than full length of hTOP1 upon long term treatment of ionomycin.

(A-B) HCT116 cells were pretreated with or without MG-132 (10 μM) for 30 min. before long term treatment of ionomycin. The cleavage patterns of hTOP1 were analyzed by immunoblotting assay with TOP1$_{\alpha\text{-Nt}}$ antibodies. The quantified hTOP1^{tr} and hTOP1 (full length) has been plotted in (C). Arrow indicates the truncated hTOP1 fragments

.

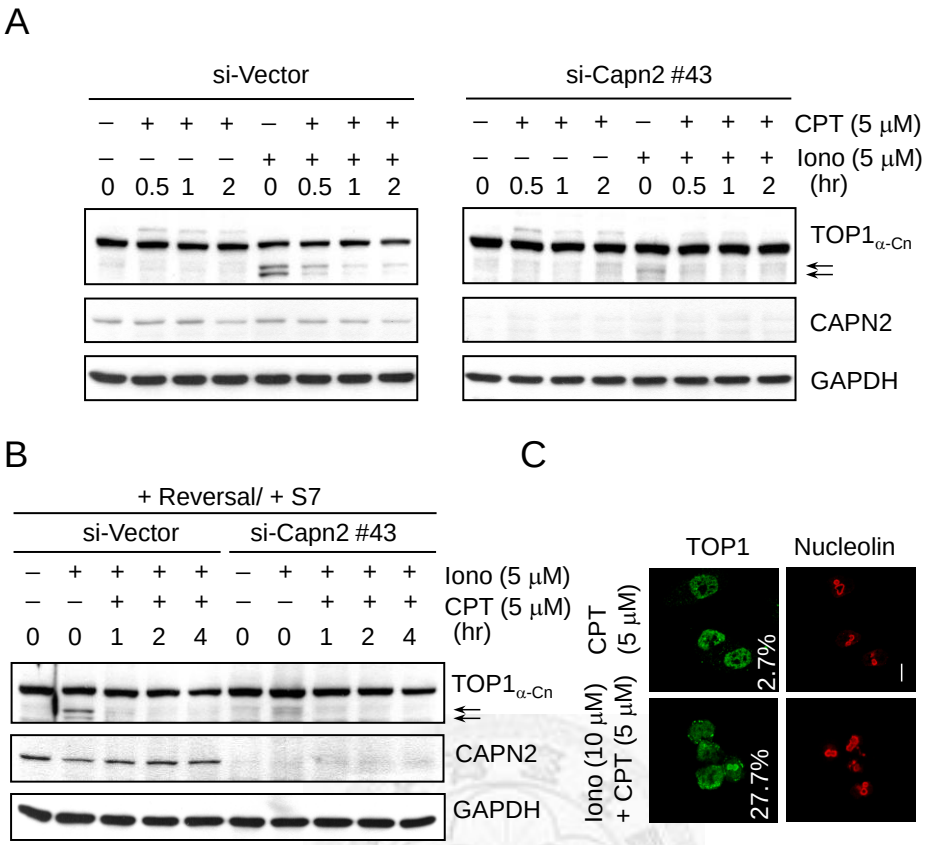

Appendix Fig. 3 CPT causes rapid degradation of ionomycin-induced hTOP1^{tr} and Ca^{2+} influx retards CPT-mediated translocation of hTOP1.

(A) Si-Vector and si-Capn2 #43 cells were treated with ionomycin (5 μM, 15 min.) before exposed to CPT (5 μM) for an additional incubation time as shown on the top of the panel. Cells were lysed with RIPA buffer and then immunoblotting assay was performed to examine the protein integrity of hTOP1 and hTOP1^{tr} with TOP1$_{α\text{-Cn}}$ antibodies. (B) As same as the above, si-Vector and si-Capn2 #43 cells were pretreated with ionomycin and followed by co-treatment with CPT (5 μM). Medium reversal with S7 nuclease treatment was performed as described in Materials and

Methods of chapter 2. (C) HCT116 cells were pretreated with or without ionomycin (10 μM, 15 min.) and co-incubated with CPT (5 μM, 30 min.). IFA was used to detect the locations of hTOP1 and nucleolin. The scored percentage of nucleolar accumulation of hTOP1 was also shown. Arrows indicate the truncated hTOP1 fragments. Bar, 8 μm

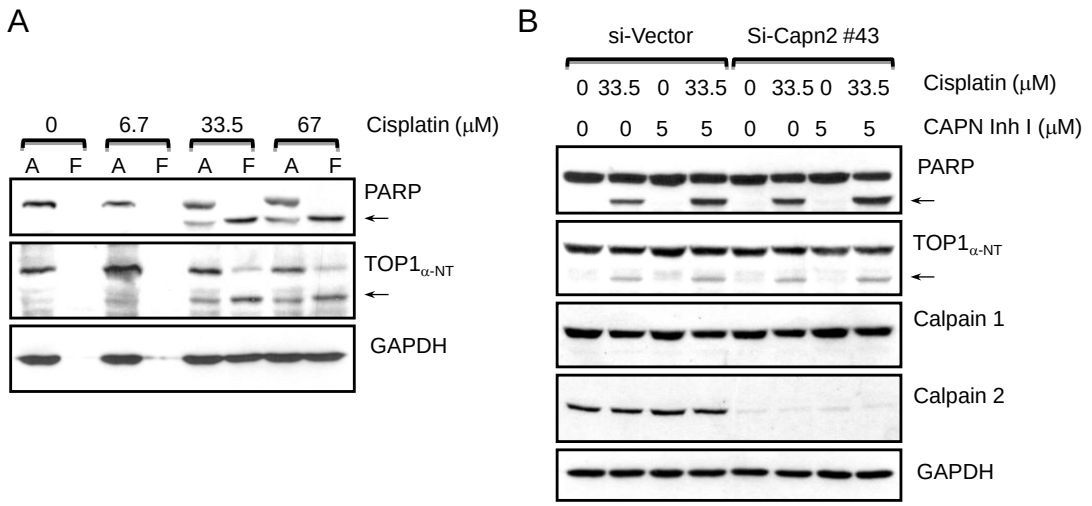

Appendix Fig. 4 Calpain is not involved in cisplatin-induced apoptosis in HCT116 cells.

(A) HCT116 cells were exposed to cisplatin (the concentrations as shown on the top of the panel) for 12 hr. Floating cells were collected from culture medium. (B) si-Vector and si-Capn2 #43 cells were incubated with cisplatin (33.5 μM) for 12 hr in the absence or presence of CAPN Inh I (5 μM). Immunoblotting was performed to determine the cleavage events of PARP and hTOP1. Arrows indicate the truncated PARP and hTOP1 fragments. A, adhering cells; F, floating cells

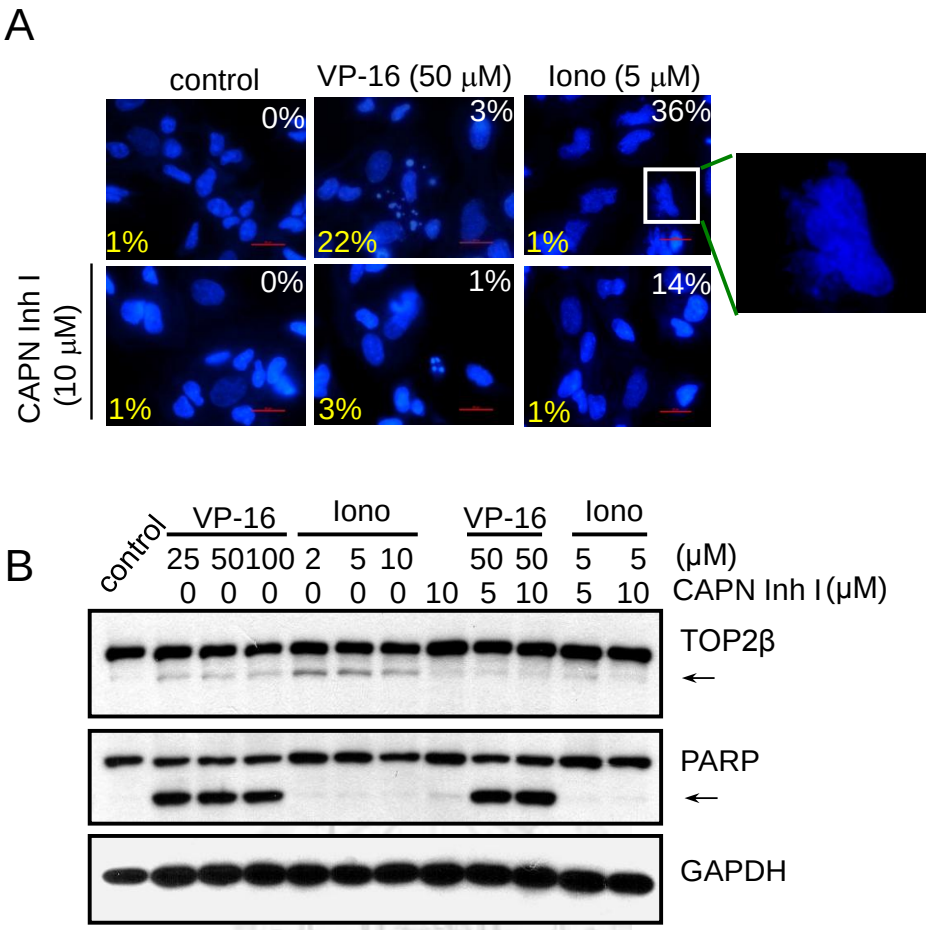

Appendix Fig. 5 Calpain inhibitor I reduces VP-16-induced formation of apoptotic bodies and ionomycin-caused breakdown of nuclear membrane.

(A-B) SK-N-SH cells seeded on coverslips for 24 hr were exposed to VP-16 (50 μM) or ionomycin (5 μM) in the absence or presence of CAPN Inh I (10 μM) for an addition 6-hr incubation. The drugs-treated samples were stained with Hoechst 33342 to observe the integrity of nucleus or lysed for immunoblotting assay to examine the proteolytic cleavage of PARP and hTOP2β. Arrows indicate the truncated PARP and hTOP2β fragments.

7. Curriculum vitae December, 2010

Shang-Min Chou

Education:

1996-2001 B.S.
Department of Plant Pathology and Microbiology
National Taiwan University
2001-2003 M.S.
Graduate Institute of Microbiology, College of Midicine
National Taiwan University
2003-2010 Ph.D.
Graduate Institute of Microbiology, College of Midicine
National Taiwan University

Publications:

1. **Chou SM**, Huang TH, Chen HC, Li TK.

Calcium-induced cleavage of DNA topoisomerase I involves the cytoplasmic-nuclear shuttling of calpain 2. ***Cell Mol Life Sci.*** 2010, Nov 18. [Epub ahead of print]

2. Huang TH, Chen HC, **Chou SM**, Yang YC, Fan JR, Li TK

Cellular processing determinants for the activation of damage signals in response to topoisomerase I-linked DNA breakage. ***Cell Res.*** 2010, Vol. 20(9), P. 1060-75

3. Kou YH, **Chou SM**, Wang YM, Chang YT, Huang SY, Jung MY, Huang YH, Chen MR, Chang MF, Chang SC.

Hepatitis C virus NS4A inhibits cap-dependent and the viral IRES-mediated translation through interacting with eukaryotic elongation factor 1A.

J Biomed Sci. 2006, Vol. 13(6), P. 861-7